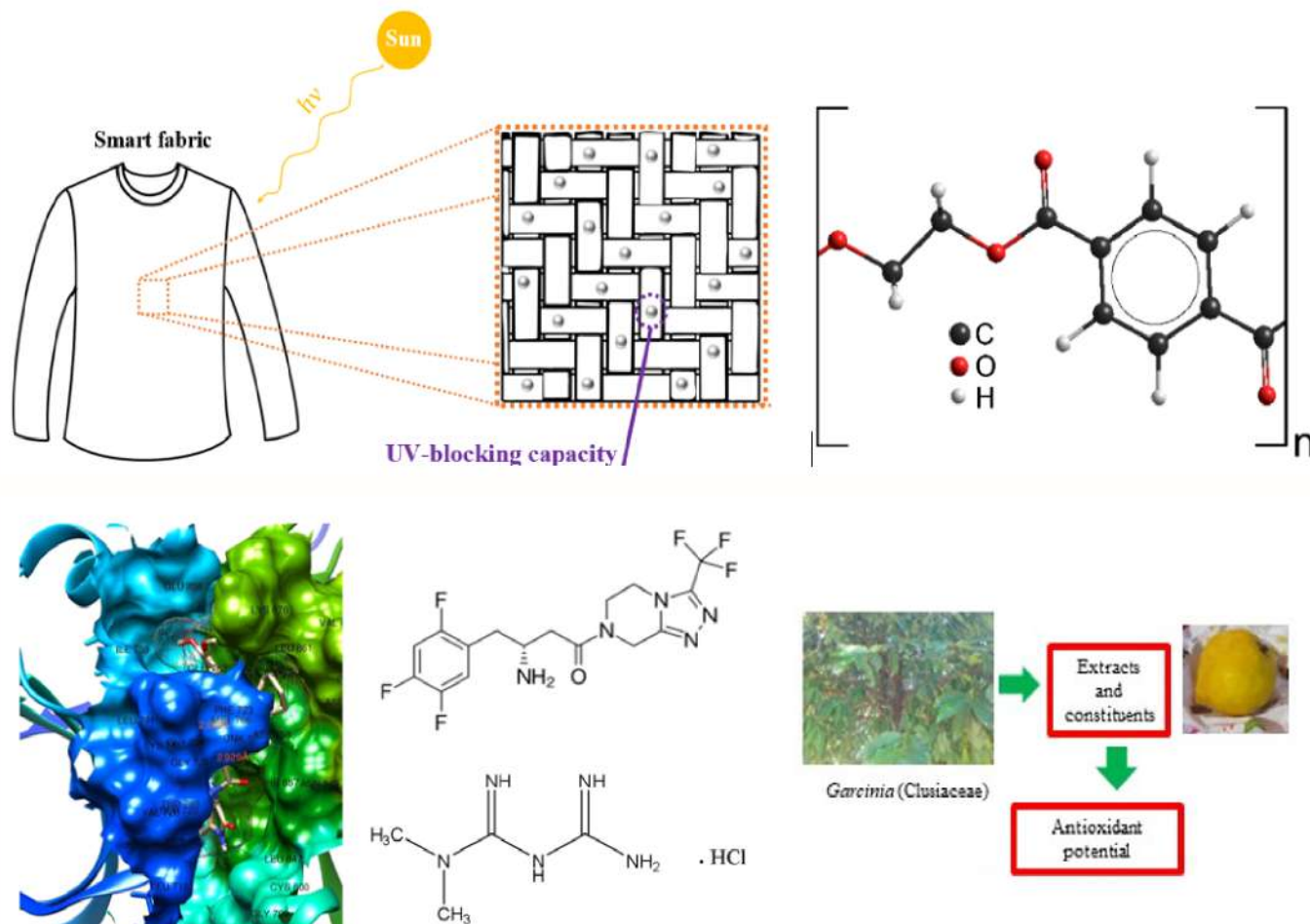


Eclética Química

Volume 48 • number 1 • year 2023



Smart fabrics

UV-protective compound-containing smart textiles: A brief overview

Benzophenones

Antioxidant property of secondary metabolites from *Garcinia* genus: A short review

Tetrahydroquinoline

Quantitative Structure-Activity relationship, Molecular Docking and ADMET Screening of Tetrahydroquinoline Derivatives as Anti-Small Cell Lung Cancer Agents

Spectrophotometric method

Development and validation of a new spectrophotometric method for simultaneous determination of sitagliptin and metformin hydrochloride in tablet pharmaceutical dosage forms using chemometrics technique in comparison with HPLC

Editorial Team

Editor-in-Chief

Prof. Assis Vicente Benedetti, São Paulo State University, Institute of Chemistry, Araraquara, Brazil.
<https://orcid.org/0000-0002-0243-6639>

Editors

Prof. Angélica María Baena Moncada, National University of Engineering, Faculty of Sciences, Lima, Peru.
<https://orcid.org/0000-0002-2896-4392>

Prof. Boutros Sarrouh, Federal University of São João Del-Rei, Department of Chemistry, Biotechnology and Bioprocess Engineering, São João Del-Rei, Brazil. <https://orcid.org/0000-0003-4476-2309>

Prof. Celly Mieko Shinohara Izumi, Federal University of Juiz de Fora, Exact Science Institute, Juiz de Fora, Brazil. <https://orcid.org/0000-0001-6489-9201>

Prof. Horacio Heinzen, University of the Republic of Uruguay, Faculty of Chemistry, Montevideo, Uruguay.
<https://orcid.org/0000-0001-8985-478X>

Prof. Irlon Maciel Ferreira, Federal University of Amapá, Course of Chemistry, Macapá, Brazil.
<https://orcid.org/0000-0002-4517-0105>

Prof. Manuel Ignacio Azocar Guzmán, University of Santiago de Chile, Facultad of Chemistry and Biology Areas, Santiago, Chile. <https://orcid.org/0000-0002-3698-4772>

Prof. Marcos Carlos de Mattos, Federal University of Ceará, Center of Sciences, Fortaleza, Brazil.
<https://orcid.org/0000-0003-4291-5199>

Prof. Mário Antônio Alves da Cunha, Federal Technological University of Paraná, Department of Chemistry, Pato Branco, Brazil. <https://orcid.org/0000-0002-1589-7311>

Prof. Michelle Jakeline Cunha Rezende, Federal University of Rio de Janeiro, Institute of Chemistry, Rio de Janeiro, Brazil. <https://orcid.org/0000-0002-8282-6636>

Prof. Natany Dayani de Souza Assai, Fluminense Federal University, Institute of Exact Sciences, Volta Redonda, Brazil. <https://orcid.org/0000-0002-0851-9187>

Prof. Natanael de Carvalho Costa, Federal University of Rio de Janeiro, Institute of Physics, Rio de Janeiro, Brazil.
<https://orcid.org/0000-0003-4285-4672>

Prof. Nuria Cinca, Polytechnic University of Catalunya, Hyperion Materials & Technologies, Martorelles, Barcelona, Spain. <https://orcid.org/0000-0002-1622-8734>

Prof. Omayra Beatriz Ferreira Balbuena, National University of Asunción, Faculty of Chemical Sciences, Asunción, Paraguay. <https://orcid.org/0000-0001-8449-1297>

Prof. Patrícia Hatsue Suegama, Federal University of Grande Dourados, Faculty of Exact and Technological Sciences, Dourados, Brazil. <http://orcid.org/0000-0001-9421-8454>

Prof. Paulo Clairmont Feitosa Lima Gomes, São Paulo State University, Institute of Chemistry, Araraquara, Brazil. <http://orcid.org/0000-0002-4837-6352>

Prof. Rogéria Rocha Gonçalves, University of São Paulo, Faculty of Philosophy, Sciences and Literature, Ribeirão Preto, Brazil. <https://orcid.org/0000-0001-5540-7690>

Editorial Advisory Board

Prof. Adalgisa Rodrigues de Andrade, University of São Paulo, Faculty of Philosophy, Sciences and Literature, Ribeirão Preto, Brazil. <https://orcid.org/0000-0002-4121-0384>

Prof. Angela Cabezas da Rosa, Technological University, South Center Regional Technological Institute, Durazno, Uruguay. <https://orcid.org/0000-0001-5460-019X>

Prof. Camila Silveira da Silva, Federal University of Paraná, Department of Chemistry, Curitiba, Brazil. <https://orcid.org/0000-0002-6261-1662>

Prof. José António Maia Rodrigues, University of Porto, Faculty of Sciences, Porto, Portugal. <https://orcid.org/0000-0002-3950-528X>

Prof. Lauro Tatsuo Kubota, University of Campinas, Institute of Chemistry, Campinas, Brazil. <https://orcid.org/0000-0001-8189-2618>

Prof. Luis Frederico Pinheiro Dick, Federal University of Rio Grande do Sul, Porto Alegre, Brazil. <https://orcid.org/0000-0002-9896-6318>

Prof. María Isabel Pividori Gugo, University Autòma of Barcelona, Barcelona, Spain. <https://orcid.org/0000-0002-5266-7873>

Prof. María Fátima Yubero de Servián, National University of Asunción, Faculty of Chemical Sciences, Asunción, Paraguay. <https://orcid.org/0000-0001-7668-1381>

Prof. Marília Oliveira Fonseca Goulart, Federal University of Alagoas, Institute of Chemistry and Biotechnology, Maceió, Brazil. <https://orcid.org/0000-0001-9860-3667>

Prof. Massuo Jorge Kato, University of São Paulo, Institute of Chemistry, São Paulo, Brazil. <https://orcid.org/0000-0002-3315-2129>

Prof. Shelley Dawn Minter, University of Utah, Department of Chemistry, Salt Lake City, USA. <http://orcid.org/0000-0002-5788-2249>

Prof. Verónica Cortés de Zea Bermudez, University of Trás-os-Montes and Alto Douro, School of Life and Environmental Sciences, Vila Real, Portugal. <https://orcid.org/0000-0002-7577-4938>

EDITORIAL PRODUCTION

Ctrl K Produção Editorial – Araraquara, Brazil
digite@ctrlk.com.br

Editorial

It is with great satisfaction and pride that the editor announces the first issue of 2023, which contains a review article on sun-protective clothing that can protect against sunburns and skin cancer caused by excessive exposure to solar ultraviolet radiation. It is known that the use of sun-protective clothing is a simple, easy, and practical method for UV protection of the human organism. In the review, the readers may find recent research efforts on the development of UV-protective compound-containing smart fabrics highlighting the UV-blocking properties and multifunctional activities. It describes an update on the progress in the incorporation, coating, and anchorage of UV-protective compounds in textile fibers that may enhance the UV-blocking ability and/or promote functional finishings to smart fabrics. Following the review, another review deals with the antioxidant activity of *Garcinia* species, reporting *in vitro* and *in vivo* assays, described from the last five years. Some species of the *Garcinia* genus are used in the treatment of many diseases and metabolic disorders frequently associated with oxidative stress. The characteristic metabolites found in this genus are xanthenes and benzophenones, which have antioxidant properties, among relevant biological potentials. Following these reviews, the readers find the *in-silico* evaluation of some tetrahydroquinoline derivatives with pyrazole and hydrazide moieties against human lung cancer cell lines and the demonstration by molecular docking analysis that some compounds show good binding affinity towards the studied protein. The results may open the door for the design and development of a library of efficient tetrahydroquinoline-based drug-like compounds as potential anti-lung carcinoma agents. In the sequence, a description of a new, quick, easy, affordable, and eco-friendly simultaneous spectrophotometric method for determining a combined sitagliptin and metformin hydrochloride in pharmaceutical formulations is presented, which was validated using two chemometrics techniques; no samples preparation or separation before analysis is needed. The proposed method is dependable to be adopted as an alternative analytical method in the pharmaceutical industry's quality control.

The Editor and his team thank all authors for their valuable contributions and reviewers for their outstanding collaboration, and convinced of the high quality of the articles, kindly invite you to submit your manuscript to **Eclética Química**.

Assis Vicente Benedetti
Editor-in-Chief of EQ

Digital Databases



Supporters



*Click on the images to follow the links.

EBSCO and FSTA has no link available. The address is for subscribers only.

INSTRUCTIONS FOR AUTHORS

BEFORE YOU SUBMIT

1. Check [Eclét. Quim.'s focus and scope](#)

Eclética Química is a peer-reviewed quarterly publication supported by Institute of Chemistry of São Paulo State University (UNESP). It publishes original researches as articles, reviews and short reviews in **all areas of Chemistry**.

2. Types of papers

- a. Original articles
- b. Reviews
- c. Short reviews
- d. Communications
- e. Technical notes
- f. Articles in education in chemistry and chemistry-related areas

Manuscripts submitted for publication as full articles and communications must contain original and unpublished results and should not have been submitted elsewhere either partially or whole.

a. Original articles

The manuscript must be organized in sections as follows:

1. Introduction
 2. Experimental
 3. Results and Discussion
 4. Conclusions
- References

Sections titles must be written in bold and sequentially numbered; only the first letter should be in uppercase letter. Subsections, numbered as exemplified, should be written in normal and italic letters; only the first letter should be in uppercase letter.

Example:

1. Introduction

1.1 History

2. Experimental

2.1 Surface characterization

2.1.1 Morphological analysis

b. Reviews

Review articles should be original and present state-of-the-art overviews in a coherent and concise form covering the most relevant aspects of the topic that is being revised and indicate the likely future directions of the field. Therefore, before beginning the preparation of a Review manuscript, send a letter (one page maximum) to the Editor with the subject of interest and the main topics that would be covered in the Review manuscript. The Editor will communicate

his decision in two weeks. Receiving this type of manuscript does not imply acceptance to be published in **Eclet. Quim.** It will be peer-reviewed.

c. Short reviews

Short reviews should present an overview of the state-of-the-art in a specific topic within the scope of the journal and limited to 5,000 words. Consider a table or image as corresponding to 100 words. Before beginning the preparation of a Short Review manuscript, send a letter (one page maximum) to the Editor with the subject of interest and the main topics that would be covered in the Short Review manuscript.

d. Communications

Communications should cover relevant scientific results and are limited to 1,500 words or three pages of the journal, not including the title, authors' names, figures, tables and references. However, Communications suggesting fragmentation of complete contributions are strongly discouraged by Editors.

e. Technical notes

Descriptions of methods, techniques, equipment or accessories developed in the authors' laboratory, as long as they present chemical content of interest. They should follow the usual form of presentation, according to the peculiarities of each work. They should have a maximum of 25 pages, including figures, tables, diagrams, etc.

f. Articles in education in chemistry and chemistry-correlated areas

Research manuscript related to undergraduate teaching in Chemistry and innovative experiences in undergraduate and graduate education. They should have a maximum of 25 pages, including figures, tables, diagrams, and other elements.

3. Special issues

Special issues with complete articles dedicated to Symposia and Congresses and to special themes or in honor of scientists with relevant contributions in Chemistry and correlate areas can be published by **Eclet. Quim.** under the condition that a previous agreement with Editors is established. All the guides of the journal must be followed by the authors.

4. Approval

Ensure all authors have seen and approved the final version of the article prior to submission. All authors must also approve the journal you are submitting to.

ETHICAL GUIDELINES

Before starting the submission process, please be sure that **all ethical aspects mentioned below were followed.** Violation of these ethical aspects may preclude authors from submitting or publishing articles in **Eclet. Quim.**

a. Coauthorship: The corresponding author is responsible for listing as coauthors only researchers who have really taken part in the work, for informing them about the entire manuscript content and for obtaining their permission to submit and publish it.

b. Nonauthors: Explicit permission of a nonauthor who has collaborated with personal communication or discussion to the manuscript being submitted to **Eclet. Quim.** must be obtained before being cited.

c. Unbiased research: Authors are responsible for carefully searching for all the scientific work relevant to their reasoning irrespective of whether they agree or not with the presented information.

d. Citation: Authors are responsible for correctly citing and crediting all data taken from other sources. This requirement is not necessary only when the information is a result of the research presented in the manuscript being submitted to **Eclet. Quim.**

e. Direct quotations: The word-for-word reproduction of data or sentences as long as placed between quotation marks and correctly cited is not considered ethical deviation when indispensable for the discussion of a specific set of data or a hypothesis.

f. Do not cite: Master's Degree dissertations and PhD theses are not accepted; instead, you must cite the publications resulted from them.

g. Plagiarism: Plagiarism, self-plagiarism, and the suggestion of novelty when the material was already published are unaccepted by **Eclet. Quim.** Before reviewing a manuscript, the **Turnitin antiplagiarism software** will be used to detect any ethical deviation.

h. Simultaneous submissions: of the same manuscript to more than one journal is considered an ethical deviation and is conflicted to the declaration has been done below by the authors.

i. Studies with humans or other animals: Before submitting manuscripts involving human beings, materials from human or animals, the authors need to confirm that the procedures established, respectively, by the institutional committee on human experimentation and Helsinki's declaration, and the recommendations of the animal care institutional committee were followed. Editors may request complementary information on ethical aspects.

COPYRIGHT NOTICE

The corresponding author transfers the copyright of the submitted manuscript and all its versions to **Eclet. Quim.**, after having the consent of all authors, which ceases if the manuscript is rejected or withdrawn during the review process.

When a published manuscript in **Eclet. Quim.** is also published in another journal, it will be immediately withdrawn from **Eclet. Quim.** and the authors informed of the Editor decision.

Self-archive to institutional, thematic repositories or personal webpage is permitted just after publication. The articles published by **Eclet. Quim.** are licensed under the [Creative Commons Attribution 4.0 International License](#).

PUBLICATION CHARGES

Eclética Química is supported by the Institute of Chemistry/UNESP and publication is free of charge for authors.

MANUSCRIPT PREPARATION

COVER LETTER

We provide a template to help you prepare your cover letter. To download it, click [here](#).

The cover letter **MUST include:**

1. Identification of authors

- a. The authors' full names (they must be written in full and complete, separated by comma)

João M. José	Incorrect
J. M. José	Incorrect
João Maria José	Correct!

- b. E-mail addresses and affiliations (**neither more nor less than two instances**) of all authors;
c. ORCID ID links;
d. A plus sign (+) indicating the corresponding author.

Example:

Author Full Name¹⁺, Author Full Name²

1. University, Faculty or Institute, City, Country.
2. Company, Division or Sector or Laboratory, City, Country.

+ Author 1: address@mail.com, ORCID: <https://orcid.org/xxxx-xxxx-xxxx-xxxx>

Author 2: address@mail.com, ORCID: <https://orcid.org/xxxx-xxxx-xxxx-xxxx>

2. Authors' contribution

We request authors to include author contributions according to CRediT taxonomy standardized contribution descriptions. **CRediT (Contributor Roles Taxonomy)** is a high-level taxonomy, including 14 roles, that can be used to represent the roles typically played by contributors to scientific scholarly output. The roles describe each contributor's specific contribution to the scholarly output.

- a. Please, visit this link (<https://casrai.org/credit/>) to find out which role(s) the authors fit into;
- b. Do not modify the role names; do not write "all authors" in any role. Do not combine two or more roles in one line.**
- c. If there are any roles that no author has engaged in (such as funding in papers that were not funded), write "Not applicable" in front of the name of the role;
- d. Write the authors' names according to the **American Chemistry Society (ACS) citation style**.

Example:

Conceptualization: Foster, J. C.; O'Reilly, R. K.

Data curation: Varlas, S.; Couturaud, B.; Coe, J.; O'Reilly, R. K.

Formal Analysis: Foster, J. C.; Varlas, S.

Funding acquisition: Not applicable.

Investigation: Foster, J. C.; O'Reilly, R. K.

Methodology: Coe, J.; O'Reilly, R. K.

Project administration: O'Reilly, R. K.

Resources: Coe, J.

Software: Not applicable.

Supervision: O'Reilly, R. K.

Validation: Varlas, S.; Couturaud, B.

Visualization: Foster, J. C.

Writing – original draft: Foster, J. C.; Varlas, S.; Couturaud, B.; Coe, J.; O'Reilly, R. K.

Writing – review & editing: Foster, J. C.; Varlas, S.; Couturaud, B.; Coe, J.; O'Reilly, R. K.

3. Indication of reviewers

We kindly ask the authors to suggest **five** suitable reviewers, providing full name, affiliation, and email.

4. Other information

- a. The authors must write one paragraph remarking the novelty and relevance of the work;
- b. The corresponding author must declare, on behalf of the other authors, that the manuscript being submitted is original and its content has not been published previously and is not under consideration for publication elsewhere;
- c. The authors must inform if there is any conflict of interest.

5. Acknowledgements and funding

Acknowledgements and funding information will be requested after the article is accepted for publication.

6. Data availability statement

A data availability statement informs the reader where the data associate with your published work is available, and under what conditions they can be accessed. Therefore, authors must inform if:

Data will be available upon request;

All dataset were generated or analyzed in the current study; or

Data sharing is not applicable.

MANUSCRIPT

We provide a template to help you prepare your manuscript. To download it, click [here](#).

1. General rules

Only manuscripts written in English are accepted. British or American usage is acceptable, but they should not be mixed. Non-native English speakers are encouraged to have their manuscripts professionally revised before submission.

Manuscripts must be sent in editable files as *.doc, *.docx or *.odt. The text must be typed using font style Times New Roman and size 12. Space between lines should be 1.5 mm and paper size A4, top and bottom margins 2.5 cm, left and right margins 2.0 cm.

All contributions must include an **abstract** (170 words maximum), **three to five keywords** and a **graphical abstract** (8 cm wide × 8 cm high).

Appendix should be included at the end of the main text of the manuscript.

Supplementary information: all type of articles accepts supplementary information (SI) that aims at complementing the main text with material that, for any reason, cannot be included in the article.

TITLE

The title should be concise, explanatory and represent the content of the work. The title must have only the first letter of the sentence in uppercase. The following are not allowed: acronyms, abbreviations, geographical location of the research, en or em dashes (which must be replaced by a colon). Titles do not have full point.

ABSTRACT

Abstract is the summary of the article. The abstract must be written as a running text not as structured topics, but its content should present background, objectives, methods, results, and conclusion. It cannot contain citations. The text

should be written in a single paragraph with a **maximum of 170 words**.

KEYWORDS

Keywords are intended to make it easier for readers to find the content of your text. As fundamental tools for database indexing, they act as a gateway to the text. The correct selection of keywords significantly increases the chances that a document will be found by researchers on the topic, and consequently helps to promote the visibility of an article within a myriad of publications.

FIGURES, TABLES AND EQUATIONS

Figures, tables and equations must be written with initial capital letter followed by their respective number and period, in bold, without adding zero “**Table 1**”, preceding an explanatory title. Tables, Figures and Equations should appear after the first citation and should be numbered according to the ascending order of appearance in the text (1, 2, 3...).

Figures, tables, schemes and photographs already published by the same or different authors in other publications may be reproduced in manuscripts of **Eclét. Quim.** only with permission from the editor house that holds the copyright.

Nomenclature, abbreviations, and symbols should follow IUPAC recommendations.

DATA AVAILABILITY STATEMENT

The data availability statement informs the reader where the data associate with your work is available, and under what conditions they can be accessed. They also include links (where applicable) to the data set.

- a. The data are available in a data repository (cite repository and the DOI of the deposited data);
- b. The data will be available upon request;
- c. All data sets were generated or analyzed in the current study;
- d. Data sharing is not applicable (in cases where no data sets have been generated or analyzed during the current study, it should be declared).

GRAPHICAL ABSTRACT

The graphical abstract must summarize the manuscript in an interesting way to catch the attention of the readers. As already stated, it must be designed with 8 cm wide × 8 cm high, and a 900-dpi resolution is mandatory for this journal. It must be submitted as *.jpg, *.jpeg, *.tif or *.ppt files as supplementary file.

We provide a template to help you prepare your GA. To download it, click [here](#).

SUPPLEMENTARY INFORMATION

When appropriate, important data to complement and a better comprehension of the article can be submitted as Supplementary File, which will be published online and will be made available as links in the original article. This might include additional figures, tables, text, equations, videos or other materials that are necessary to fully document the research contained in the paper or to facilitate the readers' ability to understand the work.

Supplementary material should be presented in appropriate .docx file for text, tables, figures and graphics. All supplementary figures, tables and videos should be referred in the manuscript body as “Table S1, S2...”, “Fig. S1, S2...” and “Video S1, S2 ...”.

At the end of the main text the authors must inform: This article has supplementary information.

Supplementary information will be located following the article with a different DOI number from that of the article, but easily related to it.

CITATION STYLE GUIDE

From 2021 on, the journal will follow the [ACS citation style](#).

Indication of the sources is made by authorship and date. So, the reference list is organized alphabetically by author.

Each citation consists of two parts: the in-text citation, which provides brief identifying information within the text, and the reference list, a list of sources that provides full bibliographic information.

We encourage the citation of primary research over review articles, where appropriate, in order to give credit to those who first reported a finding. Find out more about our commitments to the principles of [San Francisco Declaration on Research Assessment \(DORA\)](#).

What information you must cite?

- a. Exact wording taken from any source, including freely available websites;
- b. Paraphrases of passages;
- c. Summaries of another person's work;
- d. Indebtedness to another person for an idea;
- e. Use of another researchers' work;
- f. Use of your own previous work.

You do not need to cite **common knowledge**.

Example:

Water is a tasteless and odorless liquid at room temperature (common knowledge, no citation needed)

In-text citations

You can choose to cite your references within or at the end of the phrase, as showed below.

Within the cited information:

One author: Finnegan states that the primary structure of this enzyme has also been determined (2004).

Two authors: Finnegan and Roman state that the structure of this enzyme has also been determined (2004).

Three or more authors: Finnegan *et al.* state that the structure of this enzyme has also been determined (2004).

At the end of the cited information:

One author: The primary structure of this enzyme has also been determined (Finnegan, 2004).

Two authors: The primary structure of this enzyme has also been determined (Finnegan and Roman, 2004).

Three or more authors: The primary structure of this enzyme has also been determined (Finnegan *et al.*, 2004).

If you need to cite more than one reference in the same brackets, separate them with semicolon and write them in alphabetic order:

The primary structure of this enzyme was determined (Abel *et al.*, 2011; Borges, 2004; Castro *et al.*, 2021).

Bibliographic references

Article from scientific journals

Foster, J. C.; Varlas, S.; Couturaud, B.; Coe, J.; O'Reilly, R. K. Getting into Shape: Reflections on a New Generation of Cylindrical Nanostructures' Self-Assembly Using Polymer Building Block. *J. Am. Chem. Soc.* **2019**, *141* (7), 2742–2753. <https://doi/10.1021/jacs.8b08648>

Book

Hammond, C. *The Basics of Crystallography and Diffraction*, 4th ed.; International Union of Crystallography Texts on Crystallography, Vol. 21; Oxford University Press, 2015.

Book chapter

Hammond, C. Crystal Symmetry. In *The Basics of Crystallography and Diffraction*, 4th ed.; International Union of Crystallography Texts on Crystallography, Vol. 21; Oxford University Press, 2015; pp 99–134.

Book with editors

Mom the Chemistry Professor: Personal Accounts and Advice from Chemistry Professors Who Are Mothers, 2nd ed.; Woznack, K., Charlebois, A., Cole, R. S., Marzabadi, C. H., Webster, G., Eds.; Springer, 2018.

Website

ACS Publications Home Page. <https://pubs.acs.org/> (accessed 2019-02-21).

Document from a website

American Chemical Society, Committee on Chemical Safety, Task Force for Safety Education Guidelines. *Guidelines for Chemical Laboratory Safety in Academic Institutions*. American Chemical Society, 2016. <https://www.acs.org/content/dam/acsorg/about/governance/committees/chemicalsafety/publications/acs-safety-guidelines-academic.pdf> (accessed 2019-02-21).

Conference proceedings

Nilsson, A.; Petersson, F.; Persson, H. W.; Jönsson, H. Manipulation of Suspended Particles in a Laminar Flow. In *Micro Total Analysis Systems 2002*, Proceedings of the μ TAS 2002 Symposium, Nara, Japan, November 3–7, 2002; The Netherlands, 2002; pp 751–753. https://doi.org/10.1007/978-94-010-0504-3_50

Governmental and legislation information

Department of Commerce, United States Patent and Trademark Office. Section 706.02 Rejection of Prior Art [R-07.2015]. *Manual of Patent Examining Procedure (MPEP)*, 9th ed., rev. 08.2017, last revised January 2018. <https://www.uspto.gov/web/offices/pac/mpep/s706.html#d0e58220> (accessed 2019-03-20).

Patent

Lois-Caballe, C.; Baltimore, D.; Qin, X.-F. Method for Expression of Small RNA Molecules within a Cell. US 7 732 193 B2, 2010.

Streaming data

American Chemical Society. Game of Thrones Science: Sword Making and Valyrian Steel. *Reactions*. YouTube, April 15, 2015. <https://www.youtube.com/watch?v=cHRcGoje4j4> (accessed 2019-02-28).

For more information, you can access the [ACS Style Quick Guide](#) and the [Williams College LibGuides](#).

SUBMITTING YOUR MANUSCRIPT

The corresponding author should submit the manuscript online by clicking [here](#). If you are a user, register by clicking [here](#).

At the **User home** page, click in **New submission**.

In Step 1, select a section for your manuscript, verify one more time if you followed all these rules in **Submission checklist**, add Comments for the Editor if you want to, and click Save and continue.

In Step 2, you will **upload your manuscript**. Remember it will pass through a double-blind review process. So, do not provide any information on the authorship.

In Step 3, enter **submission's metadata**: authors' full names, valid e-mail addresses and ORCID ID links (with "http" not "https"). Add title, abstract, contributors and supporting agencies, and the list of references.

In Step 4, upload the **cover letter**, the **graphical abstract** and other **supplementary material** you want to include in your manuscript.

In Step 5, you will be able to check all submitted documents in the **File summary**. If you are certain that you have followed all the rules until here, click in **Finish submission**.

REVIEW PROCESS

The time elapsed between the submission and the first response of the reviewers is around three months. The average time elapsed between submission and publication is around seven months.

Resubmission (manuscripts "rejected in the present form" or subjected to "revision") must contain a letter with the responses to the comments/criticism and suggestions of reviewers/editors should accompany the revised manuscript.

All modifications made to the original manuscript must be highlighted.

If you want to check our Editorial process, click [here](#).

EDITOR'S REQUIREMENTS

Authors who have a manuscript accepted in **Eclet. Quim.** may be invited to act as reviewers.

Only the authors are responsible for the correctness of all information, data and content of the manuscript submitted to **Eclet. Quim.** Thus, the Editors and the Editorial Board cannot accept responsibility for the correctness of the material published in **Eclet. Quim.**

Proofs

After accepting the manuscript, **Eclet. Quim.** technical assistants will contact you regarding your manuscript page proofs to correct printing errors only, i.e., other corrections or content improvement are not permitted. The proofs shall be returned in three working days (72 h) via email.

Appeal

Authors may only appeal once about the decision regarding a manuscript. To appeal against the Editorial decision on your manuscript, the corresponding author can send a rebuttal letter to the editor, including a detailed response to any comments made by the reviewers/editor. The editor will consider the rebuttal letter, and if deemed appropriate, the manuscript will be sent to a new reviewer. The Editor decision is final.

Contact

If you have any question, please contact our team:

Prof. Assis Vicente Benedetti
Editor-in-Chief
ecletica.iq@unesp.br

Letícia Amanda Miguel
Technical support
ecletica@ctrlk.com.br

SUMMARY

EDITORIAL BOARD.....	2
EDITORIAL.....	4
DATABASE.....	5
INSTRUCTIONS FOR AUTHORS	6

REVIEW Article

UV-protective compound-containing smart textiles: A brief overview.....	16
<i>João Henrique Barcha Lupino, Gustavo Pereira Saito, Marco Aurélio Cebim, Marian Rosaly Davolos</i>	

SHORT REVIEW

Antioxidant property of secondary metabolites from <i>Garcinia</i> genus: A short review	41
<i>Elton Kazmierczak, Cássia Gonçalves Magalhães, Romaiiana Picada Pereira</i>	

ORIGINAL ARTICLES

Quantitative Structure-Activity relationship, Molecular Docking and ADMET Screening of Tetrahydroquinoline Derivatives as Anti-Small Cell Lung Cancer Agents	55
<i>Ehimen Annastasia Erazua, Abel Kolawole Oyebamiji, Sunday Adewale Akintelu, Pelumi Daniel Adewole, Adedayo Adelakun, Babatunde Benjamin Adeleke</i>	
Development and validation of a new spectrophotometric method for simultaneous determination of sitagliptin and metformin hydrochloride in tablet pharmaceutical dosage forms using chemometrics technique in comparison with HPLC.....	72
<i>Maher Ali Almaqtari, Najat Ahmed Al-Odaini, Fares Abdullah Alarbagi, Hussein Al-Maydama</i>	

UV-protective compound-containing smart textiles: A brief overview

João Henrique Barcha Lupino¹, Gustavo Pereira Saito¹, Marco Aurélio Cebim¹, Marian Rosaly Davolos¹⁺

1. São Paulo State University, Institute of Chemistry, Araraquara, Brazil.

+Corresponding author: Marian Rosaly Davolos, **Phone:** +55 16 33019634, **Email address:** marian.davolos@unesp.br

ARTICLE INFO

Article history:

Received: March 29, 2022

Accepted: December 12, 2022

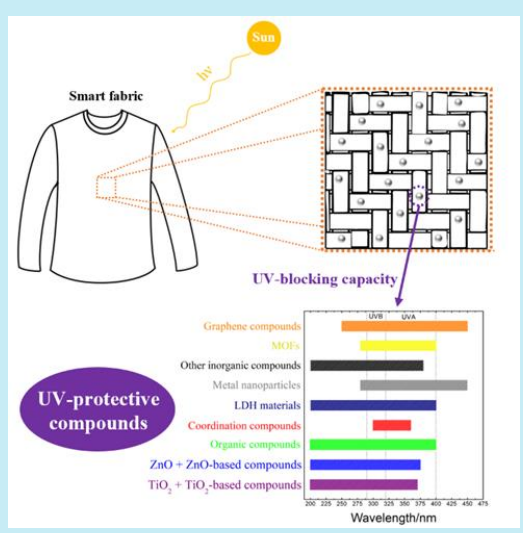
Published: January 01, 2023

Keywords:

1. smart fabrics
2. textile properties
3. different UV-protective compound classes
4. UV-blocking ability
5. ultraviolet protection factor

Section Editors: Assis Vicente Benedetti

ABSTRACT: Excessive exposure to solar ultraviolet (UV) radiation causes human health damages, such as sunburns and skin cancer. Thus, the use of sun-protective clothing is a simple, easy, and practical method for UV protection of the human organism. In this perspective, incorporation, coating, and anchorage of UV-protective compounds in textile fibers have been employed to enhance the UV-blocking ability and/or promote functional finishings to smart fabrics. This review describes recent research efforts on the development of UV-protective compound-containing smart fabrics highlighting the UV-blocking properties and multifunctional activities. Different compound class examples and discussions are presented in order to contribute to new insights into sun-protective clothing and future applications of multifunctional textiles.



CONTENTS

1. Introduction
2. Textile properties and UV protection relationships of the sun-protective clothing
3. UV-protective compound-containing smart fabrics
 - 3.1 TiO₂
 - 3.2 ZnO
 - 3.3 Graphene compounds
 - 3.4 MOFs
 - 3.5 Organic compounds
 - 3.6 Inorganic compounds, metal nanoparticles, LDH material and coordination compounds
4. Conclusions

- Authors' contribution
- Data availability statement
- Funding
- Acknowledgments
- References

1. Introduction

The sun is essential for the Earth's life and its environment (Powers and Murphy, 2019); consequently, solar radiation effects provide human health benefits, such as physical and mental well-being (Flor *et al.*, 2007) and the stimulation of melanin (Serre *et al.*, 2018) and vitamin D biosynthesis (Baker *et al.*, 2017). However, the excessive solar radiation exposure cause sunburns (Sambandan and Ratner, 2011), irregular skin pigmentation, immune system depression, premature aging (Kockler *et al.*, 2012) and skin cancer (Bagde *et al.*, 2018). Among electromagnetic radiations emitted by the sun that reach the Earth's surface, the ultraviolet (UV) radiation is the main responsible for photochemical reactions in the human organism (Baker *et al.*, 2017). UV radiation may be subdivided into following regions: UVC (200–290 nm), UVB (290–320 nm) and UVA (320–400 nm) (Velasco *et al.*, 2008). Stratospheric ozone layer blocks a high percentage of the incident UVC radiation (Baker *et al.*, 2017); therefore, a combination of UVB and UVA radiation reaches the terrestrial surface (Fourtanier *et al.*, 2012). UV radiation penetrates in the upper and deeper layers on the skin causing cellular damages and immune system function modifications (Kockler *et al.*, 2012). Thus, sunscreens and UV-blocking fabrics can be used to minimize the human health risks induced by excessive UVB and UVA radiation exposure. According to the literature, UV blocking (Faure *et al.*, 2013) and UV shielding (Parwaiz *et al.*, 2019) are scientific terms commonly used to express the solar UV protection performance of photoprotective materials. However, UV blocking term is more used than UV shielding to designate the photoprotective capacity of textiles (Mondal, 2022).

The main constituents of photoprotective products are organic and inorganic filters, which are chemical compounds that absorb and/or scatter UV radiation without changes in their physicochemical properties (Saito *et al.*, 2021). Organic filters are organic molecules composed by chromophore groups that commonly exhibit high degree of the π -conjugated system (Saito *et al.*, 2021). The UV absorption capacity of organic filters depends on both the energy differences from electronic transitions between frontier orbitals and molar absorption coefficient (ϵ). In general, $\pi \rightarrow \pi^*$ and/or $n \rightarrow \pi^*$ transitions give rise the UV absorption mechanism of organic filters (Baker *et al.*, 2017; Flor *et al.*, 2007). Some examples of organic filters are beta-diketones and organic compounds derived from: benzophenone, anthranilate, salicylic acid, cinnamic acid, p-aminobenzoic acid and camphor (Antoniou *et al.*,

2008). Organic filters are widely used in sunscreen applications due to their UVB and/or UVA absorption capacity (Kockler *et al.*, 2012). Furthermore, these organic compounds show solubility in different dispersion mediums, which facilitates the use of them in the manufacturing process of photoprotective products (Forestier, 2008; Morabito *et al.*, 2011).

Organic filter decomposition under high temperature and/or oxidizing environment exposure results in changes and/or loss of the UV shielding ability and induces the free radical's production that could cause DNA, elastin and/or collagen damages (S. Jain and N. Jain, 2010).

Inorganic filters are inorganic compounds that exhibit UV-visible (UV-VIS) absorption capacity and, depending on the refractive index and/or particle size of them, can scatter UV radiation (Abuçafy *et al.*, 2016; Seixas and Serra, 2014). In general, UV-VIS absorption process in metal oxides (e.g., ZnO and TiO₂) involves electronic transitions between valence band and conduction band (VB \rightarrow CB). The main advantages of inorganic filters are thermal stability, broad spectrum absorption (Seixas and Serra, 2014) and low toxicity to the human body (S. Wang *et al.*, 2010). For these reasons, inorganic filters are widely incorporated in cosmetic formulations and/or UV-blocking products intended for children and people with skin diseases or sensitive skin (Serpone *et al.*, 2007). However, these inorganic compounds can promote photocatalytic reactions (L. Wang *et al.*, 2018) that decompose cosmetic ingredients affecting on the UV shielding ability of photoprotective products.

The growing concern about deleterious effects of the UV radiation exposure combined with the negative aspects related to the use of commercial inorganic and organic filters has significantly promoted the development of photostable compounds with high UV protection and low toxicity to the human organism and the environment, i.e., UV-protective compounds (Saito *et al.*, 2018). In this perspective, UV-protective compounds have been obtained by the coordination of organic filters with transition metals (Ahmedova *et al.*, 2002; Pettinari *et al.*, 2016), association between inorganic and organic filters (Parisi *et al.*, 2016), encapsulation of organic (Morabito *et al.*, 2011) or inorganic filters (Frizzo *et al.*, 2019), and intercalation of organic filters into inorganic layered matrices (Franco *et al.*, 2020; Saito *et al.*, 2021).

One of the most important manufacturing steps of photoprotective products is the dispersion or incorporation of organic and/or inorganic filters in sunscreens, polymer matrices or textile fibers. Sunscreens are emulsions and/or particle dispersions,

whose main purpose is to protect the human skin from UV damages (Saito *et al.*, 2019). However, these cosmetic formulations can cause skin allergies depending on the ingredients present in their composition (Giokas *et al.*, 2007). Thus, the sun-protective clothing is a viable alternative for UV protection due to the lower occurrence of allergic reactions by skin contact and its simple, easy, and practical use. It is important to emphasize that the global smart fabrics market, which includes the promoting and selling of self-cleaning, flame retardant, antibacterial and UV-blocking fabrics, was estimated at US\$ 289.5 million in 2012. Before the COVID-19 pandemic, smart fabrics market projections for 2020 was quoted at US\$ 361.9 million, keeping similar growth rates and correcting inflation (SEBRAE, 2014).

2. Textile properties and UV protection relationships of the sun-protective clothing

The UV shielding ability of the sun-protective clothing is directly related to the physical and chemical properties of the fabric used in its manufacture. Therefore, the chemical composition, weave pattern and optical properties are the main factors that should be considered when making sun UV-blocking fabrics (Alebeid and Zhao, 2017).

In the last decades, several kinds of textile fibers or fiber blends have been used to fabric manufacturing (Jabbar and Shaker, 2016). Polyethylene terephthalate (PET), commonly named polyester, and cotton fibers are the most employed to produce sun-protective fabrics. Generally, PET (Fig. 1) is obtained by the condensation polymerization process of terephthalic acid and ethylene glycol under specific synthetic conditions (Jaffe *et al.*, 2020). In the first step of the PET polymerization, the bis(hydroxyethyl)terephthalate (BHET) monomer is produced by esterification of terephthalic acid. It is important to highlight that the esterification reaction produces a mixture of PET oligomers and BHET; consequently, water and impurity removal is essential to the ultimate achievement of the PET polymer. The next step of the PET polymerization consists in the ester interchange reaction between two BHET molecules to split off a glycol molecule, building polymer molecular weight. This condensation reaction must be catalyzed, being the antimony trioxide (Sb_2O_3) the catalyzer most used. Moreover, the melt-polymerization temperatures at or above 285°C are used to promote the uniform stirring of the reactional medium. In the last step, PET polymer is pelletized for melt spinning or putted on a spinning

machine and transformed to fiber (Jaffe *et al.*, 2020). The main reasons for the using of PET fibers in sun-protective clothing are the low cost, ease of blending with natural fibers and UVB absorption capacity (Curtzwiler *et al.*, 2017). Its UVB absorption ability is directly related to the presence of aromatic rings and carboxyl groups, i.e., chromophores groups in the polymeric structure.

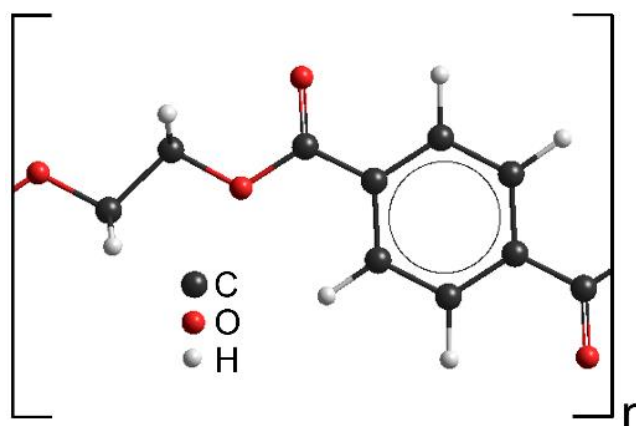


Figure 1. Polyethylene terephthalate (PET) monomer structure.

Cotton is a natural fiber formed by dried cell walls of formerly living cells of *Gossypium* genus plants (Ioelovich and Leykin, 2008; Liu, 2018). The cotton fiber formation starts in an ovary of the cotton flower and proceeds in a mature seed-containing cotton bowl (or fruit). Thus, fiber development includes initiation, primary cell wall formation for fiber elongation, secondary cell wall biosynthesis for cellulose deposition and cell wall thickening, and maturation. Cotton fibers are composed by cellulose (88.0–96.5%), proteins (1.0–1.9%), waxes (0.4–1.2%), pectins (0.4–1.2%), inorganic compounds (0.7–1.6%), and other substances (0.5–8.0%). It is important to emphasize that the chemical composition of cotton fibers depends on the cotton cultivar, growing environment and degree of fiber maturity (Liu, 2018). Cellulose, major chemical component of cotton fibers, consists in linear β -1,4-linked chains of D-glucopyranose (Fig. 2) produced by photosynthesis process (Yue *et al.*, 2012). In the cloth manufacturing, cotton fibers are widely used due to their low cost, softness, high air permeability, moisture-absorptive features, high thermal resistance, and hypoallergenic properties (H. Wang and Memon, 2020).

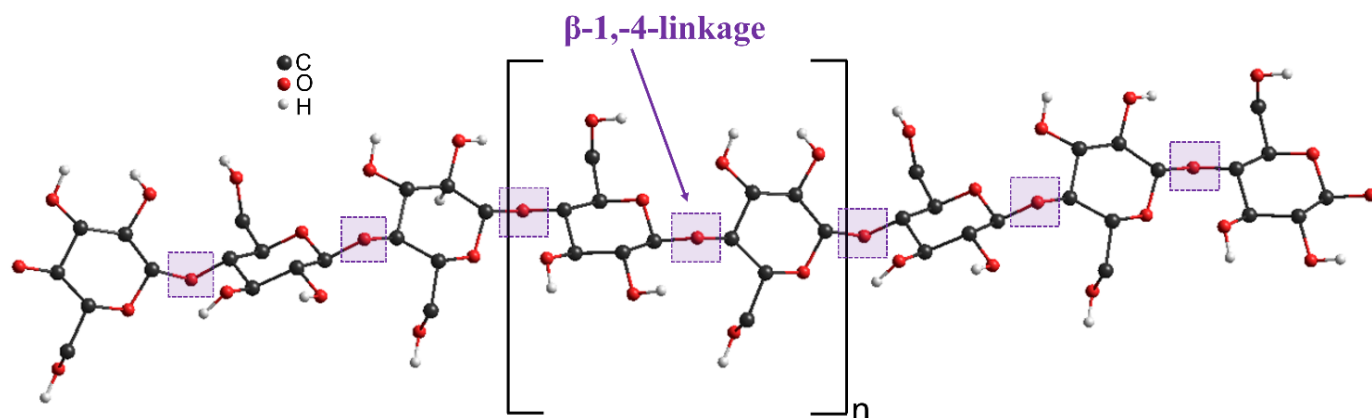


Figure 2. Schematic representation of the simplified cellulose structure.

Different weft types can be used in weaving stage of the sun-protective fabrics. The weft is the arrangement of intertwined threads that gives rise to fabric. This thread arrangement is classified into plain weave fabric and mesh (Pezzolo, 2007). In the plain weave fabric, the thread interweaving turns it more difficult to deform in shear. (Mohammed *et al.*, 2000; Pezzolo, 2007). While the mesh allows the stretching of the fabric because there are no fixed thread loops in its weft (Pezzolo, 2007).

Plain fabric's frames are commonly classified in taffeta, twill or satin. The taffeta has a weft design that

looks like a chessboard (Fig. 3a), which provides a higher mechanical resistant due to its homogeneous shape. Twill has a diagonal pattern (Fig. 3b), offering less dirt adhesion and easier cleaning, because its weft pattern provides more empty spaces among the plain weave fabric. Satin weft presents larger heels between the threads than other plain weave designs (Fig. 3c), consequently, this weft design influence on the fabric brightness (Pezzolo, 2007).

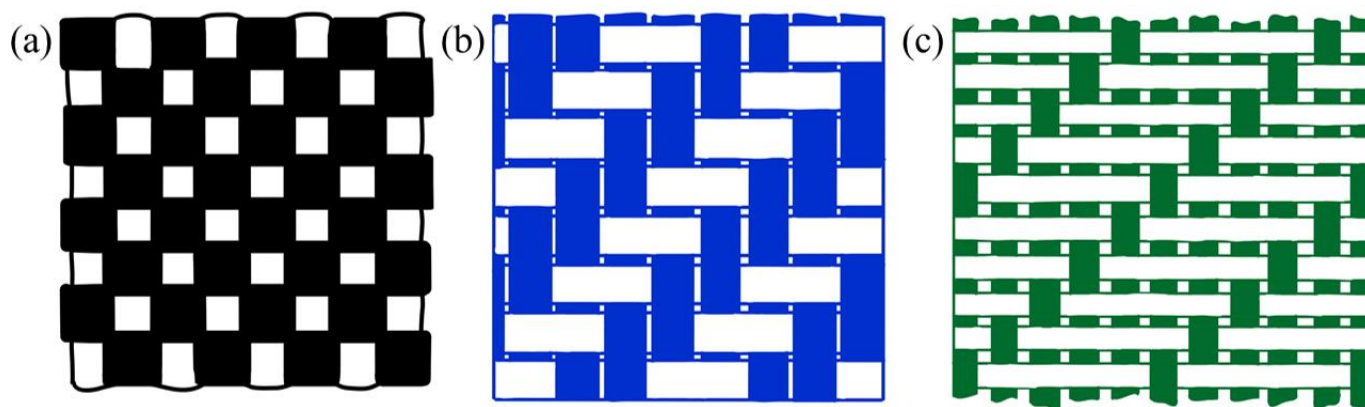


Figure 3. Schematic representations of plain fabric's frames: (a) taffeta, (b) twill and (c) satin.

After the weaving process, fabrics are submitted to the finishing stages (1st, 2nd, and 3rd stage) of the textile processing. The 1st finishing stage is mainly composed by the brushing, shaving, singeing and scouring processes. In the 2nd finishing stage, also known as dyeing and printing, pigments and/or dyes are adsorbed and/or anchored in the surface of textile fibers. Finally, the 3rd finishing stage consists in chemical processes used to generate specific physical-chemical properties in fabrics, e.g., waterproofing ability (Pezzolo, 2007). Among these chemical processes, the incorporation of

nanoparticles in textile fibers has been widely used (Chau *et al.*, 2007; Costa, 2012; Ferreira *et al.*, 2014; Sánchez, 2006) in order to create smart fabrics, i.e., fabric with self-cleaning, antibacterial or even flame-retardant properties. It is important to point that the 2nd stage can provide textile benefits similar to 3rd stage depending on the physical and chemical properties of pigments and/or dyes used. Thus, 2nd and 3rd stage can be understood as the same finishing stage of the textile processing.

UV protection on fabrics depends on the fiber type, weft design, fabric thickness, yarn linear density, and the optical properties of pigments or dyes. For example, the solar transmittance decreases, and the diffuse reflectance increases when yarn linear density, i.e., the number of weft yarns per unit length increases (Yildirim *et al.*, 2018). Besides textile properties, UV shielding capacity can be enhanced by incorporation, coating, or anchorage of UV-protective compounds in the textile fiber surface (Table 1a–d). Thus, the purpose of this review is to report

scientific results about UV-protective compound-containing smart fabrics in the period from 2010 to 2021.

It is known that the incorporation, coating and/or anchorage of UV-protective compounds in smart fabrics protects human skin against excessive UV radiation exposure and reduces the photodecomposition percentage of textile fibers. Nevertheless, this brief review focused in showing the main scientific results and potential applications of UV-blocking fabrics used to minimize the human health hazards.

Table 1a. Examples of UV-protective compound-containing textile fibers described in scientific literature between 2010 and 2012.

Textile fiber composition	UV-protective compound	Assessment method of the UV shielding performance	Additional fabric properties	Reference
PET and PET/wool (70:30) blend, PET/cotton (70:30) blend and PET/viscose (70:30) blend	Monochlorotriazinyl β -cyclodextrin, chitosan, ethylenediamine or Dyes (<i>Disperse Red FB 60</i> , <i>Disperse Blue 2BL 56</i> or <i>Disperse Orange 25</i>)	UPF	-	Ibrahim <i>et al.</i> (2010a)
Cotton	Europium(III) complex	UPF	-	Z. Chen and Yin (2010)
Linen	Metal salts ($M(CH_3COO)_2$, where $M = Cu^{2+}$, Zn^{2+} and Ca^{2+}), $ZrOCl$, Ag, ZrO , TiO_2 or Dyes (<i>C.I Basic Red 24</i> or <i>C.I Reactive Violet 5</i>)	UPF	Antibacterial	Ibrahim <i>et al.</i> (2010b)
Polyethersulfone	TiO_2	UPF	Antibacterial and self-cleaning	Mihailović <i>et al.</i> (2010)
PET	Ag/ TiO_2 nanocomposite	Diffuse reflectance spectra	Antibacterial, self-cleaning, and anti-staining	Dastjerdiā <i>et al.</i> (2010)
Wool	TiO_2	Diffuse reflectance spectra	-	Montazer and Pakdel (2010)
PET/wool (45:55) blend	TiO_2	Diffuse reflectance spectra	Antibacterial and self-cleaning	Montazer and Seifollahzadeh (2011)
Cotton	ZnO	Diffuse reflectance spectra	-	Y. Li <i>et al.</i> (2011)
Cotton or viscose	Monochlorotriazine- β -cyclodextrin, Neem seed oil and Dyes (<i>Reactive Red 120</i> , <i>Reactive Red 141</i> , <i>Reactive Blue 160</i> , <i>Reactive Red 195</i> or <i>Reactive Red 198</i>)	UPF	Antibacterial	Ibrahim <i>et al.</i> (2011)
Nylon	TiO_2	Diffuse reflectance spectra	Antibacterial	Pant <i>et al.</i> (2011)
Polyethersulfone	TiO_2	UPF	Antibacterial and self-cleaning	Mihailović <i>et al.</i> (2011)
PET	SiO_2 -coated ZnO	Transmittance spectra	Waterproofing	Xue <i>et al.</i> (2011)
Cotton	Al	UPF	Waterproofing	Pan <i>et al.</i> (2012)
Cotton	ZnO	Transmittance spectra	Waterproofing and self-cleaning	Ates and Unalan (2012)
Cotton	SiO_2 -coated TiO_2 and Dye (<i>Bezaktiv Red S-3B 150</i>)	UPF	-	Fakin <i>et al.</i> (2012)
Cotton	ZnO	UPF	Antibacterial and self-cleaning	Çakir <i>et al.</i> (2012)
Cotton	Ag	UPF	Antibacterial and waterproofing	Shateri-Khalilabad and Yazdanshenas (2013a)
Cotton	ZnO	Transmittance spectra	-	Y. Li <i>et al.</i> (2012)

PET: Polyethylene terephthalate.

Table 1b. Examples of UV-protective compound-containing textile fibers described in scientific literature between 2013-2016.

Textile fiber composition	UV-protective compound	Assessment method of the UV shielding performance	Additional fabric properties	Reference
Cotton	Mg ₂ Al-LDH intercalated with 2-hydroxy-4-methoxybenzophenone-5-sulfonate anions	UPF	Waterproofing	Zhao <i>et al.</i> (2013)
PET	SiO ₂ -coated ZnO	Transmittance spectra	Waterproofing	Xue <i>et al.</i> (2013)
Cotton	ZnO	UPF	Bacterial inhibition	Shateri-Khalilabad and Yazdanshenas (2013b)
Cotton	ZnO	UPF	Antibacterial	Zhang <i>et al.</i> (2013)
PET	TiO ₂	Transmittance spectra	-	Nazari <i>et al.</i> (2013)
Cotton	TiO ₂	Diffuse reflectance spectra	Self-cleaning	Sadr and Montazer (2014)
Cotton	TiO ₂ , ZnO or CuO	UPF	-	Emam and Bechtold (2015)
Cotton	Graphene/polyurethane composite	UPF	Electrical conductivity and far-infrared emission	Hu <i>et al.</i> (2015)
Cotton	Ag	UPF	Antibacterial and waterproofing	Nateghi and Shateri-Khalilabad (2015)
PET	TiO ₂ /carbon nanotubes or TiO ₂ /nanocarbon black nanocomposites	Diffuse reflectance spectra	Electrical conductivity	Chimeh and Montazer (2016)
Cotton	Graphene oxide/Fe ₃ O ₄ nanocomposite	UPF	Antibacterial, electrical conductivity and magnetic properties	Mirjalili (2016)
Cotton	Graphene oxide/Chitosan composite	UPF	-	Tian <i>et al.</i> (2016)
Cotton	Ag/AgBr-TiO ₂ nanocomposite	UPF	Antibacterial	Rana <i>et al.</i> (2016)
PET	Graphene oxide/SnO ₂ nanocomposite	UPF	Electrical conductivity	Babaahmadi and Montazer (2016)
Cotton	ZnO/Chitosan nanocomposite	UVA and UVB blocking percentages	Antibacterial	Raza <i>et al.</i> (2016)

PET: Polyethylene terephthalate.

Table 1c. Examples of UV-protective compound-containing textile fibers described in scientific literature between 2017 and 2018.

Textile fiber composition	UV-protective compound	Assessment method of the UV shielding performance	Additional fabric properties	Reference
Cotton	ZnO	UPF	Self-cleaning	Thi and Lee (2017)
Cotton or Silk	MIL-MOFs* (MIL-68(In)-NH ₂ or MIL-125(Ti)-NH ₂)	UPF	-	Emam and Abdelhameed (2017)
Polyamine 6	TiO ₂	UPF	Antibacterial, self-cleaning, and waterproofing	Zhou <i>et al.</i> (2017)
Cotton	TiO ₂ and Ag	UPF	Antibacterial	S. Li <i>et al.</i> (2017)
Cotton	<i>Aloe vera</i> [#] /Chitosan nanocomposite	UPF	Antibacterial and waterproofing	Subramani <i>et al.</i> (2017)
Cotton	Au	UPF	Antibacterial	Tang <i>et al.</i> (2017)
PET	CuO	UV protection enhancement	Antibacterial and self-cleaning	Rezaie <i>et al.</i> (2017a)
Wool	CuO	UV protection enhancement	Antibacterial	Rezaie <i>et al.</i> (2017b)
PET	CuO	UV protection enhancement	Antibacterial and ammonia sensing	Rezaie <i>et al.</i> (2017c)
Cotton/nylon (50:50) blend	Graphene oxide	Diffuse reflectance spectra	Antibacterial, antifungal, and electrical conductivity	Hasani and Montazer (2017a)
Cotton/nylon (50:50) blend	Graphene oxide	Diffuse reflectance spectra	Antibacterial and electrical conductivity	Hasani and Montazer (2017b)
Cotton	TiO ₂ /SiO ₂ nanocomposite	UPF	Waterproofing	Xu <i>et al.</i> (2018)
Cotton	ZnO	UPF	Gas sensor	Subbiah <i>et al.</i> (2018)
Cotton	ZnO	UPF	Antibacterial	El-Naggar <i>et al.</i> (2018)
Cotton	Polyvinylsilsesquioxane/ZnO composite	UPF	Antibacterial and waterproofing	Mai <i>et al.</i> (2018)
PET	SiO ₂ , ZnO, TiO ₂ or ZrO	UPF	Antibacterial and self-cleaning	Ibrahim <i>et al.</i> (2018)
Cotton	Polyoxotitanate (Ti ₁₈ Mn ₄ O ₃₀ (OEt) ₂₀ Phen ₃)	Diffuse reflectance spectra	Antibacterial and waterproofing	N. Li <i>et al.</i> (2018)
Cotton	TiO ₂	UPF	Waterproofing	D. Chen <i>et al.</i> (2018)
Wool	<i>Cinnamomum camphora</i> extracts	UPF	Antibacterial	Khan <i>et al.</i> (2018)
Cotton	TiO ₂	UPF	-	Morshed <i>et al.</i> (2018)
PET	3,4-ethylene dioxythiophene polymer (PEDOT)/Fe ₃ O ₄ composite	Transmittance spectra	Antibacterial, electrical conductivity, microwave attenuation, and magnetic properties	Sedighi <i>et al.</i> (2018)
Wool	Marigold (<i>Tagetes erecta</i>) flower extract	UPF	Antioxidant	Shabbir <i>et al.</i> (2018)

PET: Polyethylene terephthalate. * MIL: Materials Institute Lavoisier. MOF: metal-organic framework. # Natural herbal nanoparticles prepared from shade-dried *Aloe vera* plant.

Table 1d. Examples of UV-protective compound-containing textile fibers described in scientific literature between 2019 and 2021.

Textile fiber composition	UV-protective compound	Assessment method of the UV shielding performance	Additional fabric properties	Reference
Cotton	BiPO ₄	UPF	Self-cleaning	Jin <i>et al.</i> (2019)
Silk	ZnO	UPF	Waterproofing	Huang <i>et al.</i> (2019)
Cotton	ZnO	UPF	-	X. Wang <i>et al.</i> (2019)
Cotton, Aramid or PET	MOF (<i>InOF-1</i>)	UPF	-	G.-P. Li <i>et al.</i> (2020)
Cotton	MOFs (<i>Cu-BTC</i> , <i>ZIF-8</i> or <i>ZIF-67</i>)	UPF	Noise reduction	Zhang <i>et al.</i> (2020)
PET	MO _x /polyvinylidene fluoride/Chitosan composite (MO _x = ZnO, TiO ₂ or SiO ₂)	UPF	-	Bouazizi <i>et al.</i> (2020)
Cotton	MOFs (<i>ZIF(Ni)</i> , <i>ZIF-8(Zn)</i> or <i>ZIF-67(Co)</i>)	UPF	Antibacterial	Emam <i>et al.</i> (2020)
Cotton	ZnO	UPF	Waterproofing	Khan <i>et al.</i> (2020)
Silk	Graphene oxide	UPF	Antibacterial	S.-D. Wang <i>et al.</i> (2020)
Cotton	ZnO	UPF	Antibacterial	Noorian <i>et al.</i> (2020)
Cotton	TiO ₂ and hollow glass microspheres	UPF	Thermal insulation, flame retardancy and noise reduction	Pakdel <i>et al.</i> (2020)
Cotton	TiO ₂	Transmittance spectra	Waterproofing and self-cleaning	Suryaprabha and Sethuraman, (2021)
Wool	TiO ₂ /Ce or ZnO/Ce nanocomposite	Transmittance spectra	Antibacterial and self-cleaning	Zohoori <i>et al.</i> (2021)
Cotton	TiO ₂	UPF	-	Riaz <i>et al.</i> (2021)
Wool	Se	UV protection enhancement	Antibacterial and antifungal	Razmkhah <i>et al.</i> (2021)
Cotton	Ag	UPF	Antibacterial	Čuk <i>et al.</i> (2021)

PET: Polyethylene terephthalate. MOF: metal-organic framework.

3. UV-protective compound-containing smart fabrics

The growing request for UV-protective textiles, especially for clothes manufacturing, has driven scientific studies about textile fibers with UV shielding properties. Therefore, incorporation, coating and/or anchorage of metal oxides, dyes, organic filters, graphene compounds, metal-organic frameworks (MOFs), coordination compounds, metal nanoparticles or composites in the fiber surface are widely related in the recent literature (Table 1a–d). Several different synthetic methods have been used to produce these textile fibers, including pad-dry-cure (Z. Chen and Yin, 2010), electrospinning (Pant *et al.* 2011), hydrothermal (Y. Li *et al.*, 2011), microwave (Y. Li *et al.*, 2012; Thi and Lee, 2017), microwave assisted hydrothermal (Ates and Unalan, 2012), simple spray coating (Rana *et al.*, 2016), electrostatic layer-by-layer self-assembly approach (Zhao *et al.*, 2013), solid-phase hot-pressing procedure (G.-P. Li *et al.*, 2020) and dip-pad-cure (Ibrahim *et al.*, 2010b). Among them, the pad-dry-cure method is the most used due to the easier synthetic procedures and high-efficiency fiber coating. In the pad-dry-cure process, fabrics are soaked in UV-protective compound solution or suspension under specific conditions, e.g., liquor to fabric ratio. Then, fabric specimens are padded through two dips and two nips using a padding machine. After padding step, fabrics are dried and cured at specific temperatures and times, which are based on fabric properties. Regardless of experimental method and/or fiber type used, UV-protective compounds incorporated, coated and/or anchored improve UV-blocking properties of textile fabrics (Fig. 4) as proven by UV-VIS spectroscopic measurements, e.g., *in vitro* UV protection factor (UPF) assessment. Moreover, these UV-protective compounds can promote other beneficial functions to textile fibers such as antibacterial and self-cleaning properties (Table 1a–d). In so many cases, a superhydrophobic coating in the textile fibers is also made to provides waterproofing (Table 1a–d). It is important to highlight that multifunctional textile fibers give rise smart fabrics, which offer new insights to clothing manufacturing.

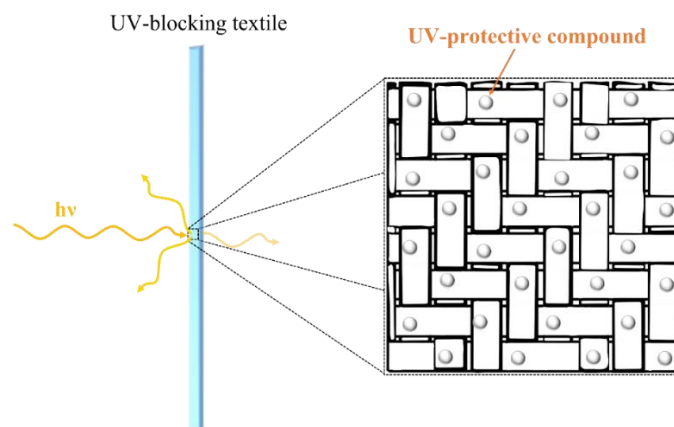


Figure 4. Schematic representation of a UV-protective compound-containing smart fabric.

3.1 TiO_2

Titanium oxide is a commercial inorganic filter commonly used in skin care products due to its UV absorption capacity (Abuçafy *et al.*, 2016; Seixas and Serra, 2014) and low skin toxicity (Abuçafy *et al.*, 2016). Besides UV shielding ability, TiO_2 exhibits photocatalytic activity that enable its use in self-cleaning systems (Banerjee *et al.*, 2015). According to the literature (Yadav *et al.*, 2016), this metal oxide also has antibacterial properties. For these reasons, TiO_2 -containing textile fibers have attracted considerable interest in the field of smart fabrics.

Mihailović *et al.* (2010; 2011), in two different scientific research publications, investigated the multifunctional properties of polyethersulfone (PES) fabrics loaded with TiO_2 prepared by oxygen, argon or air RF plasma or corona discharge pretreatment and subsequent dip-pad-cure process with titanium oxide. On both studies, oxygen, argon or air RF plasma and corona discharge pretreatments of PES fibers induced the enhanced deposition of TiO_2 nanoparticles ensuring excellent self-cleaning properties, UV protection and antibacterial activity. Considering UV blocking efficiency of PES fabrics obtained, high UPF values (UPF > 66) were reached and retained after five laundering cycles. The washing procedure used in the laundering durability test can be summarized as follows: the PES fabrics were washed in the bath containing 0.5% Felosan RG-N (Bezema) at liquor-to-fabric ratio of 40:1. After 30 min of washing at 40 °C, fabrics were rinsed once with warm water (40 °C) for 3 min and three times (3 min) with cold water. Subsequently, fabrics were dried at 70 °C.

Montazer and Pakdel (2010) reported the UV-blocking ability of TiO_2 -containing wool textiles obtained by ultrasonic bath method. The TiO_2 -protective

layer on fabric surface provided higher UV absorption in the 300-350 nm region. Moreover, the increase of the amount of TiO₂ on wool surface enhanced the UVB blocking capacity and decreased the UV photodegradation of wool fibers, i.e., photoyellowing of wool textile. In other scientific publication, [Montazer and Seifollahzadeh \(2011\)](#) prepared multifunctional textiles through enzymatic pretreatment of polyester/wool blend followed by the fiber coating with TiO₂ nanoparticles. These textile materials also exhibited higher UVB blocking ability and showed self-cleaning and antibacterial properties.

[Pant et al. \(2011\)](#) successfully prepared an electrospun nylon-6 spider-net like nanofiber mats containing TiO₂ nanoparticles. The addition of a small amount of TiO₂ NPs improved the hydrophilicity and mechanical strength of nylon-6 nanofiber mats and gave rise to antibacterial and UV blocking properties.

[Nazari et al. \(2013\)](#) developed UV-blocking polyester fabrics using TiO₂ as inorganic filter and polysiloxane as cross-linkable agent. The polysiloxane agent promoted the enhance of TiO₂ nanoparticles absorption and stabilized them on the polyester fiber surface. Consequently, the nano-TiO₂/polysiloxane coating improved the UV-blocking features of polyester fabrics as seen in UV-VIS transmission spectra.

[Zhou et al. \(2017\)](#) reported a facile and eco-friendly way to prepare a novel hybrid polyamine/nano TiO₂ fabric by a combination of UV irradiation and ultrasonic bath method. The research results indicated that TiO₂ were fixed on the fiber surface providing photocatalytic, antibacterial, UV blocking and superhydrophobic properties to polyamine fabrics. UPF values equal to 56 and 1123 were obtained.

[Sadr and Montazer \(2014\)](#), [Emam and Bechtold \(2015\)](#), [D. Chen et al. \(2018\)](#), [Morshed et al. \(2018\)](#), [Suryaprabha and Sethuraman \(2021\)](#) and [Riaz et al. \(2021\)](#) investigated the UV blocking properties of TiO₂-containing cotton fabrics. [Sadr and Montazer \(2014\)](#) reported the multifunctional features of TiO₂ nanoparticles coated cotton fabrics obtained by *in situ* sonosynthesis method. The sonochemical method had no negative influence on cotton fabric fibers and provided the formation of the nano-TiO₂ coating on the textile surface that led to UV-blocking and self-cleaning properties. Moreover, UV-protection rating of these cotton fabrics maintained even after 25 home launderings indicating an excellent washing durability. [Emam and Bechtold \(2015\)](#) immobilized TiO₂, ZnO or CuO particles into cotton and oxidized cotton fabrics by using pad-dry-cure method. The surface interactions between carboxylate groups of cotton fibers and metal oxides, mainly TiO₂, provided the enhancement of the

UV shielding capacity of cotton fabrics as seen in UV-VIS transmittance spectra and *in vitro* UPF values. [D. Chen et al. \(2018\)](#) developed UV-blocking, superhydrophobic and robust cotton fabrics by combination of polyvinylsilsesquioxane (PVS) and nano-TiO₂. Based on structural, thermal, mechanical, and spectroscopic results, the improvement on the UV protection, water repellency and rigidity of the fabrics were attributed to the synergism between the PVS polymer and nano-TiO₂. [Morshed et al. \(2018\)](#) reported to sonochemical synthesis of TiO₂ nanoparticles in cotton fibers via low temperature sol-gel technique. Ultrasonication time, ultrasonic power, and concentration of tetrabutyl titanate affected on UPF values of cotton fabrics. [Suryaprabha and Sethuraman \(2021\)](#) prepared multifunctional cotton fabrics based on the deposition of TiO₂ sol followed by surface modification using stearic acid (STA). STA-TiO₂ cotton fabrics exhibited UV-blocking ability and self-cleaning properties. Moreover, these superhydrophobic fabrics showed chemical durability and mechanical stability. Finally, [Riaz et al. \(2021\)](#) reported to the fabrication of cotton fabrics with TiO₂ nanoparticles modified with two different silane coupling agents using pad-dry-cure method. The presence of modified nanoparticles in the fiber surface improved the UV-blocking performance causing minimum effect on inherent properties of cotton textiles, e.g., sensorial comfort.

[Fakin et al. \(2012\)](#) investigated the SiO₂ coated TiO₂ particles performance in reactive dyeing of cotton fabrics. The incorporation of synthesized particles into the dyeing with reactive dyes brought about an outstanding UV blocking ability of the dyed fabrics even after 15 laundering cycles without considerable negative impact on color and comfortable properties. Washing process was performed according to the [BS EN ISO 105-C06:2010 \(2010\)](#) standard. UV protection, comfort, and dyeing properties of cotton fabrics were directly associated to dyeing temperature and amount of dye and SiO₂ coated TiO₂ particles.

[S. Li et al. \(2017\)](#) reported to the development of multifunctional cotton fabrics obtained by hydrothermal deposition of TiO₂ particles onto fiber surface followed by *in situ* deposition of Ag nanoparticles via reduction method. These fabrics exhibited high antibacterial activity with an inhibition rate higher than 99% against *Staphylococcus aureus* and *Escherichia coli* bacteria. Moreover, UPF values between 35 and 57 confirmed the UV-blocking capacity of them. Using a different two-step coating approach, [Pakdel et al. \(2020\)](#) prepared cotton fabrics coated with TiO₂ and hollow glass microspheres (HGMs). The presence of TiO₂ layer on cotton fibers gave rise to an excellent UV-blocking

activity as proved by UPF values higher than 190. In addition, HGMs coating reduced the inflammability of cotton fabrics and improved their thermal resistance and sound absorption capacity. Therefore, these TiO_2 + HGMs coated cotton fabrics exhibited multifunctional properties, i.e., UV-blocking ability, thermal insulation, flame retardancy and acoustic performance. It is important to highlighting that noise is considered a health hazard (Münzel *et al.*, 2020) and it is required to be eliminated for a better performance of humans in different areas (Pakdel *et al.*, 2020).

In different scientific publications, Dastjerdia *et al.* (2010), Rana *et al.* (2016), Chimeh and Montazer (2016), Xu *et al.* (2018), Bouazizi *et al.* (2020) and Zohoori *et al.* (2021) reported the development of UV-protective fabrics with different nanocomposites based on TiO_2 . Dastjerdia *et al.* (2010) investigated the multifunctional properties of Ag/TiO_2 nanocomposite coated polyester fabrics prepared by pad-dry-cure method. The results revealed that the nanocomposite coating gives a considerable antibacterial, self-cleaning, anti-staining and UV-blocking capacity to polyester textiles. In this scientific paper, authors focused on showing the main results of characterization techniques without in-depth discussions about physic-chemical phenomena involved. In similar scientific research, Rana *et al.* (2016) reported the preparation of multifunctional cotton fabrics with $\text{Ag}/\text{AgBr}-\text{TiO}_2$ nanocomposite coating by simple spray coating process. The results showed that the nanocomposite coating onto cotton fabrics improved textile mechanical properties and gave rise to antibacterial and UV-blocking abilities.

Chimeh and Montazer (2016) prepared polyester fabrics with nano- TiO_2 /carbon nanotubes or nano- TiO_2 /nanocarbon black composites through exhaustion method and post-curing. The composite coating increased the UV blocking capacity of PET textiles as seen in UV-VIS reflectance spectra. Furthermore, nano- TiO_2 /carbon composites imparted photocatalytic activity and electrical conductivity to fabrics. Also, Xu *et al.* (2018) successfully prepared superhydrophobic and UV-protective cotton fabrics by the incorporation of $\text{TiO}_2/\text{SiO}_2$ composite nanoparticles followed by hydrophilization with hexadecyltrimethoxysilane. $\text{TiO}_2/\text{SiO}_2$ composite nanostructures onto fibers made the textiles rougher, which contributed to the formation of superhydrophobic surfaces, and decreased the UV transmittance of cotton fabrics promoting UPF values higher than 80.

Bouazizi *et al.* (2020) reported the design and functionalization of new composite-based PET fibers with UV protection. The fixation of MO_x /polyvinylidene fluoride/Chitosan composite ($\text{MO}_x = \text{TiO}_2, \text{ZnO}$ or SiO_2)

into PET fibers improved both the thermal stability and UV protection of textiles. High UPF values (80.5 – 113.4) of textiles indicated their excellent UV-blocking capacity.

Zohoori *et al.* (2021) prepared wool fabrics coated with TiO_2/Ce or ZnO/Ce nanocomposite coated wool fabrics by ultrasonic method. XRD, EDX and SEM results showed the formation of nanocomposites and indicated a good distribution of them on the wool surface. The wool fabrics coated with TiO_2/Ce or ZnO/Ce nanocomposites showed lower UV transmission percentage than raw wool fabric indicating an improvement on the UV protection. Also, these fabrics exhibited antibacterial and self-cleaning activity.

3.2 ZnO

Zinc oxide is also a commercial inorganic filter widely used in cosmetic formulations and/or self-cleaning systems. Like TiO_2 , zinc oxide has UVB absorption capacity (Flor *et al.*, 2007; Seixas and Serra, 2014), low skin toxicity (Abuçafy *et al.*, 2016), photocatalytic and antibacterial ability (Qi *et al.*, 2017). Consequently, fabric fibers with zinc oxide or nanocomposite based on ZnO have been investigated to provide new insights in UV-protective textile manufacturing.

Y. Li *et al.* (2011) reported the preparation of cotton fabric with ZnO , in which ZnO particles were *in situ* synthesized inside of textile fibers, via two-step hydrothermal method. The results showed that zinc oxide particles were successfully assembled into the lumen and the mesoporous cotton fibers. Therefore, UV-blocking ability of the cotton fabric was significantly improved by assembling ZnO inside the fibers.

Ates and Unalan (2012) investigated to self-cleaning, superhydrophobic and UV-blocking properties of zinc oxide nanowire-containing cotton fabric prepared by microwave assisted hydrothermal method and subsequently functionalized with stearic acid. The results showed the superhydrophobic nature of textile fibers, the decrease of the transmission intensity in UV spectral region and considerable degradation of methylene blue under UV light irradiation, one of the main photodegradation methods to investigate self-cleaning properties.

Çakir *et al.* (2012) successfully prepared ZnO coated cotton fabrics that exhibit UV-blocking, self-cleaning and antibacterial properties. It is important to emphasize that ZnO nanoparticles were synthesized in reverse micelle cores of PS(10912)-b-PAA(3638) copolymer obtained by atom transfer radical polymerization. The ZnO nanoparticles coating onto textile fibers provided

photocatalytic activity on degradation of methylene blue and antibacterial activity against *Escherichia coli* and *Staphylococcus aureus* bacteria. Moreover, ZnO coated cotton fabrics exhibited UPF values greater than 60.

Y. Li *et al.* (2012) investigated UV blocking property and water-wash durability of nano-ZnO assembled cotton fibers obtained by microwave assisted precipitation and crystallization process synchronously *in situ* for the first time. UV-VIS transmission spectra showed an excellent UV-blocking activity in the 225–380 nm region. The water-washing process of nano-ZnO assembled cotton fibers did not change their UV absorption capacity as seen in UV transmission measurements. The water-washing durability test was carried out in a domestic washer (XQB45-846B National, Panasonic), where nano-ZnO assembled cotton textiles were washed with water ($v = 33$ L) for 20, 40 and, 60 min.

Shateri-Khalilabad and Yazdanshenas (2013b) and Zhang *et al.* (2013) successfully prepared smart fabrics via *in situ* synthesis of ZnO on the cotton fiber surface. In both publications, ZnO coated cotton fabric exhibited high UV-blocking ability as proven in UPF values (105.61 [Shateri-Khalilabad and Yazdanshenas, 2013b] and 136 [Zhang *et al.*, 2013]). Moreover, it showed bacterial inhibition (Shateri-Khalilabad and Yazdanshenas, 2013b) or antibacterial (Zhang *et al.*, 2013) activity.

The pad-dry-cure method was used by Raza *et al.* (2016) and El-Naggar *et al.* (2018) in the preparation of cotton fabrics coated with chitosan/ZnO nanocomposites and ZnO nanoparticles, respectively. Nanocomposite (Raza *et al.* 2016) and ZnO (El-Naggar *et al.*, 2018) coated cotton fabrics exhibited antibacterial activity and UV-blocking capacity.

Thi and Lee (2017) reported the development of self-cleaning and UV-blocking cotton fabric with modification of photoactive ZnO coating via microwave method. ZnO coated cotton fabrics synthesized at pH range equal 6–7, 8–9 and 10–11 showed UPF values of 222.52, 162.68 and 202.57, respectively. In addition, these cotton fabrics exhibited excellent self-cleaning ability proved by high removal degree of the coffee stains under UV irradiation at different air humidity levels.

Subbiah *et al.* (2018) successfully prepared nanostructured ZnO modified cotton fabrics via sol-gel and sputter seed layer-coated sol-gel techniques. All modified cotton fabrics exhibited greater UPF values than raw fabric, but the seed layer-initiated sol-gel modified cotton fabric showed the highest UPF value (378). Moreover, these modified cotton fabrics showed

room temperature gas sensing response towards volatile organic compounds enabling their use as gas sensor.

Mai *et al.* (2018) reported the development of multifunctional polyvinylsilsesquioxane/ZnO coated cotton fabrics. Composite coatings improved UV-blocking, superhydrophobic and antimicrobial properties of cotton fabrics compared to the reference textiles. In addition, polyvinylsilsesquioxane/ZnO coatings enhanced the mechanical properties of cotton fabrics and did not compromise their thermal stability.

X. Wang *et al.* (2019) successfully prepared UV-protective fabrics via grafted polymer brushes for *in situ* growth of ZnO on modified cotton fiber using the electroless deposition method. According to the results, the functionalized fabrics exhibited UV blocking properties and wash durability due to the presence of the ZnO on the inner wall of cotton fibers and the polymer-tethered structure.

Khan *et al.* (2020) reported a novel microwave hydrothermal method to grow aligned ZnO nanorods on cotton fibers. The ZnO coated cotton fabrics obtained showed greater UPF values than pristine cotton fabric, which indicated that ZnO nanorods improved the UV protection of cotton textile. Moreover, the functionalization of ZnO coated cotton fabrics with non-fluorinated silane provided superhydrophobic properties and oil–water separation performance.

Noorian *et al.* (2020) prepared antibacterial and UV-blocking fabrics by pretreatment of cotton fibers with 4-aminobenzoic acid (PABA) followed by *in situ* sonochemical synthesis of ZnO nanoparticles. The PABA treatment provided significant sites for the growth of the ZnO nanoparticles and maintained cross-linking property between oxidized cellulosic fibers and the ZnO nanoparticles. Synergistic effects from ZnO and PABA association imparted UPF values higher than 65 and antibacterial activity against *E. coli* and *S. aureus* to the cotton fabrics.

Xue *et al.* (2011; 2013), in two different scientific research publications, investigated the superhydrophobic and UV-blocking properties of PET fabrics coated with ZnO/SiO₂ core/shell particles and hexadecyltrimethoxysilane. The coated PET textiles exhibited superhydrophobic surface and UV-blocking ability as seen in water contact angle and UV-VIS spectroscopy results. In addition, the SiO₂ shell inhibited the photocatalytic activity of ZnO ensuring the superhydrophobicity of PET surfaces when exposure to UV radiation. Huang *et al.* (2019) also investigated the superhydrophobic and UV-blocking properties of silk fabrics prepared by combining a one-step *in situ* synthesis of ZnO nanorods on fiber surface and hydrophobic treatment with n-octadecanethiol. The

presence of ZnO nanorods in the silk fibers increased surface roughness and induced a rise in UPF values of fabrics indicating the improvement of UV-blocking ability. Also, obtained superhydrophobic surface showed mechanical and chemical stability.

3.3 Graphene compounds

Singular properties of graphene compounds described in the recent literature (Tiwari *et al.*, 2018) explain their several multifunctional applications in different systems and/or devices. In the smart fabric field, UV-blocking, electrical conductivity and/or antibacterial activity are mainly graphene compound properties investigated in the last scientific publications (Babaahmadi and Montazer, 2016; Hasani and Montazer, 2017a; b; Hu *et al.*, 2015; Mirjalili, 2016; Tian *et al.*, 2016; S.-D. Wang *et al.*, 2020). Electrically conducting textiles produce clothes with static dissipation, anti-spark and electromagnetic interference shielding (Varesano and Tonin, 2008) that can be used in the smart clothing design, e.g., innovative sportswear.

Hu *et al.* (2015) prepared multifunctional cotton fabrics coated with graphene and waterborne anionic aliphatic polyurethane composites by pad-dry-cure method. Graphene/polyurethane coatings significantly enhanced the UPF values indicating high UV-blocking capacity of cotton fabrics. In addition, graphene/polyurethane coated cotton fabrics exhibited far-infrared emissivity up to 0.911 in the wavelength range of 4–18 μm and lower electrical resistivity than pristine cotton fabric. Far-infrared emitting fabrics are commonly used in health care and therapeutic clothing manufacturing because the far-infrared radiation (6–15 μm) promotes the enhancement of blood microcirculation and metabolism (Vatansever and Hamblin, 2012).

Mirjalili (2016) investigated the UV-blocking, electrical conductivity, magnetic and antibacterial properties of the reduced graphene oxide/Fe₃O₄ nanocomposite coated cotton fabric. UV-blocking ability of the nanocomposite coated cotton fabric was proved by the increase of the UPF value compared to raw cotton textile. This fabric also displayed a low electrical resistivity, antibacterial activity, and magnetic properties.

Tian *et al.* (2016) successfully prepared cotton fabrics coated with graphene oxide and chitosan by the electrostatic layer-by-layer self-assembly approach. These fabrics showed higher UPF values than control cotton fabric and washing durability even after 10 times water laundering. It is important to emphasize that the water laundering durability test of cotton fabrics was

performed by following the American Association of Textile Chemists and Colorists AATCC 61 (2006).

Babaahmadi and Montazer (2016) investigated electrical conductivity and UV-blocking properties of reduced graphene oxide/SnO₂ nanocomposite coated PET textile obtained by modified exhaustion method. Electrical resistivity decreased and UPF value increased with reduced graphene oxide/SnO₂ nanocomposite coating of PET fibers, which indicated the formation of an electroconductive and UV blocking textile. Moreover, electrical resistivity and UV-blocking results demonstrated the good durability of nanocomposites on surface of PET fabrics after 10 washes with deionized water.

In different scientific papers, Hasani and Montazer (2017a; b) reported the multifunctional properties of reduced graphene oxide-coated cotton/nylon fabrics. According to the UV-VIS reflectance results, textile materials showed high UV absorption in the 200–400 nm region indicating their potential as UV-protective fabrics. These fabrics also exhibited lower electrical resistance, antibacterial activity against *Escherichia coli*, *Pseudomonas aeruginosa*, *Staphylococcus aureus* and *Enterococcus faecalis* bacteria and antifungal activity against eukaryotic fungus *C. albicans*.

S.-D. Wang *et al.* (2020) successfully prepared a multifunctional silk fabric by grafting graphene oxide (GO) nanosheet dispersion onto the fabric surface. The silk fabrics modified with GO showed higher UPF values than control silk, which indicated the enhancement of UV-blocking properties. Furthermore, modified silk fabrics exhibited excellent antibacterial activity against *Escherichia coli* and *Staphylococcus aureus* bacteria.

3.4 MOFs

Zhang *et al.* (2020) developed a series of multifunctional textiles prepared via *in situ* modified MOFs nanocrystals on the cotton surface. Based on structural and spectroscopic characterizations, it was confirmed the existence of chemical bonds between MOFs and hydroxyl and/or carboxyl groups belonging to cotton fibers. In addition, a uniform distribution of MOFs nanocrystals in textile surface was observed. The MOFs/cotton textiles exhibited greater UV blocking activity and acoustic absorption performance than blank cotton that demonstrated their potential use as fabrics for UV protection and noise reduction. According to the literature (Münzel *et al.*, 2020), excessive exposure to the noise environment induces adverse cardiovascular effects and mental annoyance.

Emam *et al.* (2020) investigated the multifunctional properties of cotton fabrics with zeolitic imidazole

frameworks (ZIFs). ZIF(Ni), ZIF-8(Zn) and ZIF-67(Co) were *in situ* synthesized into cotton fabrics before or after silicate modification on the fiber surface. When silicate functionalization was performed before the ZIFs formation, the silicate acted as cross-linker between ZIFs and cotton fibers providing the increment of MOFs amount in the fabric surface. Modified cotton fabrics showed higher UPF values than pristine cotton textile and washing durability (AATCC M6, 2010). Also, they exhibited antibacterial activity against *Staphylococcus aureus*, *Bacillus cereus*, *Escherichia coli*, and *Candida albicans* bacteria.

Emam and Abdelhameed (2017) reported the incorporation of MIL-68(In)-NH₂ or MIL-125(Ti)-NH₂ (MIL = Matériaux de l'Institut Lavoisier) into cotton or silk textiles using quite simple and one-pot process to produce UV-blocking textiles. All MIL-MOFs incorporated textiles exhibited UV-blocking activity; however, MIL-MOFs and metal contents in natural fibers influenced on the UPF values obtained. After five washing cycles (AATCC M6, 2010), these textiles showed a slight decrease of UPF values, which proved their laundering durability.

G.-P. Li *et al.* (2020) investigated the UV-blocking properties of InOF-1 coated cotton, polyester or aramid textiles prepared by hot-pressing method. Regardless of textile fiber type used, InOF-1 coating provided a significantly increasing in the UV-blocking performance. Moreover, the interactions between InOF-1 and textile fibers, as proven in FTIR results, enhanced the tensile strength and elongation at break of MOF coated textiles.

3.5 Organic compounds

Ibrahim *et al.* (2010a) investigated the transfer printability and UV blocking properties of polyester-based textiles obtained by pretreatment of polyester fibers and polyester/wool, polyester/cotton, and polyester/viscose blend fibers with monochlorotriazinyl β -cyclodextrin (MCT- β -CD), chitosan or ethylenediamine followed by transfer printing with sublimable disperse dyes. Hydrophobic cavities generated via grafting of MCT- β -CD, amine functional groups incorporated via aminolysis of the polyester and/or chitosan fixed onto textile matrix afforded an improvement of UV-blocking capacity, transfer printing and fastness properties of modified post-printed fabric samples. In other scientific publication, Ibrahim *et al.* (2011) reported the development of multifunctional cotton and viscose fabrics printed with reactive dyes through combined reactive printing and MCT- β -CD loading in one-step followed by subsequent treatment

with Neem oil. The post-treatment with Neem oil provided the improvement of the antibacterial activity of the treated reactive prints without adversely affecting the UV-blocking properties of the final products.

Subramani *et al.* (2017) investigated multifunctional properties of the Aloe vera-chitosan nanocomposite coated cotton fabric prepared by pad-dry-cure method. Cotton fabric coated with herbal nanocomposite exhibited excellent UV-blocking ability (UPF > 52), superhydrophobicity, and antibacterial activity against *Escherichia coli* and *Staphylococcus aureus* bacteria.

In different scientific publications, Khan *et al.* (2018) and Shabbir *et al.* (2018) reported the development of UV-blocking fabrics from natural plant extracts. Khan *et al.* (2018) successfully prepared UV-blocking and antibacterial fabric by wool treatment with aqueous and alkali extracts of *Cinnamomum camphora* leaves. Camphor leaves extract imparted dyeing, UV-blocking and antibacterial properties to wool fabric. Shabbir *et al.* (2018) reported UV-protective and antioxidant finishing of wool fabric dyed with marigold (*Tagetes erecta*) flower extract. Carotenoid compounds of marigold extract are main responsible for UV-blocking and antioxidant properties of this organic dye. Marigold dyed wool fabrics showed UPF values higher than 30 and capacity to capture peroxide reactive species; therefore, dyed fabrics can be used as potential UV-blocking and antioxidant textiles.

3.6 Inorganic compounds, metal nanoparticles, LDH material and coordination compounds

Z. Chen and Yin (2010) investigated the UV-blocking capacity of Eu(III) complex-containing cotton fabrics prepared by pad-dry-cure method. Based on spectroscopic results, Eu(III) complex-cotton fabrics showed higher UPF values than blank cotton fabric and red-light emission. These results are similar to the Eu(III) doped LDH intercalated with cinnamate anions reported by Saito *et al.* (2018). The Eu(III) doped LDH material exhibited UV-shielding ability and low-intensity red emission that could be inducing collagen production (Saito *et al.*, 2018). Thus, Eu(III) complex-containing cotton fabrics can be able to induce the collagen biosynthesis depending on its intensity emission.

Ibrahim *et al.* (2010b) prepared functional finishes of linen-containing fabrics by fiber surface modifications using oxygen or nitrogen plasma followed by subsequent dip-pad-cure process with metal salts, nano-scale metal or metal oxides, ionic dyes, quaternary ammonium salt or antibiotics. The linen-based textile results indicated the loading of metal salts, nano-scale metal or metal

oxides or ionic dyes onto the plasma treated substrates provided antibacterial activity and a remarkable improvement in UV blocking capacity. Moreover, these functional properties were retained even after 10 laundering cycles (AATCC 124, 1996). In other scientific publication, Ibrahim *et al.* (2018) reported the multifunctional properties of PET fibers obtained via premodification with sodium hydroxide followed by coating with SiO₂, TiO₂, ZnO or ZrO₂ nanoparticles using gelatin as a green binding agent. The results showed an improvement on antibacterial, UV blocking, self-cleaning and softness properties of PET fabrics, which are maintained after 15 laundering cycles (AATCC 135, 2000).

In a series of scientific papers (Rezaie *et al.*, 2017a; b; c) Rezaie and coworkers reported the multifunctional properties of CuO-containing wool and/or polyester fabrics. Based on the results of the UV protection enhancement (%) method described by Noorian *et al.* (2015) CuO-containing fabrics exhibited higher UV-blocking ability and self-cleaning activity. In addition, these fabrics showed antibacterial activities toward two pathogen bacteria including *Staphylococcus aureus* as Gram-positive and *Escherichia coli* as Gram-negative bacteria with no adverse effects on human dermal fibroblasts based on MMT cytotoxicity test (Montazer *et al.*, 2015). The CuO-containing PET fabrics also exhibited a rapid and effective colorimetric response for ammonia detection indicating their potential as ammonia sensing.

Zhao *et al.* (2013) successfully prepared cotton fabrics coated with amino-functionalized Mg₂Al-HMBS-LDH (HMBS = 2-hydroxy-4-methoxybenzophenone-5-sulfonate anions) by electrostatic layer-by-layer assembly technique. Based on thermal analyses, intercalated HMBS showed higher thermal stability than HMBS pristine due to host-guest interactions in the interlayer region. All cotton fabrics assembled with amino-functionalized Mg₂Al-HMBS-LDH showed water contact angles greater than 150° suggesting superhydrophobic ability. In addition, these superhydrophobic fabrics exhibited the enhancement of UPF values compared to untreated cotton textile demonstrating UV-blocking capacity.

Sedighi *et al.* (2018) investigated the multifunctional properties of 3,4-ethylene dioxythiophene polymer (PEDOT)/magnetite nanoparticles coated PET fabrics. PEDOT/magnetite nanoparticles coating improved the UV-blocking capacity of PET fabric especially in UVB and UVC regions. This nanoparticle coating also provided significant antibacterial activity against *S. aureus* bacteria, electromagnetic interference (EMI) shielding behavior and superparamagnetic properties. In

this paper, EMI shielding corresponds to microwave attenuation ability of these multifunctional PET fabrics.

N. Li *et al.* (2018) reported a novel coating technique involving *in situ* self-assembly of the polyoxotitanate (POT) cage [Ti₁₈Mn₄O₃₀(OEt)₂₀Phen₃] to fabricate multifunctional cotton fabrics in a single step. The POT cage coating imparted excellent UV-blocking performance (89% blocked at 350 nm), hydrophobicity (water contact angle > 148°) and antibacterial activity (*Escherichia coli*, *Staphylococcus epidermidis*, and *Staphylococcus aureus* bacteria) to cotton fabrics.

Jin *et al.* (2019) successfully prepared bismuth phosphate (BiPO₄) nanorods coated cotton fabrics by two-dip-two-nip technique. Chitosan and acetic acid acted as cross-linking agents between BiPO₄ and cotton fibers as seen in UV-VIS absorption and FTIR results. The coated fabrics exhibited UV-blocking ability confirmed by UPF values greater than blank cotton fabric and self-cleaning activity.

A series of scientific publications (Čuk *et al.*, 2021; Nateghi and Shateri-Khalilabad, 2015; Pan *et al.*, 2012; Razmkhah *et al.*, 2021; Shateri-Khalilabad and Yazdanshenas, 2013a; Tang *et al.*, 2017) reported multifunctional features of metal nanoparticles coated smart fabrics. In this perspective, silver nanoparticles had widely used due to their antibacterial ability. Shateri-Khalilabad and Yazdanshenas (2013a) investigated superhydrophobic, antibacterial, and UV-blocking properties of the silver nanoparticles (AgNPs) coated cotton fabric. AgNPs coating was formed on the cotton surface through an alkali preactivation followed by *in situ* reduction of silver nitrate. Then, AgNPs coated cotton fibers were subjected to superhydrophobic treatment with octyltriethoxysilane (OTES). AgNPs coated cotton fabric showed UPF value equal to 266, water contact angle greater than 150° and shedding angle equal to 8°. Also, coated fabric exhibited antibacterial activity against Gram-negative *Escherichia coli* and Gram-positive *Staphylococcus aureus* bacteria.

Nateghi and Shateri-Khalilabad (2015) also investigated multifunctional properties of the silver nanowires (AgNWs) coated cotton fabric prepared by dip-dry method followed by superhydrophobic treatment with Danasytan F 8815. SEM/EDX results indicated a thin and uniform AgNWs coating on the cotton fibers. AgNWs coated cotton fabric also exhibited UV-blocking (UPF > 113), superhydrophobic (water contact angle > 150° and shedding angle < 10°) and antibacterial properties. In other scientific paper about Ag nanoparticles coated textiles, Čuk *et al.* (2021) reported the development of multifunctional fabrics using plant food waste (green tea leaves, avocado seed and pomegranate peel) and alien invasive plant extracts

(Japanese knotweed rhizome, goldenrod flowers and staghorn sumac fruit) as reducing agents for the *in-situ* synthesis of silver nanoparticles in cotton fibers. Regardless of the reducing agent used, all silver nanoparticles containing cotton fabrics showed UPF values above 50 and antibacterial activity against *E. coli* and *S. aureus* bacteria.

Pan *et al.* (2012) successfully prepared a superhydrophobic and UV blocking cotton fabric via sol-gel method and self-assembly using inexpensive and ordinary reagents, aluminum nitrate and sodium stearate. The interactions between aluminum coating and sodium stearate in cotton fabrics was confirmed by XPS results. Cotton fabric treated with 1.5% Al sol and 20 mmol L⁻¹ sodium stearate exhibited excellent hydrophobic properties (water contact angle > 146°) and UV blocking ability (UPF = 164).

In other scientific publication about nanoparticle-containing cotton fabrics, Tang *et al.* (2017) reported the development of gold nanoparticles (AuNPs) coated cotton fabrics prepared by *in situ* synthesis of AuNPs onto fiber surface using a heating method. The localized surface plasmon resonance of the AuNPs imparted the cotton fabric with colors, showing good colorfastness to washing and rubbing. It is important to highlight that the colorfastness to washing and rubbing were evaluated in accordance with Australian Standard AS 2001.4.15–2006 and Australian Standard AS 2001.4.3–1995, respectively. The AuNPs coating improved the UV-blocking ability of cotton textiles and resulted in UV-protective fabrics with remarkable antibacterial activity. In addition, AuNPs coated cotton fabrics exhibited catalytic activity, which did not influence on their dyeing with reactive dyes.

Razmkhah *et al.* (2021) reported the UV-blocking and antibacterial properties of selenium nanoparticles coated wool fabrics. Based on the results of the UV protection enhancement (%) method (Noorian *et al.*, 2015), the coated fabrics exhibited UV-blocking ability. In addition, these fabrics showed reasonable bactericidal and fungicidal performances toward *Escherichia coli*, *Staphylococcus aureus* and *Candida albicans*.

For comparative purposes, Fig. 5 and 6 were made to analyze and discuss the main scientific information of UV-protective compound-containing smart fabrics described above. Thus, Fig. 5 shows the number of scientific publications for each UV-protective compound class presented in the chemical composition of smart fabrics and Fig. 6 illustrates the UV-blocking range of UV-protective compound-containing fabrics. It is important to highlight that UV-blocking range corresponds to the UV-shielding performance of

compound class including specific UV spectral region of each compound.

Analyzing the number of scientific publications about UV-protective compound-containing smart fabrics in the period from 2010 to 2021 (Fig. 5), it is observed that TiO₂, ZnO and nanocomposites based on TiO₂ or ZnO were the most used in the development of UV-blocking fabrics. Probably, low human skin toxicity (Abuçafy *et al.*, 2016) and UV-shielding (Abuçafy *et al.*, 2016; Flor *et al.*, 2007; Seixas and Serra, 2014), self-cleaning (Banerjee *et al.*, 2015; Qi *et al.*, 2017) and antibacterial (Qi *et al.*, 2017; Yadav *et al.*, 2016) properties of these oxides and/or nanocomposites combined with several synthetic methods used to obtain them (Montazer and Pakdel, 2011; Montazer and Amiri, 2014) encouraged this great number of scientific studies. In general, synthetic approaches use low-cost and easy-to-obtain reagents and, depending on the synthetic route, allow to control the morphology, surface, and particle size of TiO₂, ZnO and/or nanocomposites based on TiO₂ or ZnO. Despite the smaller number of scientific papers, other UV-protective compounds, mainly LDH, MOFs and Graphene compounds, demonstrate growing potential to be used in the development of novel smart fabrics due to their new multifunctional features, increasingly reported in the recent literature. Thus, a promise increasing of scientific publications about this type of smart fabrics could be expected.

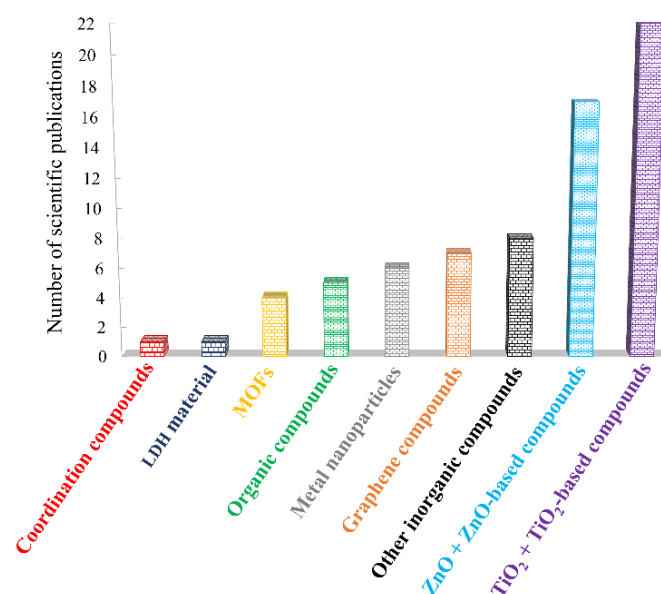


Figure 5. Number of scientific publications of the UV-protective compound-containing smart fabrics per UV-protective compound class in the period from 2010 to 2021.

Another relevant aspect to be considered is that the smart fabrics with LDH, MOFs or graphene compounds exhibited UV-blocking range situated in the UVB and UVA regions (Fig. 6) indicating broad-spectrum action, i.e., capacity to protect the human skin from both UVB and UVA radiation. Organic compounds or metal nanoparticles containing smart fabrics also had same broad-spectrum behavior, while other fabrics showed UVB-blocking capacity (Fig. 6). Therefore, UV-protective compound presented in the textile composition determines the UV radiation region that smart fabrics have higher protection efficiency.

Although organic compounds can undergo decomposition under certain conditions, e.g., high temperature and/or oxidizing environment, the synergistic effects from interactions between these compounds and textile fibers improve their thermal, chemical and/or photochemical stability. Moreover, synergistic properties reduce the fiber photodegradation of smart fabrics. In this perspective, molecular interactions between textile fibers and UV-protective compounds provide specific physicochemical properties to textile materials and ensure lower occurrence of skin allergies by fabric contact.

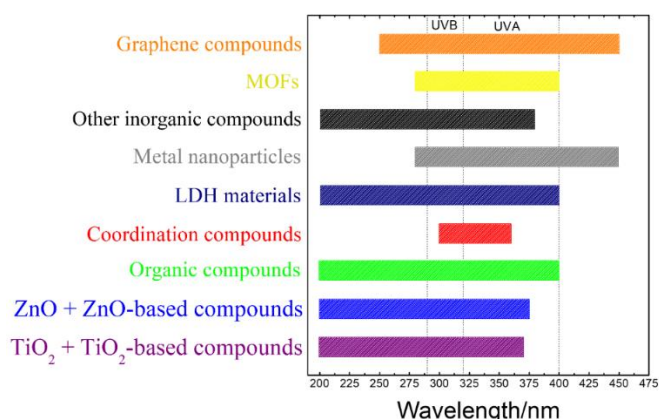


Figure 6. UV-blocking range of the UV-protective compound-containing smart fabrics per compound class.

Besides the UV-blocking range, UPF values are commonly used to indicate the UV protection of smart fabrics. Analogous to sun protection factor (SPF) of sunscreens, UPF is a parameter defined as the ratio of the average effective UV irradiance calculated for unprotected skin to the average effective UV irradiance calculated for skin protected by the smart fabric (Hoffmann *et al.*, 2001). Many scientific publications have shown that UV-VIS spectroscopic measurements are accurate and reproducible *in vitro* test method to determining UPF (Montazer and Amiri, 2014), which is obtained by Eq. 1:

$$UPF = \frac{\int_{290}^{400} E_{\lambda} S_{\lambda} d\lambda}{\int_{290}^{400} E_{\lambda} S_{\lambda} T_{\lambda} d\lambda} \quad (1)$$

where E_{λ} is the relative erythemal spectral effectiveness and S_{λ} is the solar spectral irradiance of the source. The T_{λ} corresponds to spectral transmission of the test fabric as a function of wavelength (λ) and the wavelength integration limits refers to the combined UVB and UVA wavelength range.

According to Hoffmann *et al.* (2001), UPF values between 15 to 24 (ratings 15 and 20, respectively) indicate a good UV-protection, UPFs of 25 to 39 (ratings 20, 30 and 35, respectively) demonstrate a very good UV-protection, and UPFs ≥ 40 correspond to an excellent UV-protection (ratings 40, 45, 50 and 50+). Analyzing the UPF values of scientific publications cited in this review, it is observed that more than 90% of them exhibited UPF values higher than 40. Therefore, smart fabrics had an excellent UV-protection regardless on the UV-protective compound presented in the textile fibers. However, some precautions must be considered in the analysis and interpretation of these UPF results. One of the most important aspects is the UV-VIS transmission measurements, which undergo spectral changes and/or deviations depending on the experimental conditions used and/or optical properties of smart fabrics. In this perspective, opaque and translucent smart fabrics, which exhibit nonlinear behavior of Lambert–Beer law, must be carefully analyzed to avoid mistakes in the interpretation of UPF results.

4. Conclusions

In this review, recent literature on UV-blocking textiles have been reported to give an overview of their importance and prospects in sun-protective methods. UV-protective compounds incorporated, anchored, or coated textile fibers compose a useful class of UV-blocking materials for the development of smart fabrics as proved by the large number of scientific publications in the last years. Different UV-protective compounds, mainly TiO₂ and ZnO, are used to improve UV-blocking ability of fabrics and, often, they also impart to additional fabric properties, e.g., antibacterial, and self-cleaning activities. Analyzing from spectroscopic point of view, the elucidation of UV-blocking mechanisms gives an important information about electronic structure and optical properties of UV-protective textiles; therefore, it can be more investigated and discussed in the literature. A remarkable point is the reduced number of scientific papers that reported the use of organic filters in smart fabrics although these UV-protective compounds have

high UV absorption capacity and, depending on their molecular structure, can interact to fiber surface without the presence of cross-linker compounds. UPF is a good parameter to indicate the UV-blocking ability of UV-protective compound-containing smart fabrics, however, some aspects must be considered in the analyses and interpretation of UPF results. Among them, (i) the amount of the UV-protective compound per textile area, (ii) textile thickness, and (iii) textile properties changed by the incorporation, coating and/or anchorage with UV-protective compounds, e.g., textile roughness. In this perspective, new scientific studies need to be undertaken to know the effective contribution of UV-protective compounds in the UPF values. Considering the growing requirement for simple, cheap, and practical sun-protective products, UV-blocking textiles are one of the best alternatives. Thus, scientific research in the field of smart fabric and/or UV-blocking textile, especially UV-protective compounds incorporated, anchored, or coated textile fibers, must be encourage in order to promote new insights in sun-protective clothing and future applications of multifunctional textiles.

Authors' contribution

Conceptualization: Lupino, J. H. B.; Saito, G. P.; Cebim, M. A.; Davolos, M. R.

Data curation: Lupino, J. H. B.; Saito, G. P.; Cebim, M. A.; Davolos, M. R.

Formal Analysis: Not applicable.

Funding acquisition: Davolos, M. R.

Investigation: Not applicable.

Methodology: Not applicable.

Project administration: Not applicable.

Resources: Not applicable.

Software: Not applicable.

Supervision: Davolos, M. R.

Validation: Lupino, J. H. B.; Saito, G. P.; Cebim, M. A.; Davolos, M. R.

Visualization: Lupino, J. H. B.; Saito, G. P.; Cebim, M. A.; Davolos, M. R.

Writing – original draft: Lupino, J. H. B.

Writing – review & editing: Saito, G. P.; Cebim, M. A.; Davolos, M. R.

Data availability statement

Data sharing is not applicable. In this review, all scientific publications reported were found in the Web of Science™ database (<https://www-webofscience.ez87.periodicos.capes.gov.br>).

Funding

Conselho Nacional de Desenvolvimento Científico e Tecnológico (CNPq). Grant No: 317610/2021.

Conselho Nacional de Desenvolvimento Científico e Tecnológico (CNPq) - Programa Institucional de Bolsas de Iniciação Científica (PIBIC). J.H.B.L. Scholarship No: 1127 – Edital 01/2020.

Acknowledgments

The authors acknowledge the Instituto de Química - Universidade Estadual Paulista (Unesp) for the institutional infrastructure and technical support.

References

AATCC 124. *Appearance of durable press fabrics after repeated home laundering*. American Association of Textile Chemists and Colorists, 1996. <https://law.resource.org/pub/us/cfr/ibr/001/aatcc.tm.124.1996.pdf> (accessed 2021-01-21).

AATCC 135. *Dimensional change*. American Association of Textile Chemists and Colorists, 2000. https://global.ihs.com/doc_detail.cfm?&item_s_key=00157760&item_key_date=991231&input_doc_number=&input_doc_title= (accessed 2021-01-21).

AATCC 61. *Colorfastness to laundering, home and commercial: Accelerated*. American Association of Textile Chemists and Colorists, 2006. https://global.ihs.com/doc_detail.cfm?&input_doc_number=&input_doc_title=&document_name=AATCC%2061&item_s_key=00255811&item_key_date=931231&origin=DSSC (accessed 2021-01-21).

AATCC M6. *Standardization of home laundry test conditions*. American Association of Textile Chemists and Colorists, 2010. https://global.ihs.com/doc_detail.cfm?&input_doc_number=&input_doc_title=&document_name=AATCC%20M6&item_s_key=00490394&item_key_date=891231&origin=DSSC (accessed 2021-01-21).

Abuçafy, M. P.; Manaia, E. B.; Kaminski, R. C. K.; Sarmiento, V. H.; Chiavacci, L. A. Gel based sunscreen containing surface modified TiO₂ obtained by sol-gel process: Proposal for a transparent UV inorganic filter. *J. Nanomater.* **2016**, *2016*, 8659240. <https://doi.org/10.1155/2016/8659240>

Ahmedova, A.; Mantareva, V.; Enchev, V.; Mitewa, M. 2-Acetyllindan-1,3-dione and its Cu²⁺ and Zn²⁺ complexes as promising sunscreen agents. *Int. J. Cosmet. Sci.* **2002**, *24* (2), 103–110. <https://doi.org/10.1046/j.1467-2494.2002.00126.x>

Alebeid, O. K.; Zhao, T. Review on: Developing UV protection for cotton fabric. *J. Text. Inst.* **2017**, *108* (12), 2027–2039. <https://doi.org/10.1080/00405000.2017.1311201>

- Antoniou, C.; Kosmadaki, M. G.; Stratigos, A. J.; Katsambas, A. D. Sunscreens – What’s important to know. *J. Eur. Acad. Dermatology Venereol.* **2008**, *22* (9), 1110–1119. <https://doi.org/10.1111/j.1468-3083.2007.02580.x>
- Ates, E. S.; Unalan, H. E. Zinc oxide nanowire enhanced multifunctional coatings for cotton fabrics. *Thin Solid Films.* **2012**, *520* (14), 4658–4661. <https://doi.org/10.1016/j.tsf.2011.10.073>
- Babaahmadi, V.; Montazer, M. Reduced graphene oxide/SnO₂ nanocomposite on PET surface: Synthesis, characterization and application as an electro-conductive and ultraviolet blocking textile. *Colloids Surfaces A Physicochem. Eng. Asp.* **2016**, *506*, 507–513. <https://doi.org/10.1016/j.colsurfa.2016.07.025>
- Bagde, A.; Mondal, A.; Singh, M. Drug delivery strategies for chemoprevention of UVB-induced skin cancer: A review. *Photodermatol. Photoimmunol. Photomed.* **2018**, *34* (1), 60–68. <https://doi.org/10.1111/phpp.12368>
- Baker, L. A.; Marchetti, B.; Karsili, T. N. V.; Stavros, V. G.; Ashfold, M. N. R. Photoprotection: extending lessons learned from studying natural sunscreens to the design of artificial sunscreen constituents. *Chem. Soc. Rev.* **2017**, *46* (12), 3770–3791. <https://doi.org/10.1039/C7CS00102A>
- Banerjee, S.; Dionysiou, D. D.; Pillai, S. C. Self-cleaning applications of TiO₂ by photo-induced hydrophilicity and photocatalysis. *Appl. Catal.* **2015**, *176-177*, 396–428. <https://doi.org/10.1016/j.apcatb.2015.03.058>
- Bouazizi, N.; Abed, A.; Giraud, S.; El Achari, A.; Campagne, C.; Morshed, M. N.; Thoumire, O.; El Moznine, R.; Cherkaoui, O.; Vieillard, J.; Le Derf, F. Development of new composite fibers with excellent UV radiation protection. *Phys. E Low-Dimensional Syst. Nanostructures.* **2020**, *118*, 113905. <https://doi.org/10.1016/j.physe.2019.113905>
- BS EN ISO 105-C06:2010. Textiles. Tests for colour fastness Colour fastness to domestic and commercial laundering. International Organization for Standardization, 2010. https://www.en-standard.eu/bs-en-iso-105-c06-2010-textiles-tests-for-colour-fastness-colour-fastness-to-domestic-and-commercial-laundering/?gclid=CjwKCAiAheacBhB8EiwAItVO2-iHqcpqedUsYMAatalfWKiCYHqy7ARvxEnufx5sl3ILFxrU9ntrLBoCEtcQAvD_BwE (accessed 2021-01-21).
- Çakir, B. A.; Budama, L.; Topel, Ö.; Hoda, N. Synthesis of ZnO nanoparticles using PS-b-PAA reverse micelle cores for UV protective, self-cleaning and antibacterial textile applications. *Colloids Surfaces A Physicochem. Eng. Asp.* **2012**, *414*, 132–139. <https://doi.org/10.1016/j.colsurfa.2012.08.015>
- Chau, C.-F.; Wu, S.-H.; Yen, G.-C. The development of regulations for food nanotechnology. *Trends Food Sci. Technol.* **2007**, *18* (5), 269–280. <https://doi.org/10.1016/j.tifs.2007.01.007>
- Chen, Z.; Yin, G. Suitability of a rare earth organic light conversion agent of Eu(III) complex to improve ultraviolet protection properties of cotton fabrics. *Text. Res. J.* **2010**, *80* (18), 1982–1989. <https://doi.org/10.1177/0040517510373631>
- Chen, D.; Mai, Z.; Liu, X.; Ye, D.; Zhang, H.; Yin, X.; Zhou, Y.; Liu, M.; Xu, W. UV-blocking, superhydrophobic and robust cotton fabrics fabricated using polyvinylsilsequioxane and nano-TiO₂. *Cellulose.* **2018**, *25* (6), 3635–3647. <https://doi.org/10.1007/s10570-018-1790-7>
- Chimeh, A. E.; Montazer, M. Fabrication of nano-TiO₂/carbon nanotubes and nano-TiO₂/nanocarbon black on alkali hydrolyzed polyester producing photoactive conductive fabric. *J. Text. Inst.* **2016**, *107* (1), 95–106. <https://doi.org/10.1080/00405000.2015.1012881>
- Costa, M. Nanotecnologia. O que é? *Química Têxtil.* **2012**, *106*, 3–11.
- Čuk, N.; Šala, M.; Gorjanc, M. Development of antibacterial and UV protective cotton fabrics using plant food waste and alien invasive plant extracts as reducing agents for the in-situ synthesis of silver nanoparticles. *Cellulose.* **2021**, *28* (5), 3215–3233. <https://doi.org/10.1007/s10570-021-03715-y>
- Curtzwiler, G. W.; Williams, E.B.; Maples, A. L.; Davis, N.W.; Bahns, T. L.; De Leon, J. E.; Vorst, K. L. Ultraviolet protection of recycled polyethylene terephthalate. *J. Appl. Polym. Sci.* **2017**, *134* (32), 45181. <https://doi.org/10.1002/app.45181>
- Dastjerdia, R.; Montazer, M.; Shahsavan, S. A novel technique for producing durable multifunctional textiles using nanocomposite coating. *Colloids Surf. B.* **2010**, *81* (1), 32–41. <https://doi.org/10.1016/j.colsurfb.2010.06.023>
- El-Naggar, M. E.; Shaarawy, S.; Hebeish, A. A. Multifunctional properties of cotton fabrics coated with in situ synthesis of zinc oxide nanoparticles capped with date seed extract. *Carbohydr. Polym.* **2018**, *181*, 307–316. <https://doi.org/10.1016/j.carbpol.2017.10.074>
- Emam, H. E.; Bechtold, T. Cotton fabrics with UV blocking properties through metal salts deposition. *Appl. Surf. Sci.* **2015**, *357* (Part B), 1878–1889. <https://doi.org/10.1016/j.apsusc.2015.09.095>
- Emam, H. E.; Abdelhameed, R. M. Anti-UV radiation textiles designed by embracing with nano-MIL (Ti, In)-metal organic framework. *ACS Appl. Mater. Interfaces.* **2017**, *9* (33), 28034–28045. <https://doi.org/10.1021/acsami.7b07357>
- Emam, H. E.; Darwesh, O. M.; Abdelhameed, R. M. Protective cotton textiles via amalgamation of cross-linked zeolitic imidazole frameworks. *Ind. Eng. Chem. Res.* **2020**, *59* (23), 10931–10944. <https://doi.org/10.1021/acs.iecr.0c01384>
- Fakin, D.; Veronovski, N.; Ojstršek, A.; Božič, M. Synthesis of TiO₂-SiO₂ colloid and its performance in reactive dyeing of cotton fabrics. *Carbohydr. Polym.* **2012**, *88* (3), 992–1001. <https://doi.org/10.1016/j.carbpol.2012.01.046>

- Faure, B.; Salazar-Alvarez, G.; Ahniyaz, A.; Villaluenga, I.; Berriozabal, G.; De Miguel, Y. R.; Bergström, L. Dispersion and surface functionalization of oxide nanoparticles for transparent photocatalytic and UV-protecting coatings and sunscreens. *Sci. Technol. Adv. Mater.* **2013**, *14* (2), 023001. <https://doi.org/10.1088/1468-6996/14/2/023001>
- Ferreira, A. J. S.; Ferreira, F. B. N.; Oliveira, F. R. Têxteis inteligentes: Uma breve revisão da literatura. *REDIGE.* **2014**, *5* (1), 1–22.
- Flor, J.; Davolos, M. R.; Correa, M. A. Protetores solares. *Quim. Nova.* **2007**, *30* (1), 153–158. <https://doi.org/10.1590/S0100-40422007000100027>
- Forestier, S. Rationale for sunscreen development. *J. Am. Acad. Dermatol.* **2008**, *58* (5), S133–S138. <https://doi.org/10.1016/j.jaad.2007.05.047>
- Fourtanier, A.; Moyal, D.; Seite, S. UVA filters in sun-protection products: regulatory and biological aspects. *Photochem. Photobiol.* **2012**, *11* (1), 81–89. <https://doi.org/10.1039/c1pp05152k>
- Franco, J. G.; Ataíde, J. A.; Ferreira, A. H. P.; Mazzola, P. G. Lamellar compounds intercalated with anions with solar protection function: A review. *J. Drug Deliv. Sci. Technol.* **2020**, *59*, 101869. <https://doi.org/10.1016/j.jddst.2020.101869>
- Frizzo, M. S.; Feuser, P. E.; Berres, P. H.; Ricci-Júnior, E.; Campos, C. E. M.; Costa, C.; Araújo, P. H. H.; Sayer, C. Simultaneous encapsulation of zinc oxide and octocrylene in poly (methyl methacrylate-co-styrene) nanoparticles obtained by miniemulsion polymerization for use in sunscreen formulations. *Colloids Surf., A Physicochem. Eng. Asp.* **2019**, *561*, 39–46. <https://doi.org/10.1016/j.colsurfa.2018.10.062>
- Giokas, D. L.; Salvador, A.; Chisvert, A. UV filters: From sunscreens to human body and the environment. *TrAC - Trends Anal. Chem.* **2007**, *26* (5), 360–374. <https://doi.org/10.1016/j.trac.2007.02.012>
- Hasani, M.; Montazer, M. Electro-conductivity, bioactivity and UV protection of graphene oxide-treated cellulosic/polyamide fabric using inorganic and organic reducing agents. *J. Text. Inst.* **2017a**, *108* (10), 1777–1786. <https://doi.org/10.1080/00405000.2017.1286700>
- Hasani, M.; Montazer, M. Cationization of cellulose/polyamide on UV protection, bio-activity, and electro-conductivity of graphene oxide-treated fabric. *J. Appl. Polym. Sci.* **2017b**, *134* (44), 45493. <https://doi.org/10.1002/app.45493>
- Hoffmann, K.; Laperre, J.; Avermaete, A.; Altmeyer, P.; Gambichler, T. Defined UV protection by apparel textiles. *Arch. Dermatol.* **2001**, *137* (8), 1089–1094.
- Hu, X.; Tian, M.; Qu, L.; Zhu, S.; Han, G. Multifunctional cotton fabrics with graphene/polyurethane coatings with far-infrared emission, electrical conductivity, and ultraviolet-blocking properties. *Carbon.* **2015**, *95*, 625–633. <https://doi.org/10.1016/j.carbon.2015.08.099>
- Huang, J.; Yang, Y.; Yang, L.; Bu, Y.; Xia, T.; Gu, S.; Yang, H.; Ye, D.; Xu, W. Fabrication of multifunctional silk fabrics via one step in-situ synthesis of ZnO. *Mater. Lett.* **2019**, *237*, 149–151. <https://doi.org/10.1016/j.matlet.2018.11.035>
- Ibrahim, N. A.; El-Zairy, E. M. R.; El-Zairy, M. R.; Khalil, H. M. Improving transfer printing and ultraviolet-blocking properties of polyester-based textiles using MCT- β -CD, chitosan and ethylenediamine. *Color. Technol.* **2010a**, *126* (6), 330–336. <https://doi.org/10.1111/j.1478-4408.2010.00265.x>
- Ibrahim, N. A.; Eid, B. M.; Hashem, M. M.; Refai, R.; El-Hossamy, M. Smart options for functional finishing of linen-containing fabrics. *J. Ind. Text.* **2010b**, *39* (3), 233–265. <https://doi.org/10.1177/1528083709103144>
- Ibrahim, N. A.; Eid, B. M.; El-Zairy, E. R. Antibacterial functionalization of reactive-cellulosic prints via inclusion of bioactive Neem oil/ β CD complex. *Carbohydr. Polym.* **2011**, *86* (3), 1313–1319. <https://doi.org/10.1016/j.carbpol.2011.06.032>
- Ibrahim, N. A.; Eid, B. M.; Khalil, H. M.; Almetwally, A. A. A new approach for durable multifunctional coating of PET fabric. *Appl. Surf. Sci.* **2018**, *448*, 95–103. <https://doi.org/10.1016/j.apsusc.2018.04.022>
- Ioelovich, M.; Leykin, A. Structural investigations of various cotton fibers and cotton celluloses. *Bioresources.* **2008**, *3* (1), 170–177.
- Jabbar, M.; Shaker, K. Textile Raw Materials. In *Textile engineering: An introduction*. Nawab, Y. Ed.; De Gruyter Oldenbourg, 2016; pp 7–24. <https://doi.org/10.1515/9783110413267-004>
- Jaffe, M.; Easts, A. J.; Feng, X. Polyester fibers. In *Thermal analysis of textiles and fibers: The Textile Institute Book Series*. Jaffe, M., Mencil, J. D., Eds.; Woodhead Publishing, 2020; pp 133–150. <https://doi.org/10.1016/B978-0-08-100572-9.00008-2>
- Jain, S. K.; Jain, N. K. Multiparticulate carriers for sun-screening agents. *Int. J. Cosmet. Sci.* **2010**, *32* (2), 89–98. <https://doi.org/10.1111/j.1468-2494.2010.00547.x>
- Jin, J.; Li, N.; Xie, Y. Photocatalysis and UV-blocking properties of cotton fabric functionalized with BiPO₄ nanorods. *J. Eng. Fiber. Fabr.* **2019**, *14*. <https://doi.org/10.1177/1558925019888816>
- Khan, A.; Hussain, M. T.; Jiang, H.; Gul, S. Development of functional wool fabric by treatment with aqueous and alkaline extracts of *Cinnamomum camphora* plant leaves. *J. Nat. Fibers.* **2018**, *17* (4), 472–481. <https://doi.org/10.1080/15440478.2018.1500339>
- Khan, M. Z.; Militky, J.; Baheti, V.; Fijalkowski, M.; Wiener, J.; Voleský, L.; Adach, K. Growth of ZnO nanorods on cotton fabrics via microwave hydrothermal method: effect of size and shape of nanorods on superhydrophobic and UV-blocking properties. *Cellulose.* **2020**, *27* (17), 10519–10539. <https://doi.org/10.1007/s10570-020-03495-x>

- Kockler, J.; Oelgemöller, M.; Robertson, S.; Glass, B. D. Photostability of sunscreens. *J. Photochem. Photobiol. C Photochem. Rev.* **2012**, *13* (1), 91–110. <https://doi.org/10.1016/j.jphotochemrev.2011.12.001>
- Li, Y.; Zou, Y.; Hou, Y. Fabrication and UV-blocking property of nano-ZnO assembled cotton fibers via a two-step hydrothermal method. *Cellulose*. **2011**, *18* (6), 1643–1649. <https://doi.org/10.1007/s10570-011-9600-5>
- Li, Y.; Hou, Y.; Zou, Y. Microwave assisted fabrication of Nano-ZnO assembled cotton fibers with excellent UV blocking property and water-wash durability. *Fibers Polym.* **2012**, *13* (2), 185–190. <https://doi.org/10.1007/s12221-012-0185-x>
- Li, S.; Zhu, T.; Huang, J.; Guo, Q.; Chen, G.; Lai, Y. Durable antibacterial and UV-protective Ag/TiO₂@fabrics for sustainable biomedical application. *Int. J. Nanomedicine*. **2017**, *12*, 2593–2606. <https://doi.org/10.2147/IJN.S132035>
- Li, N.; Pranantyo, D.; Kang, E.-T.; Wright, D. S.; Luo, H.-K. In situ self-assembled polyoxotitanate cages on flexible cellulosic substrates: Multifunctional coating for hydrophobic, antibacterial, and UV-blocking applications. *Adv. Funct. Mater.* **2018**, *28* (23), 1800345. <https://doi.org/10.1002/adfm.201800345>
- Li, G.-P.; Cao, F.; Zhang, K.; Hou, L.; Gao, R.-C.; Zhang, W.-Y.; Wang, Y.-Y. Design of anti-UV radiation textiles with self-assembled metal-organic framework coating. *Adv. Mater. Interfaces*. **2020**, *7* (1), 1901525. <https://doi.org/10.1002/admi.201901525>
- Liu, Y. Chemical composition and characterization of cotton fibers. In *Cotton fiber: Physics, chemistry and biology*. Fang, D. Ed.; Springer, 2018; pp 75–94. https://doi.org/10.1007/978-3-030-00871-0_4
- Mai, Z.; Xiong, Z.; Shu, X.; Liu, X.; Zhang, H.; Yin, X.; Zhou, Y.; Liu, M.; Zhang, M.; Xu, W.; Chen, D. Multifunctionalization of cotton fabrics with polyvinylsilsesquioxane/ZnO composite coatings. *Carbohydr. Polym.* **2018**, *199*, 516–525. <https://doi.org/10.1016/j.carbpol.2018.07.052>
- Mihailović, D.; Šaponjić, Z.; Molina, R.; Puač, N.; Jovančić, P.; Nedeljković, J.; Radetić, M. Improved properties of oxygen and argon RF plasma-activated polyester fabrics loaded with TiO₂ nanoparticles. *ACS Appl. Mater. Interfaces*. **2010**, *2* (6), 1700–1706. <https://doi.org/10.1021/am100209n>
- Mihailović, D.; Šaponjić, Z.; Molina, R.; Radoičić, M.; Esquena, J.; Jovančić, P.; Nedeljković, J.; Radetić, M. Multifunctional properties of polyester fabrics modified by corona discharge/air RF plasma and colloidal TiO₂ nanoparticles. *Polym. Compos.* **2011**, *32* (3), 390–397. <https://doi.org/10.1002/pc.21053>
- Mirjalili, M. Preparation of electroconductive, magnetic, antibacterial, and ultraviolet-blocking cotton fabric using reduced graphene oxide nanosheets and magnetite nanoparticles. *Fibers Polym.* **2016**, *17* (10), 1579–1588. <https://doi.org/10.1007/s12221-016-6689-z>
- Mohammed, U.; Lekakou, C.; Dong, L.; Bader, M. G. Shear deformation and micromechanics of woven fabrics. *Compos. - A: Appl. Sci.* **2000**, *31* (4), 299–308. [https://doi.org/10.1016/S1359-835X\(99\)00081-0](https://doi.org/10.1016/S1359-835X(99)00081-0)
- Mondal, S. Nanomaterials for UV protective textiles. *J. Ind. Text.* **2022**, *51* (4), 5592S–5621S. <https://doi.org/10.1177/1528083721988949>
- Montazer, M.; Pakdel, E. Reducing photoyellowing of wool using nano TiO₂. *Photochem. Photobiol.* **2010**, *86* (2), 255–260. <https://doi.org/10.1111/j.1751-1097.2009.00680.x>
- Montazer, M.; Seifollahzadeh, S. Enhanced self-cleaning, antibacterial and UV protection properties of nano TiO₂ treated textile through enzymatic pretreatment. *Photochem. Photobiol.* **2011**, *87* (4), 877–883. <https://doi.org/10.1111/j.1751-1097.2011.00917.x>
- Montazer, M.; Pakdel, E. Functionality of nano titanium dioxide on textiles with future aspects: Focus on wool. *J. Photochem. Photobiol.* **2011**, *12* (4), 293–303. <https://doi.org/10.1016/j.jphotochemrev.2011.08.005>
- Montazer, M.; Amiri, M. M. ZnO nano reactor on textiles and polymers: ex situ and in situ synthesis, application, and characterization. *J. Phys. Chem. B*. **2014**, *118* (6), 1453–1470. <https://doi.org/10.1021/jp408532r>
- Montazer, M.; Dastjerdi, M.; Azdaloo, M.; Rad, M. M. Simultaneous synthesis and fabrication of nano Cu₂O on cellulosic fabric using copper sulfate and glucose in alkali media producing safe bio-and photoactive textiles without color change. *Cellulose*. **2015**, *22* (6), 4049–4064. <https://doi.org/10.1007/s10570-015-0764-2>
- Morabito, K.; Shapley, N. C.; Steeley, K. G.; Tripathi, A. Review of sunscreen and the emergence of non-conventional absorbers and their applications in ultraviolet protection. *Int. J. Cosmet. Sci.* **2011**, *33* (5), 385–390. <https://doi.org/10.1111/j.1468-2494.2011.00654.x>
- Morshed, M. N.; Shen, X.; Deb, H.; Azad, S. A.; Zhang, X.; Li, R. Sonochemical fabrication of nanocrytalline titanium dioxide (TiO₂) in cotton fiber for durable ultraviolet resistance. *J. Nat. Fibers*. **2018**, *17* (1), 41–54. <https://doi.org/10.1080/15440478.2018.1465506>
- Münzel, T.; Kröller-Schon, S.; Oelze, M.; Gori, T.; Schmidt, F. P.; Steven, S.; Hahad, O.; Rössli, M.; Wunderli, J.-M.; Daiber, A.; Sørensen, M. Adverse cardiovascular effects of traffic noise with a focus on nighttime noise and the new WHO noise guidelines. *Annu. Rev. Public Health*. **2020**, *41*, 309–328. <https://doi.org/10.1146/annurev-publhealth-081519-062400>
- Nateghi, M. R.; Shateri-Khalilabad, M. Silver nanowire-functionalized cotton fabric. *Carbohydr. Polym.* **2015**, *117*, 160–168. <https://doi.org/10.1016/j.carbpol.2014.09.057>

- Nazari, A.; Montazer, M.; Mirjalili, M.; Nazari, S. Polyester with durable UV protection properties through using nano TiO₂ and polysiloxane softener optimized by RSM. *J. Text. Inst.* **2013**, *104* (5), 511–520. <https://doi.org/10.1080/00405000.2012.746577>
- Noorian, S. A.; Hemmatinejad, N.; Bashari, A. One-Pot Synthesis of Cu₂O/ZnO Nanoparticles at present of folic acid to improve UV-protective effect of cotton fabrics. *Photochem. Photobiol.* **2015**, *91* (3), 510–517. <https://doi.org/10.1111/php.12420>
- Noorian, S. A.; Hemmatinejad, N.; Navarro, J. A. R. Ligand modified cellulose fabrics as support of zinc oxide nanoparticles for UV protection and antimicrobial activities. *Int. J. Biol. Macromol.* **2020**, *154*, 1215–1226. <https://doi.org/10.1016/j.ijbiomac.2019.10.276>
- Pakdel, E.; Naebe, M.; Kashi, S.; Cai, Z.; Xie, W.; Yuen, A. C. Y.; Montazer, M.; Sun, L.; Wang, X. Functional cotton fabric using hollow glass microspheres: Focus on thermal insulation, flame retardancy, UV-protection and acoustic performance. *Prog. Org. Coat.* **2020**, *141*, 105553. <https://doi.org/10.1016/j.porgcoat.2020.105553>
- Pan, C.; Shen, L.; Shang, S.; Xing, Y. Preparation of superhydrophobic and UV blocking cotton fabric via sol-gel method and self-assembly. *Appl. Surf. Sci.* **2012**, *259*, 110–117. <https://doi.org/10.1016/j.apsusc.2012.07.001>
- Pant, H. R.; Bajgai, M. P.; Nam, K. T.; Seo, Y. A.; Pandeya, D. R.; Hong, S. T.; Kim, H. Y. Electrospun nylon-6 spider-net like nanofiber mat containing TiO₂ nanoparticles: A multifunctional nanocomposite textile material. *J. Hazard. Mater.* **2011**, *185* (1), 124–130. <https://doi.org/10.1016/j.jhazmat.2010.09.006>
- Parisi, O. I.; Aiello, D.; Casula, M. F.; Puoci, F.; Malivindi, R.; Scrivano, L.; Testa, F. Mesoporous nanocrystalline TiO₂ loaded with ferulic acid for sunscreen and photo-protection: safety and efficacy assessment. *RSC Adv.* **2016**, *6* (87), 83767–83775. <https://doi.org/10.1039/C6RA07653J>
- Parwaiz, S.; Khan, M. M.; Pradhan, D. CeO₂-based nanocomposites: An advanced alternative to TiO₂ and ZnO in sunscreens. *Mater. Express.* **2019**, *9* (3), 185–202. <https://doi.org/10.1166/mex.2019.1495>
- Pettinari, R.; Marchetti, F.; Petrini, A.; Pettinari, C.; Lupidi, G.; Smoleński, P.; Scopelliti, R.; Riedel, T.; Dyson, P. J. From sunscreen to anticancer agent: Ruthenium(II) arene avobenzene complexes display potent anticancer activity. *Organometallics.* **2016**, *35* (21), 3734–3742. <https://doi.org/10.1021/acs.organomet.6b00694>
- Pezzolo, D. B. *Tecidos: História, tramas, tipos e usos*; Editora Senac-São Paulo, 2007.
- Powers, J. M.; Murphy, J. E. J. Sunlight radiation as a villain and hero: 60 years of illuminating research. *Int. J. Radiat. Biol.* **2019**, *95* (7), 1043–1049. <https://doi.org/10.1080/09553002.2019.1627440>
- Qi, K.; Cheng, B.; Yu, J.; Ho, W. Review on the improvement of the photocatalytic and antibacterial activities of ZnO. *J. Alloys Compd.* **2017**, *727*, 792–820. <https://doi.org/10.1016/j.jallcom.2017.08.142>
- Rana, M.; Hao, B.; Mu, L.; Chen, L.; Ma, P.-C. Development of multi-functional cotton fabrics with Ag/AgBr-TiO₂ nanocomposite coating. *Compos. Sci. Technol.* **2016**, *122*, 104–112. <https://doi.org/10.1016/j.compscitech.2015.11.016>
- Raza, Z. A.; Anwar, F.; Ahmad, S.; Aslam, M. Fabrication of ZnO incorporated chitosan nanocomposites for enhanced functional properties of cellulosic fabric. *Mater. Res. Express.* **2016**, *3* (11), 115001. <https://doi.org/10.1088/2053-1591/3/11/115001>
- Razmkhah, M.; Montazer, M.; Rezaie, A. B.; Rad, M. M. Facile technique for wool coloration via locally forming of nano selenium photocatalyst imparting antibacterial and UV protection properties. *J. Ind. Eng. Chem.* **2021**, *101*, 153–164. <https://doi.org/10.1016/j.jiec.2021.06.018>
- Rezaie, A. B.; Montazer, M.; Rad, M. M. Photo and biocatalytic activities along with UV protection properties on polyester fabric through green *in-situ* synthesis of cauliflower-like CuO nanoparticles. *J. Photochem. Photobiol. B, Biol.* **2017a**, *176*, 100–111. <https://doi.org/10.1016/j.jphotobiol.2017.09.021>
- Rezaie, A. B.; Montazer, M.; Rad, M. M. A cleaner route for nanocolouration of wool fabric via green assembling of cupric oxide nanoparticles along with antibacterial and UV protection properties. *J. Clean. Prod.* **2017b**, *166*, 221–231. <https://doi.org/10.1016/j.jclepro.2017.08.046>
- Rezaie, A. B.; Montazer, M.; Rad, M. M. Antibacterial, UV protective and ammonia sensing functionalized polyester fabric through *in situ* synthesis of cuprous oxide nanoparticles. *Fibers Polym.* **2017c**, *18* (7), 1269–1279. <https://doi.org/10.1007/s12221-017-7263-z>
- Riaz, S.; Ashraf, M.; Hussain, T.; Hussain, M. T.; Younus, A.; Raza, M.; Nosheen, A. Selection and optimization of silane coupling agents to develop durable functional cotton fabrics using TiO₂ nanoparticles. *Fibers Polym.* **2021**, *22* (1), 109–122. <https://doi.org/10.1007/s12221-021-9245-4>
- Sadr, F. A.; Montazer, M. In situ sonosynthesis of nano TiO₂ on cotton fabric. *Ultrason. Sonochem.* **2014**, *21* (2), 681–691. <https://doi.org/10.1016/j.ultsonch.2013.09.018>
- Saito, G. P.; Romero, J. H. S.; Cebim, M. A.; Davolos, M. R. Eu(III) doped LDH intercalated with cinnamate anion as multifunctional sunscreens. *J. Lumin.* **2018**, *203*, 160–164. <https://doi.org/10.1016/j.jlumin.2018.06.039>
- Saito, G. P.; Bizari, M.; Cebim, M. A.; Correa, M. A.; Jafelicci Junior, M.; Davolos, M. R. Study of the colloidal stability and optical properties of sunscreen creams. *Eclét. Quím.* **2019**, *44* (2), 26–36. <https://doi.org/10.26850/1678-4618eqj.v44.2.2019.p26-36>

- Saito, G. P.; Matsumoto, A. C. L.; Assis, R. P.; Brunetti, I. L.; Cebim, M. A.; Davolos, M. R. Zn(Ferulate)-LSH systems as multifunctional filters. *Molecules*. **2021**, *26* (8), 2349. <https://doi.org/10.3390/molecules26082349>
- Sambandan, D. R.; Ratner, D. Sunscreens: An overview and update. *J. Am. Acad. Dermatol.* **2011**, *64* (4), 748–758. <https://doi.org/10.1016/j.jaad.2010.01.005>
- Sánchez, J. C. Têxteis inteligentes. *Química Têxtil*. **2006**, *82*, 58–77.
- SEBRAE. Tecidos inteligentes. Resposta Técnica, 2014. [https://bibliotecas.sebrae.com.br/chronus/ARQUIVOS_CHRONUS/bds/bds.nsf/aece3e5bd45d5eeced32418a25f27f56/\\$File/2014_06_30_RT_Maio_Moda_Tecidosinteligentes_pdf.pdf](https://bibliotecas.sebrae.com.br/chronus/ARQUIVOS_CHRONUS/bds/bds.nsf/aece3e5bd45d5eeced32418a25f27f56/$File/2014_06_30_RT_Maio_Moda_Tecidosinteligentes_pdf.pdf) (accessed 2021-01-21).
- Sedighi, A.; Montazer, M.; Mazinani, S. Fabrication of electrically conductive superparamagnetic fabric with microwave attenuation, antibacterial properties and UV protection using PEDOT/magnetite nanoparticles. *Mater. Des.* **2018**, *160*, 34–47. <https://doi.org/10.1016/j.matdes.2018.08.046>
- Seixas, V. C.; Serra, O. A. Stability of Sunscreens Containing CePO₄: Proposal for a New Inorganic UV Filter. *Molecules*. **2014**, *19* (7), 9907–9925. <https://doi.org/10.3390/molecules19079907>
- Serpone, N.; Dondi, D.; Albin, A. Inorganic and organic UV filters: Their role and efficacy in sunscreens and skincare products. *Inorganica Chim. Acta*. **2007**, *360* (3), 794–802. <https://doi.org/10.1016/j.ica.2005.12.057>
- Serre, C.; Busutil, V.; Botto, J.-M. Intrinsic and extrinsic regulation of human skin melanogenesis and pigmentation. *Int. J. Cosmet. Sci.* **2018**, *40* (4), 328–347. <https://doi.org/10.1111/ics.12466>
- Shabbir, M.; Rather, L. J.; Mohammad, F. Economically viable UV-protective and antioxidant finishing of wool fabric dyed with *Tagetes erecta* flower extract: Valorization of marigold. *Ind. Crops Prod.* **2018**, *119*, 277–282. <https://doi.org/10.1016/j.indcrop.2018.04.016>
- Shateri-Khalilabad, M.; Yazdanshenas, M. E. Fabrication of superhydrophobic, antibacterial, and ultraviolet-blocking cotton fabric. *J. Text. Inst.* **2013a**, *104* (8), 861–869. <https://doi.org/10.1080/00405000.2012.761330>
- Shateri-Khalilabad, M.; Yazdanshenas, M. E. Bifunctionalization of cotton textiles by ZnO nanostructures: antimicrobial activity and ultraviolet protection. *Text. Res. J.* **2013b**, *83* (10), 993–1004. <https://doi.org/10.1177/0040517512468812>
- Subbiah, D. K.; Mani, G. K.; Babu, K. J.; Das, A.; Rayappan, J. B. B. Nanostructured ZnO on cotton fabrics – A novel flexible gas sensor & UV filter. *J. Clean. Prod.* **2018**, *194*, 372–382. <https://doi.org/10.1016/j.jclepro.2018.05.110>
- Subramani, K.; Shanmugam, B. K.; Rangaraj, S.; Palanisamy, M.; Periasamy, P.; Venkatachalam, R. Screening the UV-blocking and antimicrobial properties of herbal nanoparticles prepared from *Aloe vera* leaves for textile applications. *IET Nanobiotechnol.* **2017**, *12* (4), 459–465. <https://doi.org/10.1049/iet-nbt.2017.0097>
- Suryaprabha, T.; Sethuraman, M. G. A facile approach for fabrication superhydrophobic and UV-blocking cotton fabrics with self-cleaning properties. *Fibers Polym.* **2021**, *22* (4), 1033–1040. <https://doi.org/10.1007/s12221-021-0648-z>
- Tang, B.; Lin, X.; Zou, F.; Fan, Y.; Li, D.; Zhou, J.; Chen, W.; Wang, X. In situ synthesis of gold nanoparticles on cotton fabric for multifunctional applications. *Cellulose*. **2017**, *24* (10), 4547–4560. <https://doi.org/10.1007/s10570-017-1413-8>
- Thi, V. H. T.; Lee, B.-K. Development of multifunctional self-cleaning and UV blocking cotton fabric with modification of photoactive ZnO coating via microwave method. *J. Photochem. Photobiol. A Chem.* **2017**, *338*, 13–22. <https://doi.org/10.1016/j.jphotochem.2017.01.020>
- Tian, M.; Hu, X.; Qu, L.; Du, M.; Zhu, S.; Sun, Y.; Han, G. Ultraviolet protection cotton fabric achieved via layer-by-layer self-assembly of graphene oxide and chitosan. *Appl. Surf. Sci.* **2016**, *377*, 141–148. <https://doi.org/10.1016/j.apsusc.2016.03.183>
- Tiwari, S. K.; Mishra, R. K.; Ha, S. K.; Huczko, A. Evolution of graphene oxide and graphene: From imagination to industrialization. *Chem. Nano. Mat.* **2018**, *4* (7), 598–620. <https://doi.org/10.1002/cnma.201800089>
- Varesano, A.; Tonin, C. Improving electrical performances of wool textiles: Synthesis of conducting polypyrrole on the fiber surface. *Text. Res. J.* **2008**, *78* (12), 1110–1115. <https://doi.org/10.1177/0040517507077488>
- Vatansever, F.; Hamblin, M. R. Far infrared radiation (FIR): Its biological effects and medical applications. *Photon. Lasers Med.* **2012**, *1* (4), 255–266. <https://doi.org/10.1515/plm-2012-0034>
- Velasco, M. V. R.; Sarruf, F. D.; Salgado-Santos, I. M. N.; Haroutiounian-Filho, C. A.; Kaneki, T. M.; Baby, A. R. Broad spectrum bioactive sunscreens. *Int. J. Pharm.* **2008**, *363* (1–2), 50–57. <https://doi.org/10.1016/j.ijpharm.2008.06.031>
- Wang, S. Q.; Balagula, Y.; Osterwalder, U. Photoprotection: A review of the current and future technologies. *Dermatol. Ther.* **2010**, *23* (1), 31–47. <https://doi.org/10.1111/j.1529-8019.2009.01289.x>
- Wang, L.; Zhao, J.; Liu, H.; Huang, J. Design, modification and application of semiconductor photocatalysts. *J. Taiwan Inst. Chem.* **2018**, *93*, 590–602. <https://doi.org/10.1016/j.jtice.2018.09.004>
- Wang, X.; Chen, X.; Cowling, S.; Wang, L.; Liu, X. Polymer brushes tethered ZnO crystal on cotton fiber and the application on durable and washable UV protective clothing. *Adv. Mater. Interfaces.* **2019**, *6* (14), 1900564. <https://doi.org/10.1002/admi.201900564>

Wang, S.-D.; Wang, K.; Ma, Q.; Qu, C.-X. Fabrication of the multifunctional durable silk fabric with synthesized graphene oxide nanosheets. *Mater. Today Commun.* **2020**, *23*, 100893. <https://doi.org/10.1016/j.mtcomm.2020.100893>

Wang, H.; Memon, H. *Cotton science and processing technology: Gene, ginning, garment and green recycling*; Springer, 2020.

Xu, L.; Shen, Y.; Ding, Y.; Wang, L. Superhydrophobic and ultraviolet-blocking cotton fabrics based on TiO₂/SiO₂ composite nanoparticles. *J. Nanosci. Nanotechnol.* **2018**, *18* (10), 6879–6886. <https://doi.org/10.1166/jnn.2018.15463>

Xue, C.-H.; Yin, W.; Jia, S.-T.; Ma, J.-Z. UV-durable superhydrophobic textiles with UV-shielding properties by coating fibers with ZnO/SiO₂ core/shell particles. *Nanotechnology.* **2011**, *22* (41), 415603. <https://doi.org/10.1088/0957-4484/22/41/415603>

Xue, C.-H.; Yin, W.; Zhang, P.; Zhang, J.; Ji, P.-T.; Jia, S.-T. UV-durable superhydrophobic textiles with UV-shielding properties by introduction of ZnO/SiO₂ core/shell nanorods on PET fibers and hydrophobization. *Colloids Surfaces A Physicochem. Eng. Asp.* **2013**, *427*, 7–12. <https://doi.org/10.1016/j.colsurfa.2013.03.021>

Yaday, H. M.; Kim, J.-S.; Pawar, S. H. Developments in photocatalytic antibacterial activity of nano TiO₂: A review. *Korean J. Chem. Eng.* **2016**, *33* (7), 1989–1998. <https://doi.org/10.1007/s11814-016-0118-2>

Yildirim, K.; Kanber, A.; Karahan, M.; Karahan, N. The solar properties of fabrics produced using different weft yarns. *Text. Res. J.* **2000**, *88* (13), 1543–1558. [https://doi.org/10.1016/S1359-835X\(99\)00081-0](https://doi.org/10.1016/S1359-835X(99)00081-0)

Yue Y.; Zhou, C.; French, A. D.; Xia, G.; Han, G.; Wang, Q.; Wu, Q. Comparative properties of cellulose nano-crystals from native and mercerized cotton fibers. *Cellulose.* **2012**, *19* (4), 1173–1187. <https://doi.org/10.1007/s10570-012-9714-4>

Zhang, D.; Chen, L.; Fang, D.; Toh, G. W.; Yue, X.; Chen, Y.; Lin, H. In situ generation and deposition of nano-ZnO on cotton fabric by hyperbranched polymer for its functional finishing. *Text. Res. J.* **2013**, *83* (15), 1625–1633. <https://doi.org/10.1177/0040517512474362>

Zhang, K.; Yang, Z.; Mao, X.; Chen, X.-L.; Li, H.-H.; Wang, Y.-Y. Multifunctional textiles/metal-organic frameworks composites for efficient ultraviolet radiation blocking and noise reduction. *ACS Appl. Mater. Interfaces.* **2020**, *12* (49), 55316–55323. <https://doi.org/10.1021/acsami.0c18147>

Zhao, Y.; Xu, Z.; Wang, X.; Lin, T. Superhydrophobic and UV-blocking cotton fabrics prepared by layer-by-layer assembly of organic UV absorber intercalated layered double hydroxides. *Appl. Surf. Sci.* **2013**, *286*, 364–370. <https://doi.org/10.1016/j.apsusc.2013.09.092>

Zhou, S.; Wang, F.; Balachandran, S.; Li, G.; Zhang, X.; Wang, R.; Liu, P.; Ding, Y.; Zhang, S.; Yang, M. Facile fabrication of hybrid PA6-decorated TiO₂ fabrics with

excellent photocatalytic, anti-bacterial, UV light-shielding, and super hydrophobic properties. *RSC Adv.* **2017**, *7* (83), 52375–52381. <https://doi.org/10.1039/C7RA09613E>

Zohoori, S.; Payvandy, P.; Bekrani, M. Antibacterial, self-cleaning and UV blocking of wool fabric coated with nano Ce/ZnO and Ce/TiO₂. *Indian J. Fibre Text. Res.* **2021**, *46* (1), 57–62. <https://doi.org/10.56042/ijftr.v46i1.25171>

Antioxidant property of secondary metabolites from *Garcinia* genus: A short review

Elton Kazmierczak¹⁺, Cássia Gonçalves Magalhães¹, Romaiiana Picada Pereira¹

1. State University of Ponta Grossa, Department of Chemistry, Ponta Grossa, Brazil.

+Corresponding author: Elton Kazmierczak, Phone: +55 42 999945754, Email address: kazmierczak.elton@gmail.com

ARTICLE INFO

Article history:

Received: July 27, 2022

Accepted: December 5, 2022

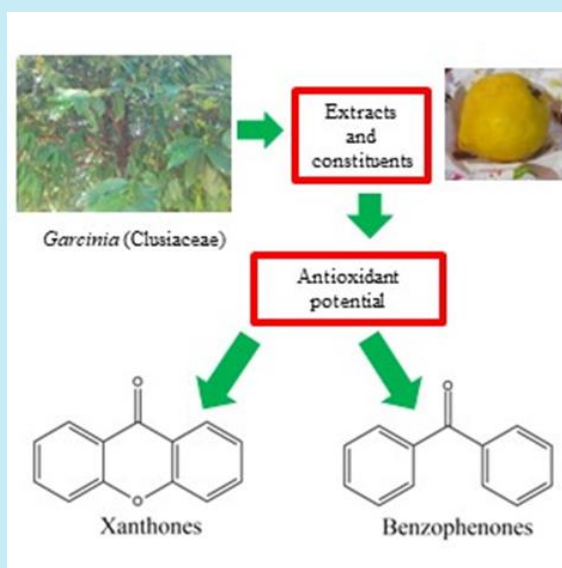
Published: January 01, 2023

Keywords:

1. Benzophenones
2. Mangosteen
3. Free radicals
4. Oxidative stress
5. Xanthonnes

Section Editors: Assis Vicente Benedetti

ABSTRACT: Species from the *Garcinia* genus (Clusiaceae family) are used in the treatment of many diseases and metabolic disorders frequently associated with the oxidative stress. The characteristic metabolites found in this genus are xanthonnes and benzophenones, which have antioxidant properties, among relevant biological potentials. This review provides a specific vision about antioxidant activity of *Garcinia* species, reporting *in vitro* and *in vivo* assays, described from the last five years. The research about antioxidant properties of *Garcinia* species and their constituents can be directed in the development of new medicines and drugs.



CONTENTS

1. Introduction
2. Methodology
3. An overview about oxidative stress and free radicals
4. Chemical constituents of *Garcinia* genus
5. Antioxidant activity of extracts and metabolites of *Garcinia* genus
6. Concluding remarks

- Authors' contribution
- Data availability statement
- Funding
- Acknowledgments
- References

1. Introduction

The increase in consumption of ultra-processed foods and other modern habits harmful to health contribute to the growth in the number of people with chronic diseases such as diabetes, hypertension and obesity (Almarshad *et al.*, 2022). This situation leads to the requirement of research for alternatives in the treatment of these problems. Due to low cost and low side effects, natural products that have health benefits are the target of studies in order to develop remedies that act in this type of disease (A. Onaolapo and O. Onaolapo, 2020).

Species of the *Garcinia* genus (Clusiaceae family) are a relevant source of bioactive compounds. They are used in traditional medicine against problems frequently associated to oxidative stress, such as chronic ulcers, dysentery, diarrhea, gonorrhoea, and diabetes (Aizat *et al.*, 2019a; Mello *et al.*, 2021). Approximately 450 species belong to this genus, and they are commonly found as trees, shrubs or subshrubs, occurring in Asia and some countries in Africa and South America (Mohamed and Ibrahim, 2020). A common feature among species of this genus is the production of yellow sap, occasionally white, in the endocarp of the fruit, bark and wood (Aizat *et al.*, 2019b; Inoue *et al.*, 2017; Machado *et al.*, 2017).

Several biological activities have been described for *Garcinia* species, including anticancer, anti-inflammatory, antimicrobial, antiviral, antidepressant, antioxidant, and neuroprotective activity against Alzheimer's disease. In addition, the antiobesity activity and appetite suppressant activity has been commercially explored through many supplements based on extracts of *Garcinia* spp. (Pandey *et al.*, 2017). This relevant and diversified biological potential is attributed to the xanthenes and benzophenones, the most abundant classes of metabolites found in these plants (Do and Cho, 2020; Inoue *et al.*, 2017; Kurniawan *et al.*, 2021; Mello *et al.*, 2021; Wairata *et al.*, 2022; Wang *et al.*, 2017; Zafar *et al.*, 2019).

Garcinia mangostana, the most studied species, is popularly known as *mangosteen*. It is cultivated for its peculiar bittersweet taste and it is also known as the *queen of fruits* due to its sweet-sour taste and the wide range of medicinal benefits (Aizat *et al.*, 2019a). In traditional medicine, the pericarp of this species has been used to treat inflammation, ulcer, skin infection, amoebic dysentery, wound healing, and diarrhea (Wang *et al.*, 2017). *G. cochinchinensis* is similar in phenotype to *G. mangostana* and is called *yellow mangosteen* or *false mangosteen*, depending on the region of occurrence. In the young fruit stage, the *G. cochinchinensis* is confused with *G. mangostana*; the latter being typical of Southeast Asian countries such as

Malaysia, Indonesia, Thailand and China. The tropical tree of *G. mangostana* can reach up to 25 m in height. The fruit in its mature stage is purple. In popular medicine, the pericarp has been used to treat inflammation, ulcer, and skin infection. In addition, several parts of *G. mangostana* are prepared by dissolving in water and after the fruit extract is commercialized as functional food and drink (Aizat *et al.*, 2019b; Wang *et al.*, 2017). *G. xanthochymus* is a perennial medium-size tree that can reach up to 20 m height and it is distributed in China, South East Asia and Western Gates of India. The *G. xanthochymus* fruit has a sub globose form, turns yellow when it is mature, and the seeds are embedded in yellow pulp. The fruits are eaten fresh or processed to make jams, vinegar, beverages and other food products. As well as other species of this genus, various subparts of the plant are used in the research like barks, leaves, seeds, stem bark and others (Hassan *et al.*, 2018; Prakash *et al.*, 2022).

In American countries there are some *Garcinia* species such as *G. brasiliensis* and *G. gardneriana*, which are used to treat inflammation, pain and urinary infections. These species are native to the Amazonian region; *G. brasiliensis*, for example is known as *bacuri*, *bacupari* or *bacuripari*. The fruit of *G. brasiliensis* is yellow and has a sour-sweet pulp. It has also anti-inflammatory, antinociceptive, antitumoral and antioxidant properties (Demenciano *et al.*, 2020; Espirito Santo *et al.*, 2020).

Species like *G. atroviridis*, *G. cola*, *G. cambogia* and *G. indica* are used to treat degenerative diseases, such as obesity, diabetes mellitus, and arthritis, as well as other metabolic syndromes (Kuswandi *et al.*, 2022). *G. cambogia* is used as an antiobesity supplement and can be effective in terms of weight loss (Andueza *et al.*, 2021; Han *et al.*, 2021). Andueza *et al.*, (2021) warn about the negative effect of *Garcinia* supplements for weight loss because it can be associated with liver damage and to lesser extent with serotonin toxicity.

The responsible compounds by antioxidant property in *Garcinia* species are phenolic compounds, flavonoids, phenolic acids, anthocyanins, xanthenes and benzophenones, because there is relationship between free radical scavenging and total phenolic content and total flavonoids content (Espirito Santo *et al.*, 2020; Kainama *et al.*, 2020). Another important compound present in the genus *Garcinia* is hydroxycitric acid, which, together with hydroxylated xanthenes and benzophenones, has a significant antioxidant activity. It controls the oxidative stress with hydroxycitric acid and others bioactive compounds from *Garcinia* regulating the concentration of reactive oxygen species, being one important therapeutic strategy (Han *et al.*, 2021).

Bioactive compounds, such as phenolics compounds, flavonoids and biflavonoids, xanthenes and benzophenones, found in this genus are strong antioxidants that complement and enhance the functions of vitamins and enzymes, protecting against oxidative stress (Mello *et al.*, 2021). These compounds may be used in the food industry, mainly in meat products, in which oxidation is one of the main problems related to their deterioration (Beya *et al.*, 2021). Another strong trend in the study of natural antioxidants is their use to preserve the quality of raw food, suggesting another possible application for plant extracts and isolated metabolites that show this property.

Based on the relevant potential of plants as a source of antioxidant compounds, the present review aims to describe the antioxidant property of species of the *Garcinia* genus, reported between 2017 and 2022.

2. Methodology

Data relating to *Garcinia* spp. and their antioxidant potential were obtained through PubMed and Google Scholar published in the last 5 years. The species of *Garcinia* shown here were chosen due to the number of publications such as *G. mangostana*, *G. kola*, *G. xanthochymus* and others. Another reason was the relation with metabolic disorders. The following exclusion criteria were adopted: 1- article whose full text was not accessible in the database; 2- publications that did not include the terms “*Garcinia*” and “antioxidant activity” search phrases in the abstract or title; 3- articles which are not written in English; and 4- articles in which the phytochemicals used in the biological activity assays were not isolated from these species but were acquired from industries. The chemical structures of compounds mentioned in this text were drawn using ChemDrawn 12.0 software.

3. An overview about oxidative stress and free radicals

The terms oxidants or pro-oxidants are related to the reactive oxygen species (ROS) and reactive nitrogen species (RNS). Both of them can be described as free radicals, although ROS can be found as non-free radical species. Free radicals are atoms or molecules containing one or more unpaired electrons in the valence shell (Elmund and Hartrianti, 2020). Because of its odd and unpaired electron, the radical becomes unstable, short-lived, and reactive. Due to their high reactivity, radicals interact with other substances to remove their electrons and achieve stability. The substance that has suffered the

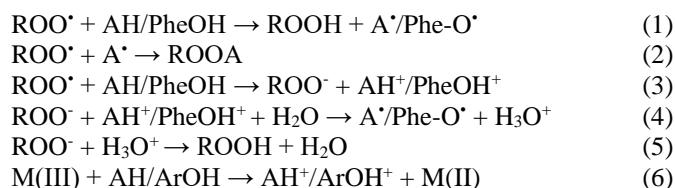
electron removal can turn into a radical and reacts with a subsequent one and, thus, start a chain reaction, which ultimately causes cellular damage (Kumar *et al.*, 2021; Omidifar *et al.*, 2021). These free radicals can be generated in normal mitochondrial processes. This phenomenon, oxidative stress, occurs when pro-oxidant substances are in higher concentration than antioxidant substances. Then, they may cause oxidative damage due to the absence of antioxidant defense. The examples for the radicals include superoxide ($O_2^{\cdot-}$), oxygen radical (O_2^{\cdot}), hydroxyl (OH^{\cdot}), alkoxy radical (RO^{\cdot}), Peroxy radical (ROO^{\cdot}), Nitric oxide (NO^{\cdot}) and nitrogen dioxide (NO_2^{\cdot}) (Abubakar *et al.*, 2020; Kumar *et al.*, 2021).

When the number of oxidizing substances, whether free radicals or nonradical reactive species, are at a higher level, the body is able to neutralize by the action of antioxidant substances and, by the enzymatic antioxidant system, the phenomenon oxidative stress occurs. This phenomenon describes the level and state of oxidative damage to tissues and cells caused by ROS and other radicals. Oxidative stress can be defined as an imbalance between concentration of free radical and other oxidative compounds and the decrease of concentration of antioxidants, which lead to a disruption of redox signaling, control and molecular damage (Cassidy *et al.*, 2020; Kumar *et al.*, 2021; Mohamed and Ibrahim, 2020). In mental illness, for example, the concentration of antioxidants and their markers can indicate the level of oxidative damage and suggest the presence of a particular disease or disorder. In this context, the reduction in the level of antioxidants such as glutathione, glutathione transferase and catalase, as well as the increase in ROS and RNS and the variability of their concentrations, may indicate differences in the initial and final stages of healthy problems related to this balance (Ashton *et al.*, 2019).

In order to control the undesired action of radicals, the search for compounds that perform this function is increasing. In this case, these substances are called antioxidants. They can be present in the body and convert radicals and other reactive species into stable species. Antioxidants act by different mechanisms of action, including radical scavengers, singlet oxygen inhibitors, peroxide inactivators and metal chelators (Gulcin, 2020). Redox markers are also used as evaluation parameters for oxidative stress, there is an increase in malondialdehyde and thiobarbituric acid reactive substances markers. The antioxidant enzymes themselves can be used as markers that are altered in the context of serious diseases, such as superoxide dismutase, catalase and glutathione peroxidase, as they indicate the active level of the body's antioxidant defense. High levels of oxidative stress may originate in the mitochondria and are associated with

their dysfunction or, in part, when the oxidative damage to the mitochondria happens (Ashton *et al.*, 2019).

A variety of assays are used to evaluate antioxidant property of secondary metabolites from plants, by different mechanisms. Among them, it is possible to cite assays of radical capture activity or reactive species, reducing power and metal chelation. The most common methods for evaluating antioxidant activity to be used is the radical scavenging activity assay of 2,2-diphenyl-1-picrylhydrazyl (DPPH), radical 2,2'-azino-bis (3-ethylbenzothiazoline-6-sulfonic acid) (ABTS), ferric reducing antioxidant power (FRAP) and metal chelation capacity (Wairata *et al.*, 2022). Depending on the reagents involved, the type of antioxidant and oxidant reactions can occur in two distinct mechanisms in order to convert the radical into a stable species. Both mechanisms lead to the same results (Gulcin, 2020). So, the basis of the chemical reactions involved is categorized into hydrogen atoms transfer (HAT) and single electron transfer (SET). HAT (Eqs. 1 and 2) is defined as one H atom is transferred to a radical target resulting in a stable product and SET (Eqs. 3–6) as one or more electrons are transferred to reduce target free radicals.



Reactions HAT and SET, where AH = any antioxidant with donatable H or electron, PheOH = phenol or polyphenol antioxidants, M = redox metal. Reactions based in SET involve one redox reaction with the antioxidant compound.

Antioxidant assays like DPPH, ABTS and FRAP occur by SET mechanisms. The DPPH radical capture assay is among the most used assays in the evaluation of antioxidant activity (Benzie and Devaki, 2017; Sethi *et al.*, 2020). DPPH is a stable radical of purple color and soluble in ethanol. After reacting with antioxidants, electrons or hydrogen atoms, it loses its purple color, becoming colorless or slightly yellowish. The colorless compound formed is also called 2,2-diphenyl-picrylhydrazyl or reduced DPPH (Gulcin, 2020).

The ABTS^{•+} radical is prepared from nonradical ABTS by reacting with a strong oxidizing agent, such as persulfate ion (Sethi *et al.*, 2020). ABTS^{•+} is a bluish green cation radical with maximum absorption at 734 nm, which gradually loses its color intensity when it

reacts with antioxidant species (AH, Ar-OH) (Gulcin, 2020).

The FRAP of extracts from plant samples occurs through single electron transfer reactions. This is a method that measures the ability of the potential antioxidant to transfer an electron to reduce any compound, in this case the transition metal iron, as well as carbonyls and other oxidizing radicals (Benzie and Devaki, 2017; Sethi *et al.*, 2020). The need to investigate the ability to reduce iron ions in their involvement in the oxidative process, increasing the concentration of ROS, consequently, aggravating the oxidative stress. Iron participates in the Fenton reaction, present in the body (Benzie and Devaki, 2017). Some ROS are moderately reactive such as superoxide (O₂^{•-}) like most biological molecules. However, through the Haber–Weiss reaction catalyzed by the Fenton reaction, other extremely reactive ROS are generated (Gulcin, 2020). Fe³⁺ reacts with the superoxide to form Fe²⁺ (Eq. 7). This cation reacts rapidly with hydrogen peroxide (H₂O₂) producing ion of iron III, radical hydroxyl and the hydroxyl ion (Eq. 8), ROS that are extremely harmful to the body (Benzie and Devaki, 2017; Lakey-Beitia *et al.*, 2021). The combination of Eqs. 7 and 8 results in the iron-catalyzed Haber–Weiss reaction (Eq. 9), which turns out to be possible *in vivo* (Engwa, 2018).



The importance of evaluating FRAP is in reducing of the Fe³⁺ in Eq. 7, as this prevents the formation of ROS, whereas in chelation of iron, the antioxidant compounds present in the extracts chelate the ion Fe²⁺ in Eq. 8, also preventing the formation of ROS. In general, the chelation capacity of metals is determined by measuring the chelating effect of antioxidants for iron ions, Fe²⁺ (Gulcin and Alwaseel, 2022). The chelating capacity of antioxidant compounds can be measured to chelate both Fe and Cu, and in turn, phenolic and flavonoid species are both able to chelate these transition metals (Lakey-Beitia *et al.*, 2021). The chelation of transition metals prevents them from participating in reactions that generate oxidant species, for example, in Fenton and Haber–Weiss reactions generating ROS (García-Diez *et al.*, 2021).

4. Chemical constituents of *Garcinia* genus

The major classes of secondary metabolites found in species from *Garcinia* genus are phenolics compounds, flavonoids, biflavonoids, xanthenes, benzophenones and

terpenes (Hassan *et al.*, 2018). These phytochemicals can be isolated by different parts of the plant, using different techniques, such as conventional fractionated extraction, ultrasound assisted extraction and microwave assisted extraction (Carrillo-Hormaza *et al.*, 2020; Chang *et al.*, 2020; Ramirez *et al.*, 2019).

The two main classes of bioactive compounds found in species of the genus *Garcinia* are xanthenes and benzophenones, associated with isoprenyl groups and glycosides. The base skeleton of xanthone is composed of two benzene rings linked by a γ -pyran ring, and its tricycle structure can be associated with its biological activities (Ashton *et al.*, 2019; Zafar *et al.*, 2019). The name *xanthone* comes from Greek language, where *xanthos* means yellow color, because xanthenes are commonly obtained as yellow solids (Kurniawan *et al.*, 2021). Xanthenes can be found in various parts of plants from the *Garcinia* genus, such as the fruit, peel of the fruit, bark, and seeds (Mohamed and Ibrahim, 2020). The biosynthesis of xanthenes is given based on the numbering of ring A and B from xanthenes. The biosynthesis pathway of ring A (carbon 1-4) comes from the acetate pathway, while the ring B (carbon 5-8) is given by the shikimic acid pathway (Pinto *et al.*, 2021). Several xanthenes analogs and their glycosides are obtained by adding substituents to the side chain of the aromatic rings of the skeleton base, but in different positions. Thus, there are reported hydroxylated xanthenes, from mono to polyhydroxylated, prenylated, alkylated, linked to charged groups, linked to glycoside groups, linked to alkoxide groups and xanthenes found in the form of dimers and trimers (Zafar *et al.*, 2019).

The xanthenes found in *Garcinia* species exhibit important diverse biological properties, such as antioxidant, antitumor, antiviral, anti-HIV, antiglycemic, antimicrobial and neuroprotective activities such as in Alzheimer's disease, Parkinson's disease and depression, anticancer (Do and Cho, 2020; Inoue *et al.*,

2017; Kurniawan *et al.*, 2021; Wairata *et al.*, 2022; Wang *et al.*, 2017; Zafar *et al.*, 2019).

The xanthenes isolated from *Garcinia* species exhibit important diverse biological properties, such as antioxidant, antitumor, antiviral, anti-HIV, antiglycemic, antimicrobial and neuroprotective activities (Kurniawan *et al.*, 2021; Wairata *et al.*, 2022; Wang *et al.*, 2017). Examples of these metabolites include α -mangostin, β -mangostin, γ -mangostin, gartanin, 8-desoxygartanin, garcinexanthone A, cabalaxanthone, garcixanthone A, garcinone C, lichexanthone, subelliptenone H, 12b-hydroxy-des-D-garcigerrin A, garcinaxanthone B, garcigerin A, garcinone-E, smeathxanthone A, and 1,3,5-tridroxixanthone (Fig. 1) (Kusmayadi *et al.*, 2019; Wairata *et al.*, 2022; Zafar *et al.*, 2019).

Benzophenones are a class of compounds similar to xanthenes. However, there is no oxygen present between the two aromatic rings. The base form for benzophenones is characterized by phenol-carbonyl-phenol (Inoue *et al.*, 2017; Murthy *et al.*, 2020). They can also be in the form of polyisoprenylated, linked to glycosides and other substituents, as well as xanthenes. Examples of known benzophenones are isogarcinol, garcinol and 7-epiclusianone, xanthochymol, 2,4,6,3',4',6'hexahydroxybenzophenone.

Morelloflavone and volkensiflavone are biflavonoid found in *G. brasiliensis* (Fig. 2) (Moreira *et al.*, 2017; Pasaribu *et al.*, 2021b). The A ring of benzophenones usually have one or two substituents present. On the other hand, the B ring can undergo prenylation and cyclization, producing a variety of different compounds. The benzophenones can be unique with bi-, tri- and tetracyclic ring systems and show different biological activities, such as antioxidant, antimicrobial, anti-HIV, cytotoxic, hepatoprotective, antiparasitic, and antidiabetic. Benzophenones are the main intermediates in the biosynthetic pathway of xanthenes (Inoue *et al.*, 2017).

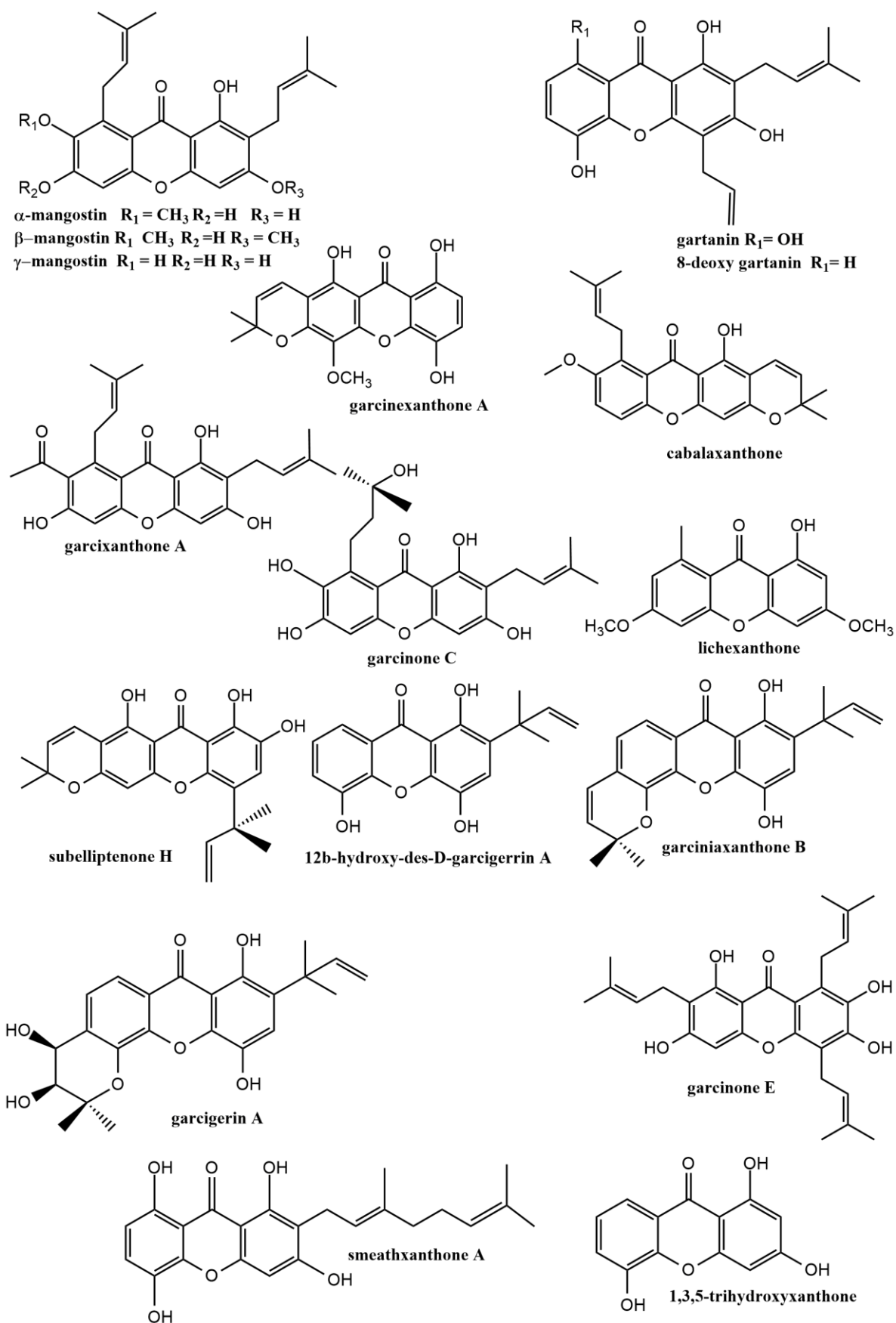


Figure 1. Examples of xanthones found in the *Garcinia* species.

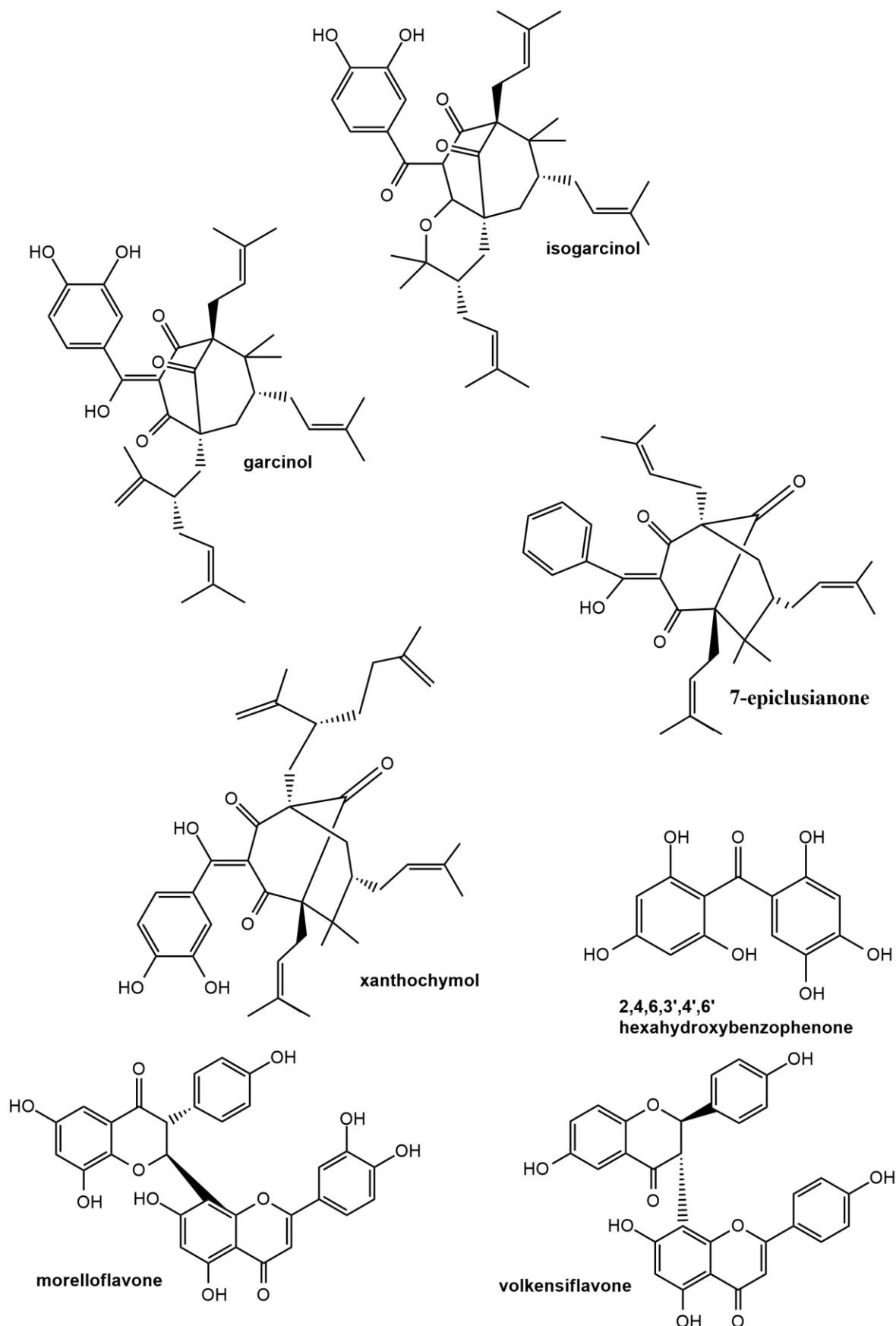


Figure 2. Examples of benzophenones and flavonoids presents in *Garcinia* species.

5. Antioxidant activity of extracts and metabolites of *Garcinia* genus

Xanthenes and benzophenones can be classified as primary antioxidants because they are capable of donating hydrogen or electrons to ROS. In consequence, they delay, inhibit or prevent the initiation step or interrupt reaction in the chain. Xanthenes react with free radicals through electron transfer or hydrogen atom transfer. The antioxidant activity of phenolics compounds may vary according to the amount of hydroxyl substituents and the position of other substituents in the skeleton (Gulumian *et al.*, 2018). This happens because hydroxyl groups attached to aromatic rings, forming phenolic groups, act effectively to capture free radicals. The number of hydroxyl groups present in xanthenes, flavonoids and other classes of compounds also affects their antioxidant potential. Although dihydroxy and trihydroxy xanthenes or flavonoids have significant antioxidant activity, tetrahydroxy xanthenes or flavonoids have higher values than di- and trisubstituted. However, it is necessary to take into account the presence of other substituents that alter the interaction between the xanthone and the oxidizing compound. Among these substituents it can be listed alkoxide, prenyl groups. In addition, several natural xanthenes that have antioxidant property also exhibit other activities and the scientific community has developed studies to evaluate the structure-activity relationship to better investigate the biological potential of these molecules (Gulcin, 2020; Gulumian *et al.*, 2018; Zafar *et al.*, 2019)

Virgolin *et al.* (2017) investigated the antioxidant activity by FRAP assay of extracts of the fruits of *G. humilis* and *G. xanthochymus* using 70% acetone. It was observed a good potential for these samples, 2995.88 ± 3.23 and 489.39 ± 0.48 $\mu\text{mol trolox } 100 \text{ g}^{-1}$ pulp, respectively.

Considering the evaluation of isolated compounds from the *Garcinia* genus, Wairata *et al.* (2021) investigated the antioxidant, antidiabetic and antiplasmodial properties of xanthenes from *G. forbesii*. From the stem bark of *G. forbesii*, it was isolated five xanthenes: lichexanthone, subelliptenone H, 12b-hydroxy-des-D-garcigerrin A, garciniaxanthone B and garcigerin A (Fig. 2). These authors evaluated the antioxidant property of the compounds described by scavenging DPPH, ABTS, and FRAP methods, and verified that those metabolites showed strong antioxidant activity by those methods. The most effective

compounds were garciniaxanthone B for DPPH assay and 12b-hydroxy-des-D-garcigerrin A for ABTS assay. The antioxidant activity of these compounds can be explained by the presence of hydroxyl groups linked in aromatic rings, which react with radical DPPH through the SET mechanism. From *G. brasiliensis*, fukugetin, 7-epiclusianone and guttiferone-A were found in its fruits and seeds. These compounds performed relevant antioxidant activity (Melo *et al.*, 2021).

Considering the chelation of metals, Chew and Lim (2018) evaluated the FRAP of *G. mangostana*, *G. atroviridis* and *G. hombroniana* extracts from leaves, pulps and pericarps of these species. Considering leaves and pulp extracts, *G. hombroniana* was more effective in chelating power (60% and 30%, respectively). The pericarp extract of *G. mangostana* showed more activity (78%) than *G. hombroniana* and *G. atroviridis* (45% and 11%, respectively). The parts of the same *Garcinia* species were compared in terms of antioxidant activity and total phenolic content and total flavonoids content.

Nguyen *et al.* (2021) evaluated the antioxidant activity of *G. fusca*, *G. hopii*, *G. planchonii*, *G. nigrolineata*, *G. gaudichaudii*, and *G. tinctoria*. The extracts were obtained with hexane, ethyl acetate and methanol in solid-liquid extraction. The antioxidant activity methods used were DPPH assay, hydroxyl radical scavenging and total antioxidant capacity. The higher values of IC_{50} for the DPPH assay were found in ethyl acetate extract and methanolic extract in all *Garcinia* species. For hydroxyl radical scavenging capacity, the strongest antioxidant activity is shown in ethyl acetate extract of *G. tinctoria* with 83.5% at IC_{50} of $1.5 \mu\text{g mL}^{-1}$. About the total antioxidant capacity assay, the extracts obtained from *G. tinctoria* have the highest values 265.

Ramirez *et al.* (2019) evaluated the antioxidant activity by DPPH, ABTS and FRAP assays of seeds, epicarp and leaves of *G. madruno*. A sequential extraction of these parts with hexane, dichloromethane, ethyl acetate and methanol were done. The ethyl acetate fraction from leaves was more effective in the three assays. Research like this makes possible discussions and analysis between fractions of the same plant part and between all parts studied. The different polarity of solvent used influences directly the yield of antioxidant compounds and the IC_{50} value of antioxidant activity, solvents such as ethyl acetate, dichloromethane and others with medium polarity are good to extract phenolics compounds. Other articles are shown in Table 1.

Table 1. Antioxidant property of *Garcinia* species.

Species (part of plant)	Compounds or extracts assayed	Assay for determination of antioxidant activity	References
<i>G. cochinchinensis</i> (pulp and leaves)	Acetone extract	DPPH	Machado <i>et al.</i> (2017)
<i>G. morella</i> (tree's latex)	Acetone extract	DPPH, TAC, hydrogen peroxide scavenging activity (H ₂ O ₂) and FRAP	Murthy <i>et al.</i> (2017)
<i>G. morella</i> (fruit)	Methanol extract	DPPH and FRAP	Choudhury <i>et al.</i> (2018)
<i>G. mangostana</i> (fruit peels)	Extraction with ethanol, acetone, ethyl acetate, methanol, hexane, acetic acid and distilled water	DPPH	Kusmayadi <i>et al.</i> (2019)
<i>G. mangostana</i> (pericarps)	α -mangosteen and γ -mangosteen	Determination of intracellular ROS, DPPH, lipid peroxidation	Lee <i>et al.</i> (2019)
<i>G. brasiliensis</i> (leaves, barks and seeds)	Ethanol and aqueous extract	DPPH	Naves <i>et al.</i> (2019)
<i>G. mangostana</i> (pectin from rind)	Aqueous extract acidified at pH 2	DPPH	Wathoni <i>et al.</i> (2019)
<i>G. gardneriana</i> (fruits and leaves)	extracts of sequential extraction (ethanol, hexane, chloroform, ethyl acetate and hydromethanol fraction)	DPPH	Demenciano <i>et al.</i> (2020)
<i>G. kola</i> (leaves, roots and stem bark)	Hydro-ethanolic and methanol extract	DPPH, ABTS and FRAP	Djague <i>et al.</i> (2020)
<i>G. mangostana</i> (fruit)	Methanol extract	DPPH and FRAP	Abey Suriya <i>et al.</i> (2020)
<i>G. mangostana</i> (pericarp)	Isolated compounds: 2,4,6,3',4',6'-hexa hydroxybenzophenone; 6-O- β -D-glucopyranosyl-2,4,6,3',4',6'-hexa hydroxybenzophenone and 2R,3R-5,7-dihydroxy-8-C- β -D-glucopyranosyl-4'-methoxy-2,3-dihydroflavon-3-ol	DPPH	Mohamed and Ibrahim (2020)
<i>G. lasoar</i> (stem bark)	Extracts obtained by ethanol, ethyl acetate, dichloromethane and n-hexane; Petroleum ether; Extract obtained by aqueous infusion and other with methanol by maceration;	DPPH and ABTS	Kainama <i>et al.</i> (2020)
<i>G. mangostana</i> (pericarp)	Ultrasonic assisted extraction	DPPH	Sungpud <i>et al.</i> (2020)
<i>G. latifolia</i> (dried fruits)	Methanol fruit extract	DPPH	Reddy <i>et al.</i> (2021)
<i>G. macrophylla</i> (stem bark)	Macrophylloflavone isolated from ethyl acetate fraction	DPPH	Cane <i>et al.</i> (2020)
<i>G. pedunculata</i> (fruit)	Dry extract	DPPH	Hossain <i>et al.</i> (2021)
<i>G. celebica</i> (root bark)	Extracts (n-hexane, dichloromethane, ethyl acetate and methanol); (-)-cycloanthochymol, isoxanthochymol and xanthochymol.	DPPH, ABTS and FRAP	Pasaribu <i>et al.</i> (2021b)
<i>G. mangostana</i> (pericarp)	Methanol extract	DPPH	Pasaribu <i>et al.</i> (2021a)
<i>G. kola</i> and <i>G. afzelii</i> (stem and bark)	Methanol extract (70%)	DPPH, ABTS and FRAP	Essuman <i>et al.</i> (2021)
<i>G. xanthochymus</i> (peel, pulp, rind and seeds)	Methanol extract of lyophilized peel; Methanol extract of lyophilized pulp; Ethanol extract of sun-dried rind; Methanol extract of sun-dried seed	DPPH, ABTS and FRAP	Prakash <i>et al.</i> (2022)

FRAP = ferric reducing antioxidant power; TAC = total antioxidant activity; DPPH = 2,2-diphenyl-1-picrylhydrazyl scavenging assay; ABTS = 2,2'-azinobis-(3-ethylbenzothiazoline-6-sulphonate) radical scavenging assay.

It is important to highlight that many researchers report the relationship between antioxidant activity with other biological activities or alternative methods of extraction. Between them, the research of [Chang et al. \(2020\)](#) was based on the effect of a concentrated mangosteen (*G. mangostana*) drink, MCD, in rats after long-term running exercise in order to investigate changes in the antioxidant system and lactate clearance. Since aerobic exercise can lead to significant fatigue, oxidative stress and muscle damage, the authors investigated the level of lactate clearance and the levels of endogenous antioxidants such as superoxide dismutase, glutathione peroxidase and catalase, in addition to blood glucose, cholesterol, triglycerides and muscle malondialdehyde levels. The levels of glutathione peroxidase and catalase increased with the ingestion of concentrated mangosteen drink and the supplementation of this drink also increased lactate clearance, contributing to a better physical recovery of rats after exhaustion from running exercise. MDA concentration also decreased with mangosteen drink supplementation compared to the control group; however, there was no decrease of malondialdehyde in muscle.

[Araújo et al. \(2019\)](#) performed *in vivo* tests in mice that were ingesting ethanolic extract of *G. brasiliensis* leaves daily to evaluate its antioxidant activity, modulation of the intestinal microbiota and anti-inflammatory activity. The ethanolic extract of the leaf contained the biflavonoid morelloflavone and the benzophenone 7-epiclusianone. They concluded that the extract was able to reduce oxidative stress, demonstrated by the increase in the amount of antioxidant enzymes. It inhibited the inflammatory process, modulated the intestinal microbiota, favoring beneficial bacteria and regulating lipid metabolism, which reduces obesity ([Araújo et al., 2019](#)). The ethyl acetate extract of the seeds e from *G. kola* was evaluated by [Idris et al. \(2020\)](#) for *in vivo* antioxidant, anti-inflammatory and antidiabetic activities. Biochemical markers related to these processes such as glutathione peroxidase levels, lipid peroxidation revealed by malondialdehyde levels and biochemical markers for antidiabetic activity were evaluated. The levels of glutathione found in the group administered with *G. kola* were near to the healthy group, but the highest value was found in the treated group with insulin. The malondialdehyde levels increased in the group treated with insulin and the *G. kola* extract group compared to diabetic control group. These results emphasize that *G. kola* extract is a candidate for therapeutic uses in diabetes and oxidative stress treatment ([Idris et al., 2020](#)). [Tjahjani, et al. \(2019\)](#) demonstrated antioxidant and antimalarial activity of

G. mangostana's ethyl acetate fraction for *in vivo* models.

All these reports highlight the relevant scientific potential of species from the *Garcinia* genus and stimulate the search for new sources of antioxidant compounds.

6. Concluding remarks

Garcinia genus shows significant free radical scavenging and antioxidant potential by the presence of xanthenes and benzophenones. The isolated compounds and extracts from these species have potential to be applied in pharmaceutical and food industries. This emphasizes the continuation of studies involving these plants, because they can lead to the discovering new possibilities of application of these natural resources, increasing their scientific value.

Authors' contribution

Conceptualization: Kazmierczak, E.; Pereira, R. P.; Magalhães, C. G.

Data curation: Kazmierczak, E.

Formal analysis: Kazmierczak, E.

Funding acquisition: Not applicable.

Investigation: Kazmierczak, E.

Methodology: Kazmierczak, E.; Pereira, R. P.; Magalhães, C. G.

Project administration: Kazmierczak, E.; Pereira, R. P.; Magalhães, C. G.

Resources: Kazmierczak, E.

Software: Not applicable.

Supervision: Pereira, R. P.; Magalhães, C. G.

Validation: Pereira, R. P.; Magalhães, C. G.

Visualization: Kazmierczak, E.; Pereira, R. P.; Magalhães, C. G.

Writing – original draft: Kazmierczak, E.

Writing – review & editing: Pereira, R. P.; Magalhães, C. G.

Data availability statement

The data will be available upon request.

Funding

Coordenação de Aperfeiçoamento de Pessoal de Nível Superior (CAPES). Finance Code 2013/2998/2014.

Conselho Nacional de Desenvolvimento Científico e Tecnológico (CNPq). Grant No: 307546/2014.

Acknowledgments

Not applicable.

References

- Abeyesuriya, H. I.; Bulugahapitiya, V. P.; Pulukkuttige, J. L. Total Vitamin C, Ascorbic Acid, Dehydroascorbic Acid, Antioxidant Properties, and Iron Content of Underutilized and Commonly Consumed Fruits in Sri Lanka. *Int. J. Food Sci.* **2020**, *2020*, 4783029. <https://doi.org/10.1155/2020/4783029>
- Abubakar, A.; Olorunkemi, M. R.; Musa, B.; Hamzah, R. U.; Abdulrasheed-Adeleke, T. Comparative *In vitro* Antioxidant Activities of Aqueous Extracts of *Garcinia kola* and *Buchholzia coriacea* Seeds. *Tanz. J. Sci.* **2020**, *46* (2), 498–507.
- Aizat, W. M.; Ahmad-Hashim, F. H.; Jaafar, S. N. S. Valorization of mangosteen, “The Queen of Fruits,” and new advances in postharvest and in food and engineering applications: A review. *J. Adv. Res.* **2019a**, *20*, 61–70. <https://doi.org/10.1016/j.jare.2019.05.005>
- Aizat, W. M.; Jamil, I. N.; Ahmad-Hashim, F. H.; Noor, N. M. Recent Updates on Metabolite Composition and Medicinal Benefits of Mangosteen Plant. *PeerJ.* **2019b**, *7*. <https://doi.org/10.7717/peerj.6324>
- Almarshad, M. I.; Algonaiman, R.; Alharbi, H. F.; Almujaydil, M. S.; Barakat, H. Relationship between Ultra-Processed Food Consumption and Risk of Diabetes Mellitus: A Mini-Review. *Nutrients.* **2022**, *14* (12), 2366. <https://doi.org/10.3390/nu14122366>
- Andueza, N.; Giner, R. M.; Portillo, M. P. Risks Associated with the Use of Garcinia as a Nutritional Complement to Lose Weight. *Nutrients.* **2021**, *13* (2), 450. <https://doi.org/10.3390/nu13020450>
- Araújo, F. O.; Moreira, M. E. C.; Lima, C. F.; Toledo, R. C. L.; Sousa, A. R.; Veloso, M. R.; Freitas, P. G.; Santos, M. H.; Souza, E. C. G.; Mantovani, H. C.; Martino, H. S. D. Bacupari (*Garcinia brasiliensis*) extract modulates intestinal microbiota and reduces oxidative stress and inflammation in obese rats. *Food Res. Int.* **2019**, *122*, 199–208. <https://doi.org/10.1016/j.foodres.2019.04.012>
- Ashton, M. M.; Dean, O. M.; Walker, A. J.; Bortolasci, C. C.; Ng, C. H.; Hopwood, M.; Harvey, B. H.; Möller, M.; McGrath, J. J.; Marx, W.; Turner, A.; Dodd, S.; Scott, J. G.; Khoo, J.-P.; Walder, K.; Sarris, J.; Berk, M. The Therapeutic Potential of Mangosteen Pericarp as an Adjunctive Therapy for Bipolar Disorder and Schizophrenia. *Front. Psychiatry.* **2019**, *10*, 115. <https://doi.org/10.3389/fpsy.2019.00115>
- Benzie, I. F. F.; Devaki, M. The ferric reducing/antioxidant power (FRAP) assay for non-enzymatic antioxidant capacity: Concepts, procedures, limitations and applications. In *Measurement of Antioxidant Activity & Capacity: Recent Trends and Applications*, Apak, R., Capanolu, E., Shahidi, F. Eds.; Wiley & Sons, **2018**; Chap5, 77–106. <https://doi.org/10.1002/9781119135388.ch5>
- Beya, M. M.; Netzel, M. E.; Sultanbawa, Y.; Smyth, H.; Hoffman, L. C. Plant-Based Phenolic Molecules as Natural Preservatives in Comminuted Meats: A Review. *Antioxidants.* **2021**, *10* (2), 263. <https://doi.org/10.3390/antiox10020263>
- Cane, H. P. C. A.; Saidi, N.; Yahya, M.; Darusman, D.; Erlidawati, E.; Safrida, S.; Musman, M. Macrophylloflavone: A New Biflavonoid from *Garcinia macrophylla* Mart. (Clusiaceae) for Antibacterial, Antioxidant, and Anti-Type 2 Diabetes Mellitus Activities. *Sci. World J.* **2020**, *2020*, 2983129. <https://doi.org/10.1155/2020/2983129>
- Carrillo-Hormaza, L.; Duque, L.; López-Parra, S.; Osorio, E. High-intensity ultrasound-assisted extraction of *Garcinia madruno* biflavonoids: Mechanism, kinetics, and productivity. *Biochem. Eng. J.* **2020**, *161*, 107676. <https://doi.org/10.1016/j.bej.2020.107676>
- Cassidy, L.; Fernandez, F.; Johnson, J. B.; Naiker, M.; Owoola, A. G.; Broszczak, D. A. Oxidative stress in Alzheimer’s disease: A review on emergent natural polyphenolic therapeutics. *Complement. Ther. Med.* **2020**, *49*, 102294. <https://doi.org/10.1016/j.ctim.2019.102294>
- Chang, C.-C.; Chen, C.-W.; Owaga, E.; Lee, W.-T.; Liu, T.-N.; Hsieh, R.-H. Mangosteen Concentrate Drink Supplementation Promotes Antioxidant Status and Lactate Clearance in Rats after Exercise. *Nutrients.* **2020**, *12* (5), 1447. <https://doi.org/10.3390/nu12051447>
- Chew, Y.-L.; Lim, Y.-Y. Evaluation and Comparison of Antioxidant Activity of Leaves, Pericarps and Pulps of Three *Garcinia* Species in Malaysia. *Free Radic. Antioxid.* **2018**, *8* (2), 130–134. <https://doi.org/10.5530/fra.2018.2.19>
- Choudhury, B.; Kandimalla, R.; Elancheran, R.; Bharali, R.; Kotoky, J. Garcinia Morella Fruit, a Promising Source of Antioxidant and Anti-Inflammatory Agents Induces Breast Cancer Cell Death via Triggering Apoptotic Pathway. *Biomed. Pharmacother.* **2018**, *103* (December 2017), 562–573. <https://doi.org/10.1016/j.biopha.2018.04.068>
- Demenciano, S. C.; Silva, M. C. B. L.; Alexandrino, C. A. F.; Kato Junior, W. H.; Figueiredo, P. O.; Garcez, W. S.; Campos, R. P.; Guimarães, R. C. A.; Sarmiento, U. C.; Bogo, D. Antiproliferative Activity and Antioxidant Potential of Extracts of *Garcinia gardneriana*. *Molecules.* **2020**, *25* (14), 3201. <https://doi.org/10.3390/molecules25143201>
- Djague, F.; Lungu, P. K.; Toghueo, K. R. M.; Melogmo, D. Y. K.; Fekam, B. F. *Garcinia kola* (Heckel) and *Alchornea cordifolia* (Schumacher & Thonn.) Müll. Arg. from Cameroon possess potential antisalmonellal and antioxidant properties.

- PLoS One* **2020**, *15* (8), 0237076. <https://doi.org/10.1371/journal.pone.0237076>
- Do, H. T. T.; Cho, J. Mangosteen Pericarp and Its Bioactive Xanthonenes: Potential Therapeutic Value in Alzheimer's Disease, Parkinson's Disease, and Depression with Pharmacokinetic and Safety Profiles. *Int. J. Mol. Sci.* **2020**, *21* (17), 6211. <https://doi.org/10.3390/ijms21176211>
- Elmund, B.; Hartrianti, P. Evaluation of mangosteen (*Garcinia mangostana*) antioxidant activity in clinical trials and *in vivo* animal studies: A systematic review. *J. Appl. Pharm. Sci.* **2020**, *10* (12), 114–129. <https://doi.org/10.7324/JAPS.2020.101216>
- Engwa, G. A. Free Radical and the Role of Plant Phytochemicals as Antioxidants Against Oxidative Stress-Related Diseases. In *Phytochemicals - Source of Antioxidants and Role in Disease Prevention*, Asao, T., Asaduzzaman, M. Eds.; IntechOpen; 2018, Vol. 7; 49–74. <https://doi.org/10.5772/intechopen.76719>
- Espirito Santo, B. L. S.; Santana, L. F.; Kato Junior, W. H.; Araújo, F. O.; Bogo, D.; Freitas, K. C.; Guimarães, R. C. A.; Hiane, P. A.; Pott, A.; Filiú, W. F. O.; Asato, M. A.; Figueiredo, P. O.; Bastos, P. R. H. O. Medicinal Potential of *Garcinia Species* and Their Compounds. *Molecules*. **2020**, *25* (19), 4513. <https://doi.org/10.3390/molecules25194513>
- Essuman, E. K.; Boakye, A. A.; Tettey, C. O.; Hunkpe, G.; Kortei, N. K.; Kwansa-Bentum, H.; Waikhom, S. D.; Aninagyei, E. Evaluation of the Antidiarrheal and Antioxidant Effects of Some Chewing Sticks Commonly Used for Oral Hygiene in Ghana. *Evid. Based Complementary Altern. Med.* **2021**, *2021*, 7270250. <https://doi.org/10.1155/2021/7270250>
- García-Díez, G.; Monreal-Corona, R.; Mora-Díez, N. Complexes of Copper and Iron with Pyridoxamine, Ascorbic Acid, and a Model Amadori Compound: Exploring Pyridoxamine's Secondary Antioxidant Activity. *Antioxidants*. **2021**, *10* (2), 208. <https://doi.org/10.3390/antiox10020208>
- Gulcin, İ. Antioxidants and antioxidant methods: an updated overview. *Arch. Toxicol.* **2020**, *94* (3), 651–715. <https://doi.org/10.1007/s00204-020-02689-3>
- Gulcin, İ.; Alwasel, S. H. Metal Ions, Metal Chelators and Metal Chelating Assay as Antioxidant Method. *Processes*. **2022**, *10* (1), 132. <https://doi.org/10.3390/pr10010132>
- Gulumian, M.; Yahaya, E. S.; Steenkamp, V. African Herbal Remedies with Antioxidant Activity: A Potential Resource Base for Wound Treatment. *Evid. Based Complementary Altern. Med.* **2018**, *2018*, 4089541. <https://doi.org/10.1155/2018/4089541>
- Han, J.-H.; Park, M.-H.; Myung, C.-S. *Garcinia cambogia* Ameliorates Non-Alcoholic Fatty Liver Disease by Inhibiting Oxidative Stress-Mediated Steatosis and Apoptosis through NRF2-ARE Activation. *Antioxidants*. **2021**, *10* (8), 1226. <https://doi.org/10.3390/antiox10081226>
- Hassan, N. K. N. C.; Taher, M.; Susanti, D. Phytochemical constituents and pharmacological properties of *Garcinia xanthochymus* - a review. *Biomed. Pharmacother.* **2018**, *106*, 1378–1389. <https://doi.org/10.1016/j.biopha.2018.07.087>
- Hossain, M. A.; Dey, P.; Joy, R. I. Effect of osmotic pretreatment and drying temperature on drying kinetics, antioxidant activity, and overall quality of taikor (*Garcinia pedunculata* Roxb.) slices. *Saudi J. Biol. Sci.* **2021**, *28* (12), 7269–7280. <https://doi.org/10.1016/j.sjbs.2021.08.038>
- Idris, A. E.; Seke Etet, P. F.; Saeed, A. A.; Farahna, M.; Satti, G. M. H.; AlShammari, S. Z.; Hamza, M. A. Evaluation of metabolic, antioxidant and anti-inflammatory effects of *Garcinia kola* on diabetic rats. *Saudi J. Biol. Sci.* **2020**, *27* (12), 3641–3646. <https://doi.org/10.1016/j.sjbs.2020.08.006>
- Inoue, T.; Kainuma, M.; Baba, K.; Oshiro, N.; Kimura, N.; Chan, E. W. C. *Garcinia subelliptica* Merr. (Fukugi): A multipurpose coastal tree with promising medicinal properties. *J. Intercult. Ethnopharmacol.* **2017**, *6* (1), 121–127. <https://doi.org/10.5455/jice.20161229060034>
- Kainama, H.; Fatmawati, S.; Santoso, M.; Papilaya, P. M.; Ersam, T. The Relationship of Free Radical Scavenging and Total Phenolic and Flavonoid Contents of *Garcinia lasoara* PAM. *Pharm. Chem. J.* **2020**, *53* (12), 1151–1157. <https://doi.org/10.1007/s11094-020-02139-5>
- Kumar, M.; Pratap, V.; Nigam, A. K.; Sinha, B. K.; Singh, M. K.; Gour, J. K. Plants as a Source of Potential Antioxidants and Their Effective Nanoformulations. *J. Sci. Res.* **2021**, *65* (3), 57–72.
- Kurniawan, Y. S.; Priyanga, K. T. A.; Jumina; Pranowo, H. D.; Sholikhah, E. N.; Zulkarnain, A. K.; Fatimi, H. A.; Julianus, J. An Update on the Anticancer Activity of Xanthone Derivatives: A Review. *Pharmaceuticals*. **2021**, *14* (11), 1144. <https://doi.org/10.3390/ph14111144>
- Kusmayadi, A.; Adriani, L.; Abun, A.; Muchtaridi, M.; Tanuwiria, U. H. Antioxidant activity of mangosteen peel (*Garcinia mangostana* L.) extracted using different solvents at the different times. *Drug Invent. Today*. **2019**, *11* (1), 44–48.
- Kuswandi, A.; Tarawaan, V.; Goenawan, H.; Muchtaridi, M.; Lesmana, R. Potential Roles of *Garcinia* Family as Antimetabolic Syndrome. *J. Adv. Pharm. Technol. Res.* **2022**, *13* (1), 1–6.
- Lakey-Beitia, J.; Burillo, A. M.; La Penna, G.; Hegde, M. L.; Rao, K. S. Polyphenols as Potential Metal Chelation

- Compounds Against Alzheimer's Disease. *J. Alzheimer's Dis.* **2021**, 82 (S1), S335–S357. <https://doi.org/10.3233/JAD-200185>
- Lee, Y.; Kim, S.; Oh, Y.; Kim, Y. M.; Chin, Y. W.; Cho, J. Inhibition of Oxidative Neurotoxicity and Scopolamine-Induced Memory Impairment by γ -Mangostin: In Vitro and in Vivo Evidence. *Oxid. Med. Cell. Longev.* **2019**, 2019. <https://doi.org/10.1155/2019/3640753>
- Mello, R. F. A.; Pinheiro, W. B. S.; Benjamim, J. K. F.; Siqueira, F. C.; Chisté, R. C.; Santos, A. S. A fast and efficient preparative method for separation and purification of main bioactive xanthenes from the waste of *Garcinia mangostana* L. by high-speed countercurrent chromatography. *Arab. J. Chem.* **2021**, 14 (8), 103252. <https://doi.org/10.1016/j.arabjc.2021.103252>
- Machado, F. M. V. F.; Mariano-Nasser, F. A. C.; Furlaneto, K. A.; Fiorini, A. M. R.; Vieites, R. L. Compostos fenólicos e atividade antioxidante *in vitro* dos frutos e folhas da *Garcinia cochinchinensis* Choisy. *Rev. Energ. Agric.* **2017**, 32 (4), 393–400. <https://doi.org/10.17224/EnergAgric.2017v32n4p393-400>
- Melo, A. M.; Almeida, F. L. C.; Cavalcante, A. M. M.; Ikeda, M.; Barbi, R. C. T.; Costa, B. P.; Ribani, R. H. *Garcinia brasiliensis* fruits and its by-products: Antioxidant activity, health effects and future food industry trends – A bibliometric review. *Trends Food Sci. Technol.* **2021**, 112, 325–335. <https://doi.org/10.1016/j.tifs.2021.04.005>
- Mohamed, G. A.; Ibrahim, S. R. M. New benzophenones and a dihydroflavanonol from *Garcinia mangostana* pericarps and their antioxidant and cytotoxic activities. *Phytochem. Lett.* **2020**, 39, 43–48. <https://doi.org/10.1016/j.phytol.2020.07.007>
- Moreira, M. E. C.; Natal, D. I. G.; Toledo, R. C. L.; Ramirez, N. M.; Ribeiro, S. M. R.; Benjamin, L. A.; de Oliveira, L. L.; Rodrigues, D. A.; Demuner, A. J.; Veloso, M. P.; Santos, M. H.; Martino, H. S. D. Bacupari peel extracts (*Garcinia brasiliensis*) reduce high-fat diet-induced obesity in rats. *J. Funct. Foods* **2017**, 29, 143–153. <https://doi.org/10.1016/j.jff.2016.11.001>
- Murthy, H. N.; Joseph, K. S.; Payamalle, S.; Dalawai, D.; Ganapumane, V. Chemical Composition, Larvicidal and Antioxidant Activities of Latex from *Garcinia morella* (Gaertn.) Desr. *J. Parasit. Dis.* **2017**, 41 (3), 666–670. <https://doi.org/10.1007/s12639-016-0863-5>
- Murthy, H. N.; Dalawai, D.; Dewir, Y. H.; Ibrahim, A. Phytochemicals and Biological Activities of *Garcinia morella* (Gaertn.) Desr.: A Review. *Molecules* **2020**, 25 (23), 1–15. <https://doi.org/10.3390/molecules25235690>
- Naves, V. M. L.; Santos, M. H.; Ribeiro, I. S.; Silva, C. A.; Silva, N. C.; Silva, M. A.; Silva, G. A.; Dias, A. L. T.; Ionta, M.; Dias, D. F. Antimicrobial and antioxidant activity of *Garcinia brasiliensis* extracts. *South African J. Bot.* **2019**, 124, 244–250. <https://doi.org/10.1016/j.sajb.2019.05.021>
- Nguyen, N. H.; Nguyen, M. T.; Nguyen, H. D.; Pham, P. D.; Thach, U. D.; Trinh, B. T. D.; Nguyen, L. T. T.; Dang, S. V.; Do, A. T.; Do, B. H. Antioxidant and Antimicrobial Activities of the Extracts from Different *Garcinia* Species. *Evid. Based Complementary Altern. Med.* **2021**, 2021, 5542938. <https://doi.org/10.1155/2021/5542938>
- Omidifar, N.; Nili-Ahmadabadi, A.; Nakhostin-Ansari, A.; Lankarani, K. B.; Moghadami, M.; Mousavi, S. M.; Hashemi, S. A.; Gholami, A.; Shokripour, M.; Ebrahimi, Z. The modulatory potential of herbal antioxidants against oxidative stress and heavy metal pollution: plants against environmental oxidative stress. *Environ. Sci. Pollut. Res.* **2021**, 28 (44), 61908–61918. <https://doi.org/10.1007/s11356-021-16530-6>
- Onaolapo, A. Y.; Onaolapo, O. J. Nutraceuticals and Diet-based Phytochemicals in Type 2 Diabetes Mellitus: From Whole Food to Components with Defined Roles and Mechanisms. *Curr. Diabetes Rev.* **2020**, 16 (1), 12–25. <https://doi.org/10.2174/1573399814666181031103930>
- Pandey, R.; Kumar, B.; Rameshkumar, K. B. Rapid estimation of bioactive constituents of *Garcinia* species in the Western Ghats using UHPLC-MS/MS method. In *Diversity of Garcinia species in the Western Ghats: Phytochemical Perspective*. Rameshkumar, K. B. Ed.; Jawaharlal Nehru Tropical Botanic Garden and Research Institute, 2017; 113–122.
- Pasaribu, T.; Sinurat, A. P.; Wina, E.; Cahyaningsih, T. Evaluation of the phytochemical content, antimicrobial and antioxidant activity of *Cocos nucifera* liquid smoke, *Garcinia mangostana* pericarp, *Syzygium aromaticum* leaf, and *Phyllanthus niruri* L. extracts. *Vet. World.* **2021a**, 14 (11), 3048–3055. <https://doi.org/10.14202/vetworld.2021.3048-3055>
- Pasaribu, Y. P.; Fadlan, A.; Fatmawati, S.; Ersam, T. Biological Activity Evaluation and in Silico Studies of Polyphenylated Benzophenones from *Garcinia celebica*. *Biomedicines.* **2021b**, 9 (11), 1654. <https://doi.org/10.3390/biomedicines9111654>
- Pinto, M. M. M.; Palmeira, A.; Fernandes, C.; Resende, D. I. S. P.; Sousa, E.; Cidade, H.; Tiritan, M. E.; Correia-da-Silva, M.; Cravo, S. From Natural Products to New Synthetic Small Molecules: A Journey through the World of Xanthenes. *Molecules.* **2021**, 26 (2), 431. <https://doi.org/10.3390/molecules26020431>
- Prakash, J.; Sallaram, S.; Martin, A.; Veeranna, R. P.; Peddha, M. S. Phytochemical and Functional Characterization of Different Parts of the *Garcinia Xanthochymus* Fruit. *ACS Omega.* **2022**, 7 (24), 21172–21182. <https://doi.org/10.1021/acsomega.2c01966>

- Ramirez, C.; Gil, J. H.; Marín-Loaiza, J. C.; Rojano, B.; Durango, D. Chemical Constituents and Antioxidant Activity of *Garcinia Madruno* (Kunth) Hammel. *J. King Saud Univ. - Sci.* **2019**, *31* (4), 1283–1289. <https://doi.org/10.1016/j.jksus.2018.07.017>
- Reddy, Y. M.; Kumar, S. P. J.; Saritha, K. V.; Gopal, P.; Reddy, T. M.; Simal-Gandara, J. Phytochemical Profiling of Methanolic Fruit Extract of *Gardenia latifolia* Ait. By LC-MS/MS Analysis and Evaluation of Its Antioxidant and Antimicrobial Activity. *Plants.* **2021**, *10* (3), 545. <https://doi.org/10.3390/plants10030545>
- Sethi, S.; Joshi, A.; Arora, B.; Bhowmik, A.; Sharma, R. R.; Kumar, P. Significance of FRAP, DPPH, and CUPRAC assays for antioxidant activity determination in apple fruit extracts. *Eur. Food Res. Technol.* **2020**, *246* (3), 591–598. <https://doi.org/10.1007/s00217-020-03432-z>
- Sungpud, C.; Panpipat, W.; Yoon, A. S.; Chaijan, M. Ultrasonic-assisted virgin coconut oil based extraction for maximizing polyphenol recovery and bioactivities of mangosteen peels. *J. Food Sci. Technol.* **2020**, *57* (11), 4032–4043. <https://doi.org/10.1007/s13197-020-04436-z>
- Tjahjani, S.; Biantoro, Y.; Tjokropranoto, R. Ethyl Acetate Fraction of *Garcinia Mangostana* L Rind Study as Antimalaria and Antioxidant in *Plasmodium Berghei* Inoculated Mice. *Open Access Maced. J. Med. Sci.* **2019**, *7* (12), 1935–1939.
- Virgolin, L. B.; Seixas, F. R. F.; Janzantti, N. S. Composition, Content of Bioactive Compounds, and Antioxidant Activity of Fruit Pulps from the Brazilian Amazon Biome. *Pesq. Agropec. Bras.* **2017**, *52* (10), 933–941. <https://doi.org/10.1590/s0100-204x2017001000013>
- Wairata, J.; Sukandar, E. R.; Fadlan, A.; Purnomo, A. S.; Taher, M.; Ersam, T. Evaluation of the Antioxidant, Antidiabetic, and Antiplasmodial Activities of Xanthones Isolated from *Garcinia Forbesii* and Their *In Silico* Studies. *Biomedicines.* **2021**, *9* (10), 1380. <https://doi.org/10.3390/biomedicines9101380>
- Wairata, J.; Fadlan, A.; Purnomo, A. S.; Taher, M.; Ersam, T. Total phenolic and flavonoid contents, antioxidant, antidiabetic and antiplasmodial activities of *Garcinia forbesii* King: A correlation study. *Arab. J. Chem.* **2022**, *15* (2), 103541. <https://doi.org/10.1016/j.arabjc.2021.103541>
- Wang, M.-H.; Zhang, K.-J.; Gu, Q.-L.; Bi, X.-L.; Wang, J.-X. Pharmacology of mangostins and their derivatives: A comprehensive review. *Chin. J. Nat. Med.* **2017**, *15* (2), 81–93. [https://doi.org/10.1016/S1875-5364\(17\)30024-9](https://doi.org/10.1016/S1875-5364(17)30024-9)
- Wathoni, N.; Yuan Shan, C.; Yi Shan, W.; Rostinawati, T.; Indradi, R. B.; Pratiwi, R.; Muchtaridi, M. Characterization and Antioxidant Activity of Pectin from Indonesian Mangosteen (*Garcinia Mangostana* L.) Rind. *Heliyon* **2019**, *5* (8), e02299. <https://doi.org/10.1016/j.heliyon.2019.e02299>
- Zafar, S.; Jian, Y.-Q.; Li, B.; Peng, C.-Y.; Choudhary, M. I.; Rahman, A.-u.; Wang, W. Antioxidant Nature Adds Further Therapeutic Value: an updated review on natural xanthones and their glycosides. *Digit. Chinese Med.* **2019**, *2* (3), 166–192. <https://doi.org/10.1016/j.dcm.2019.12.005>

Quantitative Structure-Activity relationship, Molecular Docking and ADMET Screening of Tetrahydroquinoline Derivatives as Anti-Small Cell Lung Cancer Agents

Ehimen Anastasia Erazua¹, Abel Kolawole Oyebamiji²⁺, Sunday Adewale Akintelu³, Pelumi Daniel Adewole⁴, Adedayo Adelakun⁵, Babatunde Benjamin Adeleke¹

1. University of Ibadan, Department of Chemistry, Ibadan, Nigeria.
2. Bowen University, Department of Chemistry and Industrial Chemistry, Iwo, Nigeria.
3. Beijing Institute of Technology, School of Chemistry and Chemical Engineering, Beijing, China.
4. Elizade University, Department of Medical Laboratory Science, Ilara-Mokin, Nigeria.
5. Southeast Iowa Regional Medical Center, Iowa, United States.

+Corresponding author: Abel Kolawole Oyebamiji, **Phone:** +2348032493676, **Email address:** abeloyebamiji@gmail.com

ARTICLE INFO

Article history:

Received: April 19, 2022

Accepted: November 7, 2022

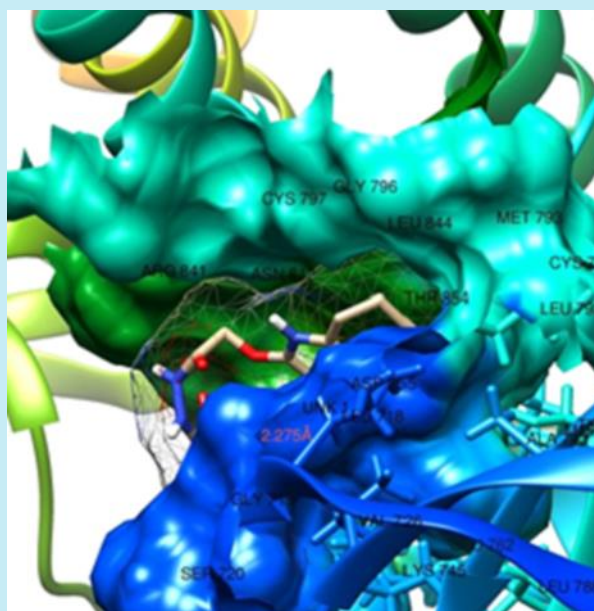
Published: January 01, 2023

Keywords:

1. Tetrahydroquinoline
2. Lung cancer
3. QSAR
4. Molecular docking
5. ADMET

Section Editors: Assis Vicente Benedetti

ABSTRACT: Lung carcinoma (LC) is responsible for almost one-third of all cancer fatalities worldwide. Tetrahydroquinoline is an organic molecule that is the semi-hydrogenated derivative of quinoline and could be found in several naturally occurring compounds such as flindersine, oricine etc. Some tetrahydroquinoline derivatives with pyrazole and hydrazide moieties were evaluated in silico against A549 (human lung cancer cell lines). The quantitative structural-activity relationship (QSAR) model created was statistically significant with validation metrics of R^2 (0.9525), R^2_{adj} (0.9314), and CV.R (0.9719). The molecular docking analysis revealed that compound C14 demonstrated the best binding affinity towards the studied protein with binding affinity value of $-10.1 \text{ kcal mol}^{-1}$ (4LRM). This is in accordance with the experimental result ($IC_{50} = 0.69$). The factors observed for ADME&T correlated well with the factors observed for the referenced drug. This study indicates that compounds C1 and C9 can be further developed as anti-epidermal growth factor receptor (EGFR) compounds. Thus, our findings may open door for the design and development of library of efficient Tetrahydroquinoline-based drug-like compounds as potential anti-LC agents.



1. Introduction

Lung carcinoma (LC) leads to the greatest number of cancer-associated morbidity and death across the globe (Siegel *et al.*, 2016). It accounted for around one-third of all cancer deaths worldwide (Ibrahim *et al.*, 2020) and is now the fourth most common reason for respiratory disease patients to be admitted to the hospitals (Salim *et al.*, 2011). This disease begins as a primary metastatic tumor in the lungs and escalate to other region of the body. Weight loss, difficulty in breathing, cough (sometimes with blood), and chest pain (Wang *et al.*, 2016) are all known signs of LC. Genetic factors, tobacco use, nutrition, air pollution, and obesity are some of the factors that have been linked to lungs cancer (Cassidy *et al.*, 2008).

Small cell lung cancer (SCLC) and non-small cell lung carcinoma (NSCLC) are the two main types of lung cancer (Collins *et al.*, 2007). NSCLC constitutes 85% of total cases and 40% of NSCLCs are adenocarcinoma (Devesa *et al.*, 2005; Morgensztern *et al.*, 2010). The most effective strategy to treat NSCLC adenocarcinoma is to target the adenosine triphosphate (ATP) binding cleft of the tyrosine kinase binding domain of epidermal growth factor receptor (EGFR) using possible inhibitors (such as gefitinib and erlotinib) (Zhang *et al.*, 2012). However, the establishment of acquired drug resistance in patients restricts its usage in therapeutic settings (Stella *et al.*, 2012). The underlying molecular reason of medication resistance is thought to be steric interferences in the EGFR and inhibitor binding properties caused by mutations. Although irreversible inhibitors such as afatinib and osimertinib were created to combat EGFR molecule acquired resistance, they were discovered to change the covalent connections in the EGFR protein structure, restricting their practical application (Sato *et al.*, 2012). As a result, there is a pressing need to find and develop novel, safe treatment regimens that can quickly overcome medication resistance caused by EGFR mutations.

Quinolines and their derivatives are a class of chemical compounds that have been shown to have a variety of biological actions, including anticancer activity (Hayat *et al.*, 2010; Mekheimer *et al.*, 2020). Tetrahydroquinolines are significant building blocks in the chemical structure of a variety of physiologically active derivatives, such as pyrazolo[3,4-b]quinolines, and have strong anticancer properties (Faidallah and

Rostomb, 2013). The quinoline and pyrazole moieties in the pyrazoloquinolines framework are excellent anticancer medicines with a wide range of pharmacological efficacies (Opoku-Temeng *et al.*, 2018). In the creation of anticancer medicines, the quinoline hydrazide scaffold plays a significant role (Mandewale *et al.*, 2017). Currently, there is a lot of interest in pyrazoloquinolines framework physiologically active molecules.

Computational studies based on ligand and structure-based techniques are regarded useful tools in medicinal chemistry for speeding up the drug design process. Molecular docking is a computer-aided drug design process that uses in silico virtual screening to determine how ligands and receptors interact utilizing their specific 3D architectures (Lapa *et al.*, 2013). A drug's drug-likeness, lipophilicity, pharmacokinetic, and toxicity qualities provide information about how the body reacts to its administration. As a result, before this medicine reaches the final (clinical) stage, it must be studied for drug-likeness and pharmacokinetic features.

Therefore, this research was aimed at identifying the descriptors that are responsible for anti-EGFR activities thereby downregulating human lung cancer and developing valid quantitative structural relationship activity (QSAR) model using the obtained descriptors as well as observing the nonbonding interactions between the selected phytochemicals (synthesized by Fathy *et al.*, 2020) and EGFR (PDB ID: 4LRM) (Yasuda *et al.*, 2013).

2. Methodology

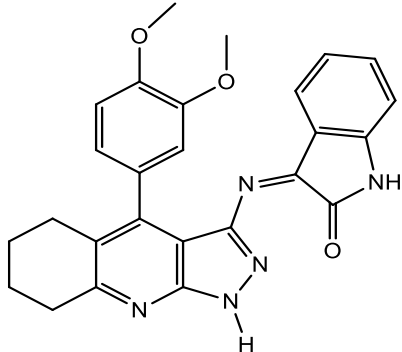
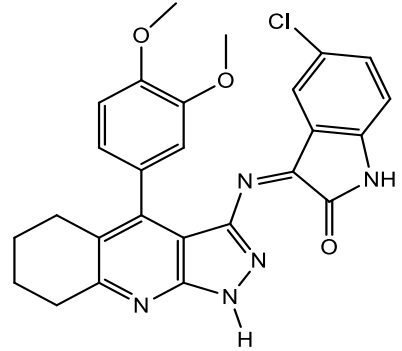
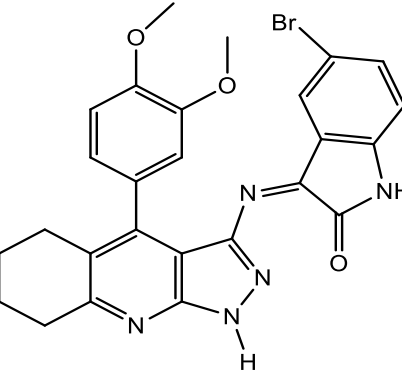
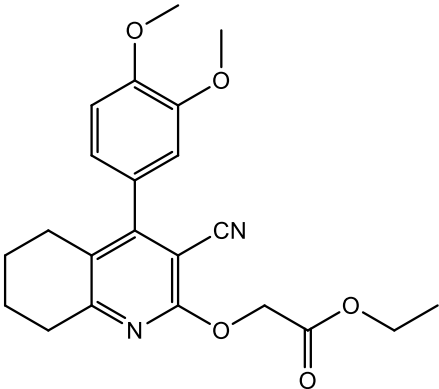
2.1 Quantum Chemical Study

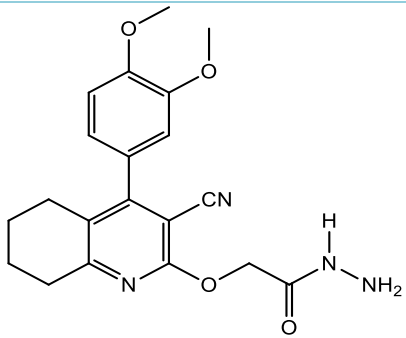
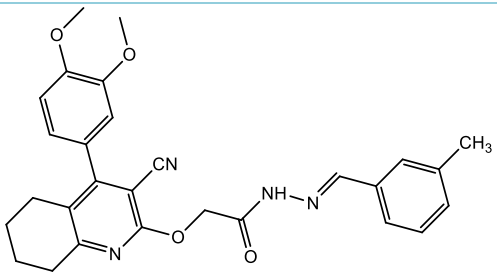
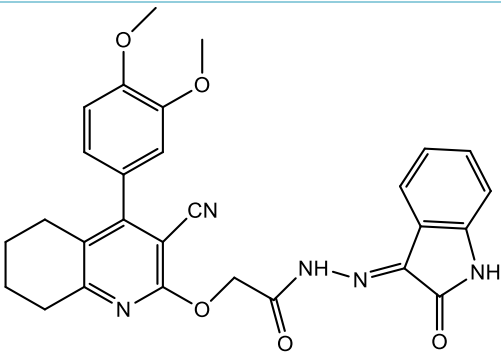
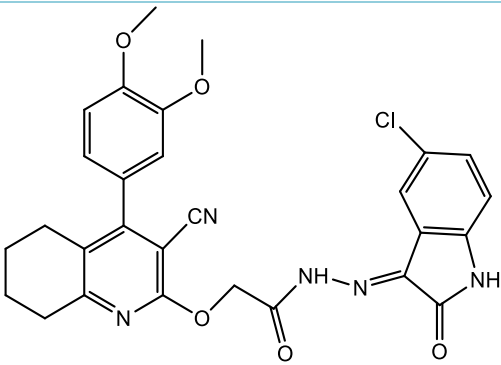
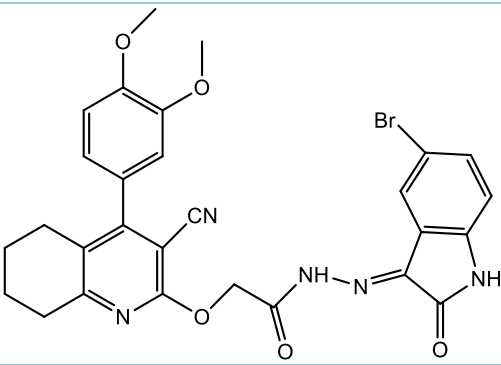
For this study, a set of 14 tetrahydroquinoline derivatives obtained from Fathy *et al.* (2020) as potential anti-EGFR agents with inhibitory activities (IC_{50}) in $\mu\text{mol L}^{-1}$ (Table 1) was investigated. All the studied compounds were optimized using Spartan 14 software (Waziri *et al.*, 2023) to achieve a stable conformation with the least amount of energy. Molecular mechanics force field (Vanommeslaeghe *et al.*, 2014) was used to remove the strain energy from the molecules, and density functional theory was used to execute the optimization using the standard 6-31+G* (d, p) basis set, which includes Becke's (1993) gradient, exchange correlation and the Yang *et al.* (2005), Parr *et al.* (1999) correlation functional (i.e., B3LYP).

Table 1. Chemical structure, IUPAC name and IC₅₀ of studied compounds.

Code	Chemical structure	IUPAC name	IC ₅₀ (μmol L ⁻¹)
C1		2-chloro-4-(3,4-dimethoxyphenyl)-5,6,7,8-tetrahydroquinoline-3-carbonitrile	85.50
C2		4-(3,4-dimethoxyphenyl)-5,6,7,8-tetrahydro-2H-pyrazolo[3,4-b]quinolin-3-amine	58.60
C3		(E)-4-(3,4-dimethoxyphenyl)-N-(4-(dimethylamino)benzylidene)-5,6,7,8-tetrahydro-1H-pyrazolo[3,4-b]quinolin-3-amine	17.90
C4		(E)-N-(2,4-dichlorobenzylidene)-4-(3,4-dimethoxyphenyl)-5,6,7,8-tetrahydro-1H-pyrazolo[3,4-b]quinolin-3-amine	35.40
C5		(E)-4-(3,4-dimethoxyphenyl)-N-(3-methylbenzylidene)-5,6,7,8-tetrahydro-1H-pyrazolo[3,4-b]quinolin-3-amine	15.40

Continue...

C6		(Z)-3-((4-(3,4-dimethoxyphenyl)-5,6,7,8-tetrahydro-1H-pyrazolo[3,4-b]quinolin-3-yl)imino)indolin-2-one	1.37
C7		(Z)-5-chloro-3-((4-(3,4-dimethoxyphenyl)-5,6,7,8-tetrahydro-1H-pyrazolo[3,4-b]quinolin-3-yl)imino)indolin-2-one	1.20
C8		(Z)-5-bromo-3-((4-(3,4-dimethoxyphenyl)-5,6,7,8-tetrahydro-1H-pyrazolo[3,4-b]quinolin-3-yl)imino)indolin-2-one	1.10
C9		Ethyl-2-((3-cyano-4-(3,4-dimethoxyphenyl)-5,6,7,8-tetrahydroquinolin-2-yl)oxy)acetate	39.60
<i>Continue...</i>			

C10		2-((3-cyano-4-(3,4-dimethoxyphenyl)-5,6,7,8-tetrahydroquinolin-2-yl)oxy)acetohydrazide	4.24
C11		(E)-2-((3-cyano-4-(3,4-dimethoxyphenyl)-5,6,7,8-tetrahydroquinolin-2-yl)oxy)-N'-(3-methylbenzylidene)acetohydrazide	3.10
C12		(E)-2-((3-cyano-4-(3,4-dimethoxyphenyl)-5,6,7,8-tetrahydroquinolin-2-yl)oxy)-N'-(2-oxoindolin-3-ylidene)acetohydrazide	2.00
C13		(E)-N'-(5-chloro-2-oxoindolin-3-ylidene)-2-((3-cyano-4-(3,4-dimethoxyphenyl)-5,6,7,8-tetrahydroquinolin-2-yl)oxy)acetohydrazide	1.06
C14		(E)-N'-(5-bromo-2-oxoindolin-3-ylidene)-2-((3-cyano-4-(3,4-dimethoxyphenyl)-5,6,7,8-tetrahydroquinolin-2-yl)oxy)acetohydrazide	0.69
5-FU		5-flurouracil	0.60

5-FU: 5-Flurouracil.

Source: [Fathy et al. \(2020\)](#)

2.3 QSAR Modelling

The obtained descriptors were extracted from the optimized compounds together and were used in developing valid and reliable QSAR model. The extracted descriptors were used as independent variable and the experimental inhibition concentration (IC_{50}) was used as dependent variable. The QSAR model development was achieved using genetic function approximation (GFA) via material studio software (Puzyn *et al.*, 2010) and the MLR-GFA equation for the model is shown in Eq. 1 below:

$$\text{Predicted } IC_{50} = \alpha + \beta_1 X_1 + \beta_2 X_2 + \dots + \beta_n X_n \quad (1)$$

where α is the regression constant, X_1, X_2, \dots, X_n are the descriptors and $\beta_1, \beta_2, \dots, \beta_n$ are the coefficient of the corresponding descriptors. The developed QSAR model was validated by considering series of statistic factors such cross validation R^2 ($CV.R^2$) and Adjusted R^2 (R_a^2) (Eqs. 2 and 3) and the developed model will be considered valid when the calculated value for R_a^2 and $CV.R^2$ were ≥ 0.6 and ≥ 0.5 respectively.

$$CV.R^2 = 1 - \frac{\sum(Y_{obs} - Y_{cal})^2}{\sum(Y_{obs} - \bar{Y}_{obs})^2} \quad (2)$$

where Y_{obs} = experimentally observed IC_{50} , Y_{cal} = calculated IC_{50} and \bar{Y}_{obs} = average of the experimentally observed IC_{50}

$$R_a^2 = \frac{(N-1) \times R^2 - P}{N-1-P} \quad (3)$$

where N = no of compounds observed, P = no of molecular descriptors used in the QSAR model and R^2 = R -squared value obtained from the QSAR model.

2.4 Molecular Docking

Crystal structure of the EGFR (PDB ID: 4LRM) (Yasuda *et al.*, 2013) was retrieved from the Protein Data Bank (<https://www.rcsb.org/>) (Yasuda *et al.*, 2013) and employed as target receptors in this study. Also, the tetrahydroquinoline derivatives (Table 1) synthesized by Fathy *et al.* (2020) were used as ligands. The 2D structures of the ligands were drawn with the help of Chem Professional 15.0 and saved as structure-data files (SDFs).

Chimera 1.14 was employed to prepare the protein by eliminating water molecules, numerous ligands, nonprotein component, and other extraneous substances

downloaded together with the proteins (Pettersen *et al.*, 2004). The ligands were saved as SDF files and treated protein was converted to PDBQT format using Autodock tool 4.2. Grid box size $x = 18.49 \text{ \AA}$, $y = 22.59 \text{ \AA}$, size $z = 17.09 \text{ \AA}$ and grid center dimensions $x = 41.77$, $y = 361.60$ and $z = 17.09$ were set for 4LRM.

The prepared ligands were docked into the binding site of the receptor which was determined by using CastP online server) and the docking calculation was performed using Autodock Vina from PyRX workspace (Trott and Olson, 2010). The inhibitors were treated as flexible throughout the docking simulations. A force-field-based energy scoring function was used to score the ligand orientations, and the highest-scoring binding structure was chosen. Finally, 3D views of the protein-ligand complex were analyzed by using UCSF Chimera 1.14 and Discovery Studio 2020 was used to create the 2D images of the molecular interactions (Capra *et al.*, 2009; Oyeneyin *et al.*, 2022).

2.5 ADMET Screening

The biological action of medications and their metabolic fate in an organism are intimately related to their absorption, distribution, metabolism, and excretion (ADME) and toxicity (ADMET) qualities. In silico predictive models were used to determine the ADMET properties of the test substances. The ADME properties of the substances were determined using the SwissADME online server (<http://www.swissadme.ch/index.php/>) (Daina *et al.*, 2017). The acute toxicity class, LD50, hepatotoxicity, carcinogenicity, mutagenicity, cytotoxicity, and immunotoxicity of the substances were all predicted using the ProTox-II web server (Banerjee *et al.*, 2018).

The Swiss ADME and ProTox-II online servers take one or more query molecules in canonical SMILES format as input and use a large database to accurately predict the physicochemical properties, pharmacokinetics, solubility, lipophilicity, drug-likeness, bioavailability score, therapeutic properties, and toxicity of compounds.

3. Results and Discussion

3.1 Calculated Descriptors

The calculated descriptors from optimized compounds were screened and for further processing. The calculated descriptors were the energy of the highest occupied molecular orbital (E_{HOMO}), lowest unoccupied

molecular orbital energy (E_{LUMO}), dipole moment (DM), volume, area, lipophilicity (log P), polar surface area (PSA), number of hydrogen bond donor (HBD), hydrogen bond acceptor (HBA). The calculated descriptors also helped in QSAR study. As shown in Table 2, C3 possess higher E_{HOMO} value and according to report by Semire *et al.* (2017), compound with high E_{HOMO} value possess greater tendency to donate electron

to the neighboring compounds and it is expected to interact with the target; therefore, C3 with -4.29 eV is expected to interact well with neighboring compounds. As reported by Oyebamiji *et al.* (2018), the lower the E_{LUMO} value the better the tendency of the compound to interact with the target; therefore, C8 proved to have a tendency to interact than other studied compounds (Table 2).

Table 2. Selected descriptors for the QSAR model.

	E_{HOMO} eV	E_{LUMO} eV	DM debye	MW	Area	Vol	PSA	Log p	Pol	HBD	HBA
C1	-5.27	-2.24	7.73	328.8	339.08	322.96	36.526	1.24	66.86	0	4
C2	-5.03	-1.31	11.48	324.38	340.27	325.26	67.428	-0.16	66.88	2	6
C3	-4.29	-1.99	6.56	455.56	492.87	474.59	54.06	0.66	79.33	1	7
C4	-6.05	-1.99	3.39	481.38	471.57	452.07	52.682	1.12	77.09	1	6
C5	-5.93	-1.78	3.43	426.5	461.31	43.34	52.55	1.66	76.36	1	6
C6	-5.94	-2.54	8.35	453.5	453.91	445.24	79.11	0.56	76.69	2	8
C7	-5.86	-2.91	9.09	487.94	467.07	459.43	79.3	0.42	77.95	2	8
C8	-6.12	-3.78	5.63	532.4	475.79	465.79	80.499	0.69	78.61	2	8
C9	-6.35	-1.67	8.61	396.44	430.16	404.16	62.633	0.64	73.05	0	6
C10	-6.35	-1.66	9.72	382.42	407.97	380.79	98.07	-0.86	71.15	2	8
C11	-6.09	-1.68	8.6	484.56	524.08	498.26	77.218	2.3	80.75	1	8
C12	-5.93	-2.25	13.74	511.54	523.44	501.31	98.47	-0.37	81.17	2	10
C13	-5.92	-2.38	11.48	545.98	533.57	514.42	95.51	-0.51	82.27	2	10
C14	-5.91	-2.39	11.62	590.43	536.62	518.51	94.66	-0.24	82.6	2	10

DM: dipole moment; MW: molecular weight; Vol: volume; PSA: polar surface area; POL: polarizability; HBD: hydrogen bond donor and HBA: hydrogen bond acceptor.

3.2 QSAR Study

Five distinct models were developed and the best model was chosen and reported among them, since it met the minimum conditions for the evaluation of a valid

QSAR model, as reported by Veerasamy *et al.* (2011). Tables 2–5 as well as Figs. 1 and 2 present the findings of the QSAR study and the developed QSAR model was presented in Eq. 4. The selected and reported model is given by the Eq. 4 with the following validation terms: $R^2 = 0.9525$, $adj.R^2 = 0.9314$ and $CV.R^2 = 0.9719$.

$$\text{Predicted IC}_{50} = 179.0741 + 6.54433 (\text{DM}) - 5.73413 (\text{Log P}) - 28.2133 (\text{HBA}) + 0.215819 (\text{MW}) \quad (4)$$

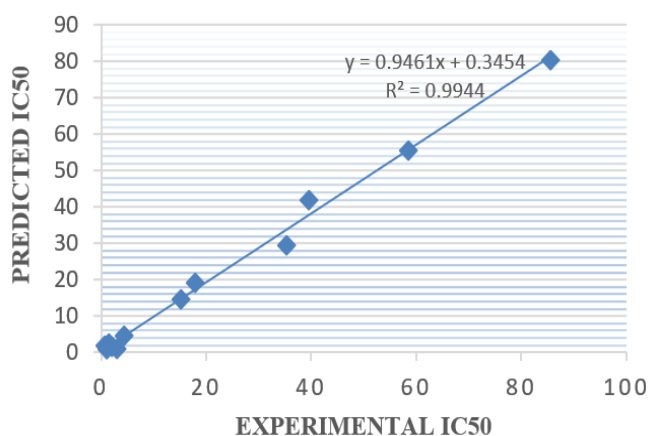


Figure 1. Scatter plot of predicted IC_{50} versus the experimental IC_{50} for the reported model.

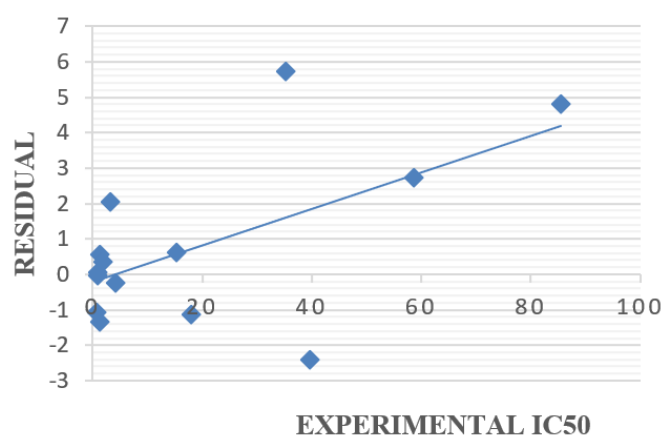


Figure 2. Scatter plot of residual versus the experimental IC_{50} for the reported model.

The negative coefficients of the Log P and HBA descriptors clearly suggested that they have a negative contribution to the compounds inhibitory actions. This suggests that reduction in the amount of these independent descriptors improves the inhibition concentration of the studied compounds, and vice versa. The positive coefficients of dipole moment and molecular weight in the model, on the other hand, indicated that these independent descriptors contributed positively to the inhibitory effects of the ligands under study. It suggests that by increasing the amount of these descriptors in the structures with

potential anti-EGFR therapeutic agents, the inhibition concentration these drug-like compounds increases and vice versa (Ibrahim *et al.*, 2020; Oke *et al.*, 2022).

Also, as reported by Oyebamiji *et al.* (2021), inhibition concentration of any developed QSAR model is not enough to judge the potency of such model and this therefore called for validation of the developed QSAR model. The calculated factors considered for validation were cross validation (CV.R²) and adjusted squared correlation coefficient (adj.R²).

Table 3. Statistical parameters and limit needed for the QSAR model assessment.

Statistical Parameters	Details	Accepted Value	Selected model
R ²	correlation coefficient	≥ 0.6	0.9525
R ² _{adj}	Squared correlation coefficient	≥ 0.6	0.9314
CV.R	Cross-validation coefficient	≥ 0.5	0.9719
CV.R – R ² _{adj}	Difference between CV.R and R ²	≥ 0.3	0.0405

The validation factors revealed in this study matched the validation parameters in Table 3, indicating that the model created is both predictive and resilient.

For the compounds under examination, Table 4 displays the experimental IC₅₀, predicted IC₅₀, and residual values. The minimal residual values observed between the experimental and predicted IC₅₀ in the table validated the model's high anticipated power (meaning that the reported model was reliable with high predicted power). Figure 1 also shows a plot of the predicted IC₅₀ versus experimental IC₅₀ for the compounds, and the

distribution of the predicted IC₅₀ and experimental IC₅₀ of the compounds along the line reaffirmed the model's dependability. The R² values of the internal validation (0.9525) and the plot (0.9944) agreed with one another, confirming the reported model's stability and reliability (Grisoni *et al.*, 2018). Furthermore, Fig. 2 shows a scatter plot of residuals against the experimental IC₅₀ which the remarkable appearance of both sets of residuals on the plot's top and lower sides confirms that the reported model was free of methodological mistake (systematic deviations).

Table 4. The experimental IC₅₀, predicted IC₅₀ and the residual values for the studied compounds.

	Experimental IC ₅₀	Predicted IC ₅₀	Residual
C1	85.5	80.66	4.84
C2	58.6	55.85	2.75
C3	17.9	19.05	-1.15
C4	35.14	29.45	5.69
C5	15.4	14.77	0.63
C6	1.37	2.68	-1.31
C7	1.2	1.75	0.55
C8	1.1	1.16	-0.06
C9	39.6	42.03	-2.43
C10	4.2	4.44	-0.24
C11	3.1	1.04	2.06
C12	2.0	1.62	0.38
C13	1.06	1.01	0.05
C14	0.69	1.79	-1.10

Table 6 shows the correlation statistical analysis of the independent descriptors in the presented model, which revealed that there is no relationship between the descriptors in the model. This demonstrated the good performance of the descriptors utilized in creating the reported model.

The variation inflation factor (VIF) data were also examined to see if the descriptors employed in the model had any multicollinearity issues. In general, a VIF value of 1 or a value between 1 and 5 indicates that there is no intercorrelation between the descriptors. Nevertheless, if the VIF value is larger than 10, the produced model is

unstable, and the model should be rechecked if desired (Beheshti *et al.*, 2016). Table 5 shows that the VIF values for each descriptor were less than 5, indicating that the descriptors were highly orthogonal to each other and that there was no intercorrelation between them. This demonstrates that the descriptors used to construct the provided model do not have a multicollinearity problem.

A one-way analysis of variance was used to determine the association between the descriptors and each compound's biological activity (ANOVA). Table 5

shows the probability value of each descriptor at the 95% confidence level ($p = 0.05$). As a result, the alternative hypothesis stating that there is a direct relationship between the biological activity of each compound and the descriptor swaying the built model is accepted; however, the null hypothesis stating that there is no direct relationship between the biological activity of each compound and the descriptor swaying the created model is rejected.

Table 5. Statistical parameters that affect the model.

Descriptors	Regression coefficient	P-value (confidence interval)	VIF	Standard error
DM	-4.43867	0.2580	3.297	3.47832
MW	-0.31745	0.5345	3.541	0.476184
HBA	-8.97918	0.4406	4.349	10.7244
Log P	-1.51775	0.8604	2.202	8.19602

Table 6. Coefficient of Pearson's correlation for descriptor in QSAR model.

Intercorrelation	Constant	DM	MW	HBA	Log P
Constant	225.902				
DM	-10.9752	1.29913			
MW	-0.607345	0.0415951	0.00386242		
HBA	20.7074	-2.59999	-0.197066	11.9110	
Log P	-12.6244	0.728923	-0.0698522	4.41221	10.2917

3.2 Molecular Docking Studies

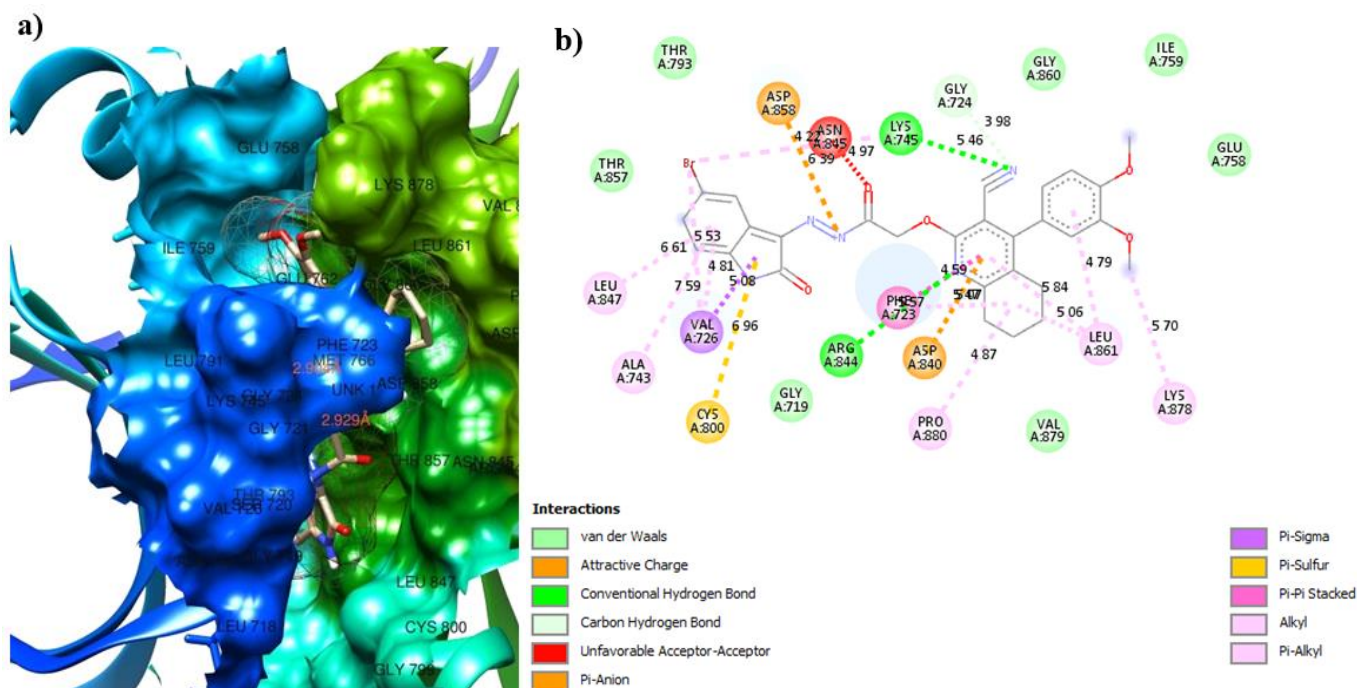
Molecular docking technique was used to recognize the compounds which bind well to the EGFR pocket. All tested compounds had strong binding affinity with the receptor. They perfectly fit into the active site of the receptor by interacting with the amino acid residue in the active site of the receptor. The protein residues involved in the interaction, types of interaction involved, distance and binding affinity obtained for each complex formed by the studied compounds and standard were displayed in Tables 7 and 8. The protein residues involved in the interaction and type of interactions observed for C14-EGFR complex was also displayed in Fig. 3.

The complexes formed by 4LRM receptor showed good interactions (Fig. 3). The tested compounds showed binding affinity ranging from -4.6 to -10.1 kcal mol⁻¹. According to Adepoju *et al.* (2022), the lower the binding affinity value of any compound, the better the

inhibiting ability of such compound; thus, Compound C14 with -10.1 kcal mol⁻¹ was observed to have highest tendency to inhibit the studied receptor than other studied compounds. Pi-anion interaction was observed in all the complexes except in compounds C5, C7, C8, and C9. A salt bridge was formed between Asp858, and the nitro group of the ligand in complex formed by compound C12. Complexes formed by compound C4, C6, C8, C11, and C14 showed a pi-sulfur interaction between Cys800 and the respective ligands. Pi-sigma bond was observed for all complexes except for complexes formed by C2, C5, C9, C12 and C13. only the complex formed by C14 had unfavorable acceptor-acceptor interaction. Complexes formed by compound C2, C5, C9, C10, C11, C12, and C14 showed a conventional hydrogen bond while others do not. Other interactions observed in the complexes are carbon hydrogen bond, pi-pi stacked, alkyl and pi-alkyl (Table 7).

Table 7. Binding Interactions and Binding Affinity between Ligands and Receptor 4LRM.

	Hydrogen interaction	Hydrophobic Interaction	ΔG (kcal mol ⁻¹)
C1	-	Thr793, Ala743, Cys800, Ser720, Gly724, Gly719, Arg844, Asn845, Asp858, Lys745, Glu762, Leu718, Thr857, Met766, Leu847, Val726	-8.4
C2	Glu762, Asp858	Leu847, Thr793, Thr857, Met766, LEU791, Lys745, Phe859, Ser720, Gly719, Gly724, Arg844, Phe723, Asn845, Ala743, Val726, Leu718,	-8.1
C3	-	Ala743, Val726, Leu847, Leu718, Gly799, Cys800, Gly719, Arg844, Ser720, Gly721, Phe723, Gly724, Asp858, Asn854, Lys745, Met766, Thr857, Thr793,	-8.2
C4	-	Thr857, Thr793, Val726, Leu718, Gly799, Leu847, Gly719, Cys800, Ser720, Arg844, Leu802, Gly724, Asp803, Phe723, Asp840, Asp858, Asn845, Lys745	-8.7
C5	Asp858, Lys745	Lys878, Phe723, Val879, Pro880, Asp840, Leu861, Gly860, Glu762, Ala755, Ile759, Leu747, Glu758, Lys754, Ala722,	-8.0
C6	-	Arg844, Asp803, Cys800, Gly719, Asn845, Leu847, Val726, Ala743, Leu718, Thr857, Lys745, Asp840, Phe723, Gly724, Asp858, Ser720, Gly721	-7.8
C7	-	Asp803, Arg844, Leu802, Cys800, Glu762, Thr857, Leu847, Val726, Leu718, Asp858, Lys745, Gly719, Thr725, Gly724, Ser720, Phe723, Gly721	7.6
C8	-	Arg844, Asp803, Leu802, Cys800, Gly762, Lys 745, Thr857, Val726, Leu847, Leu718, Asp856, Gly719, Gly724, Phe723, Asp840, Asn845, Ser720, Gly721	-8.4
C9	Thr793, Lys745	Met766, Thr793, Asp858, Gly724, Asn845, Arg844, Phe723, Asp840, Gly721, Ser720, Gly719, Val726, Cys800, Leu718, Leu847, Aa743, Thr857	-8.4
C10	Gln794, Met796	Leu795, Leu718, Leu847, Cys800, Gly719, Ser720, Gly724, Arg844, Phe723, Asp858, Asn845, Glu762, Lys745, Met766, Thr857, Val726, Ala743, Thr793	-6.9
C11	-	Glu762, Lys745, Val726, Met766, Thr793, Ala743, Thr857, Arg 844, Cys800, Ser720, Gly724, Asp840, Leu861, Phe723, Asn845, Asp858, Gly719, Leu847	-8.4
C12	Lys745	Cys800, Asn845, Asp858, Gly724, Glu758, Leu747, Leu861, Gly860, Lys878, Pro880, Val879, Phe723, Asp840, Arg844, Val726, Thr857, Leu847	-9.5
C13	Arg844	Thr793, Thr857, Lys745, Glu762, Cys800, Gly724, Asp840, Leu861, Asp858, Phe723, Asn845, Gly721, Ser720, Gly719, Gly799, Ala743, Leu718, Leu847, Leu795, Val726	-9.4
C14	Lys745, Arg844	Thr857, Thr793, Asp858, Asn845, Gly724, Gly860, Ile759, Glu758, Lys878, Leu861, Val879, Pro880, Asp840, Phe723, Gly719, Cys800, Val726, Ala743, leu847 Thr857	-10.1

**Figure 3.** (a) 3D and (b) 2D views of the molecular interactions of amino acid residues of receptor 4LRM with compound 14.

3.3 ADMET Profiling

Regardless of the compounds inhibitory capability against target proteins, the ADMET properties of the compounds are a critical element in determining their pharmacological activities such as drug-likeness, lipophilicity, pharmacokinetics, and toxicity profile when used as drug. In silico ADMET prediction is a quick and low-cost method of determining whether a molecule will be well distributed to its intended site of action, metabolized efficiently, and quickly removed from the body without causing hazardous side effects (Ntie-Kang, 2013). The prediction output for drug likeness, lipophilicity pharmacokinetics, and toxicity profiles of test molecules are displayed on Tables 9–11 respectively.

Drug-likeness analysis is a qualitative evaluation of oral bioavailability based on structural or physicochemical examination of molecules. In this study the rule base filters which include Lipinski's *et al.*

(2013), Veber *et al.* (2002), and Muegge and Ghose (2001) rules were employed to determine if a molecule is impermeable or badly absorbed. If a molecule does not break more than two rules, it is deemed orally bioavailable. As indicated on Table 8, the molecular weights of the compounds range from 130 (5-FU) to 590 g mol⁻¹ (C14). The HBA ranged from 3 to 8 and HBDs ranged from 0 to 2; number of rotatable bonds are between 0 (5-FU) to 9 (C11). The TPSA are between 55.14 (5-FU) and 134.93 (C13 and C14). MR ranged from 27.64 (5-FU) to 150.11 (C14). The less the drug candidate can infiltrate, the higher the TPSA and molecular weight values are, and vice versa.

A target molecule's synthetic accessibility (SA) score is used to evaluate it before it is synthesized. It is a parameter used to rate the ease or difficulty of synthesizing a compound. The SA score runs from 1 (very easy) to 10 (very tough) (Swierczewska *et al.*, 2015). The studied compounds possess good SA, with SA scores ranging from 1.52 to 4.13 as shown in Table 8.

Table 8. Drug-likeness prediction output of test compounds.

Sample code	Chemical formula	MW (g mol ⁻¹)	Rotatable bond	HBA	HBD	TPSA	MR	SA
C1	C ₁₈ H ₁₇ ClN ₂ O ₂	328.79	3	4	0	55.14	89.81	2.93
C2	C ₁₈ H ₂₀ N ₄ O ₂	324.38	3	4	2	86.05	94.15	3.11
C3	C ₂₇ H ₂₉ N ₅ O ₂	455.55	6	5	1	75.63	137.64	4.04
C4	C ₂₅ H ₂₂ Cl ₂ N ₄ O ₂	481.37	5	5	1	72.39	133.46	3.82
C5	C ₂₆ H ₂₆ N ₄ O ₂	426.51	5	5	1	72.39	128.4	3.89
C6	C ₂₆ H ₂₃ N ₅ O ₃	453.49	4	6	2	101.49	133.76	3.91
C7	C ₂₆ H ₂₂ ClN ₅ O ₃	487.94	4	6	2	101.49	138.77	3.92
C8	C ₂₆ H ₂₂ BrN ₅ O ₃	532.39	4	6	2	101.49	141.46	3.97
C9	C ₂₂ H ₂₄ N ₂ O ₅	396.44	8	7	0	90.67	107.00	3.55
C10	C ₂₀ H ₂₂ N ₄ O ₄	382.41	7	7	2	119.49	101.81	3.36
C11	C ₂₈ H ₂₈ N ₄ O ₄	484.55	9	7	1	105.83	137.05	4.02
C12	C ₂₈ H ₂₅ N ₅ O ₅	511.53	8	8	2	134.93	142.41	4.06
C13	C ₂₈ H ₂₄ ClN ₅ O ₅	545.97	8	8	2	134.93	147.42	4.06
C14	C ₂₈ H ₂₄ BrN ₅ O ₅	590.42	8	8	2	134.93	150.11	4.13
5-FLU	C ₄ H ₃ FN ₂ O ₂	130.08	0	3	2	65.72	27.64	1.52

5-FLU: 5-fluorouracil; MW: molecular weight; MR: molar refractivity; HBA: hydrogen bond acceptor; HBD: hydrogen bond donor; TPSA: topology polar surface area; MR: molar refractivity; SA: synthetic accessibility.

The partition coefficient between n-octanol and water (log P_{o/w}) is the fundamental descriptor for lipophilicity (Log P). The tested compounds' log P values, water solubility, and bioavailability are reported in Table 9. Lipophilicity and water solubility are two important physicochemical qualities that influence a drug's behavior. An orally delivered medicine should be lipophilic enough to pass through the intestinal lining, permeate target cell membranes, and be hydrophilic enough to move through the aqueous blood. The higher a compound's log P value, the more lipophilic it is and the less water soluble it is (Johnson *et al.*, 2021). The log P values for the studied compounds ranged from

–0.13 (5-FU) to 5.77 (C4), which revealed that C4 is not as soluble as the referenced drug (Table 9).

The Silicos-IT prediction model was used to calculate water solubility as the logarithm of molar solubility in water (log S). The log S value of a drug affects its capacity to dissolve, and the lower the value, the better (Darvas *et al.*, 2002). The compounds had log S values ranging from –0.76 (poorly soluble, C4) to –3.5 (soluble, C10) indicating. This trend is in accordance with the values of log P earlier discussed.

The bioavailability score employs the total charge, the TPSA, and the Lipinski filter to provide a semiquantitative indication of the compounds'

likelihood of being effective oral medicines (Testa and Krämer, 2009). The less the drug candidate can penetrate, the higher the TPSA and molecular weight values are, and vice versa. The bioavailability score of the test compounds is 0.55, which means that these

compounds have a 55% chance of a minimum of 10% oral absorption in rat or human colon carcinoma (Caco-2) permeability (Testa and Krämer, 2009) indicating that they could be useful as oral drug.

Table 9. Predicted lipophilicity (Log P) values, water solubility and bioavailability of the studied compounds.

Sample code	iLOGP	XLOGP3	WLOGP	MLOGP	Silicos-IT Log P	Consensus Log P	ESOL Log S	Solubility Class	BS
C1	3.13	4.33	4.17	2.23	5.03	3.78	-4.79	Moderately soluble	0.55
C2	2.08	3.27	3.11	2.17	3.64	2.85	-4.18	Moderately soluble	0.55
C3	3.45	5.37	5.34	3.96	6	4.82	-6.11	Poorly soluble	0.55
C4	3.15	6.5	6.58	5.03	7.58	5.77	-7.06	Poorly soluble	0.55
C5	3.25	5.61	5.58	4.29	6.83	5.11	-6.17	Poorly soluble	0.55
C6	2.18	4.58	4.02	3.31	5.62	3.94	-5.73	Moderately soluble	0.55
C7	2.46	5.21	4.68	3.78	6.26	4.48	-6.33	Poorly soluble	0.55
C8	2.35	5.27	4.78	3.88	6.3	4.52	-6.64	Poorly soluble	0.55
C9	3.44	3.96	3.46	1.6	4.72	3.44	-4.57	Moderately soluble	0.55
C10	2.46	2.27	1.88	0.78	2.77	2.03	-3.5	Soluble	0.55
C11	3.44	5.02	4.35	2.16	6.04	4.2	-5.78	Moderately soluble	0.55
C12	2.51	4.53	2.8	1.22	4.83	3.18	-5.69	Moderately soluble	0.55
C13	2.91	5.16	3.45	1.68	5.48	3.74	-6.29	Poorly soluble	0.55
C14	2.74	5.23	3.56	1.78	5.52	3.77	-6.61	Poorly soluble	0.55
5-FU	0.44	-0.89	-0.38	-0.32	1.78	0.13	-0.58	Very soluble	0.55

5-FU: 5-fluorouracil; BS: bioavailability score.

Table 10 showed the result of pharmacokinetics prediction of the test molecules. P-glycoprotein (P-gp), a well-studied plasma membrane ATP-binding cassette transporter, is responsible for the active efflux of xenobiotics through biological membranes to protect the body against foreign substances. This efflux pump contributes to drug resistance by preventing some medications from entering sensitive regions. Except for C13 and C14, all the chemicals had a high likelihood of being absorbed in the gastrointestinal tract. This shows that when these chemicals are taken orally, they have the potential to be absorbed in the gastrointestinal tract (Lynch and Price, 2007).

The enzyme cytochrome P450 monooxygenase plays an important role in the metabolism and removal of drugs. It is a group of isoenzymes that catalyzes several processes in the first phase of drug metabolism (Hollenberg, 2002). The suppression of five main isoforms (CYP1A2, CYP2C19, CYP2C9, CYP2D6, and CYP3A4), which are substrates of 50–90% of medications and primary sources of pharmacokinetics-related drug-drug interactions. Because these enzymes are not inhibited, the chemicals have a high chance of being converted and, as a result, of becoming bioavailable when taken orally. Inhibition of the CYP isomers by the substances, on the other hand, can result in poor bioavailability due to failure to be metabolized and severe side effects due to their retention (Sahin and Benet, 2008). Compounds C1, C2, and C9 are potential

inhibitor of CYP1A2 among the tested compounds. All the compounds are potential inhibitor of CYP2C19 except compound C2, C10, and standard 5-FU. As shown in table 10, only compound C2 and 5-FU (referenced drug) were non-inhibitors of CYP2C9 while other studied compounds proved to possess the ability to inhibit CYP2C19. Compounds C1, C2, C3, C6, C9, and C12 are potential inhibitor of CYP2D6 while others are not. All compounds are potential inhibitors of CYP3A4, except compounds C4, C7, C8, 5-FU. It was observed that the standard 5-FU was is not an inhibitor of any cytochrome P450, which suggests that the standard is more likely to be converted and bioavailable after oral delivery than the compounds investigated.

The skin is a selective barrier that allows diverse compounds to permeate through at different rates based on their physicochemical properties (Dixon *et al.*, 2006). Hence, the skin permeability (LogKp) is a key parameter for the evaluation of molecules that might require transdermal administration (Dixon *et al.*, 2006). The more negative the log Kp (with Kp in cm s^{-1}), the less skin permeant is the molecule. As highlighted in Table 10 log Kp (cm s^{-1}) of the test compounds ranged from -7.73 (least permeant) to -4.62 (most permeant).

The skin acts as a selective barrier, allowing various molecules to infiltrate at varied rates depending on their physicochemical qualities (Cheng and Dixon, 2003). As a result, skin permeability (LogKp) is an important characteristic to consider when evaluating compounds

that may need to be administered transdermally. The lower the log K_p (in cm s⁻¹), the less permeant the molecule is to the skin. The test compounds' log K_p (cm s⁻¹) ranged from -7.73 (least

permeant) to -4.62 (most permeant), as shown in Table 9. The values indicate that the compounds show low skin permeability.

Table 10. Pharmacokinetics prediction output of test compounds.

Sample code	GI absorption	P-gp	CYP 1A2 inhibitor	CYP2C19 inhibitor	CYP2C9 inhibitor	CYP2D6 inhibitor	CYP3A4 inhibitor	Log K _p (cm s ⁻¹)
C1	High	No	Yes	Yes	Yes	No	Yes	-5.23
C2	High	Yes	Yes	No	No	Yes	Yes	-5.96
C3	High	Yes	No	Yes	Yes	Yes	Yes	-5.27
C4	High	Yes	No	Yes	Yes	No	No	-4.62
C5	High	Yes	No	Yes	Yes	No	Yes	-4.92
C6	High	Yes	No	Yes	Yes	Yes	Yes	-5.81
C7	High	Yes	No	Yes	Yes	No	No	-5.58
C8	High	Yes	No	Yes	Yes	No	No	-5.81
C9	High	No	Yes	Yes	Yes	Yes	Yes	-5.91
C10	High	Yes	No	No	Yes	No	Yes	-7.02
C11	High	Yes	No	Yes	Yes	Yes	Yes	-5.69
C12	High	Yes	No	Yes	Yes	Yes	Yes	-6.2
C13	Low	Yes	No	Yes	Yes	No	Yes	-5.97
C14	Low	Yes	No	Yes	Yes	No	Yes	-6.19
5-FU	High	No	No	No	No	No	No	-7.73

5-FLU: 5-fluorouracil; GI: gastrointestinal; and P-gp: P-glycoprotein.

The toxicity prediction output of the compounds is shown in Table 11. Compounds C8, C12, C13, and C14 fall under the oral toxicity class 5, while other tested compounds fall under oral toxicity class 4. Human hepatotoxicity (H-HT) is a term that describes and illustrates numerous types of liver damage that can lead to the organ failing or death (Cheng and Dixon, 2003). Compounds C10, C11, C12, C13, and C14 were hepatotoxic. Carcinogenicity compounds can damage the genome, the disrupt cellular metabolic processes and cause cancer. Compounds C2, C3, C4, C5, C6, C11, C12 and the standard are carcinogenic. Immunotoxicity is defined as the negative impact of toxic compounds on the functioning of both the local and systemic immune

systems. Only compounds C1, C9, C10 and the standard are nonimmunotoxic. The mutagenicity test is used to identify substances that can cause mutations or malignant growth in humans (Loving *et al.*, 2009). Compounds C2, C3, C4, C5, C6, and C12 are mutagenic, and only compound C2 is cytotoxic among the test compounds. The study clearly revealed that most of the compounds possess one form of toxicity except for compounds C1 and C9, which did not show any tendency for hepatotoxicity, carcinogenicity, immunotoxicity, mutagenicity and cytotoxicity, indicating that they are safe as possible therapeutic agents. These two compounds did not violate any of the base rule filter, they are moderately soluble and not P-gp substrate.

Table 11. Toxicity profiles of test compounds.

Code	C1	C2	C3	C4	C5	C6	C7	C8	C9	C10	C11	C12	C13	C14	5-FU
LD50 (mg kg ⁻¹)	753	1000	1000	1000	1000	1000	1000	4000	750	750	750	3000	2001	3009	1923
Toxicity Class	4	4	4	4	4	4	4	5	4	4	4	5	5	5	4
Hepatotoxicity	-	-	-	-	-	-	-	-	-	+	+	+	+	+	-
Carcinogenicity	-	+	+	+	+	+	-	-	-	-	+	+	-	-	+
Immunotoxicity	-	+	+	+	+	+	+	+	-	-	+	+	+	+	-
Mutagenicity	-	+	+	+	+	+	-	-	-	-	-	+	-	-	-
Cytotoxicity	-	-	-	-	-	-	-	-	-	-	-	-	-	+	-

5-FLU: 5-fluorouracil.

4. Conclusions

Fourteen selected tetrahydroquinoline derivatives having pyrazole and hydrazide moieties were evaluated in silico against human lung cancer cell lines A549. QSAR technique was used to build a model found to be statistically fit with a very high predictive power and the predicted bioactivity represented the experimental results well. Molecular docking analysis showed that compound C14 demonstrated the best binding affinity, but the drug-likeness, pharmacokinetic properties and toxicity profile of the test compounds revealed that compound C1 and C9 are better NSCLC therapeutic agents because they possess better drug-likeness, pharmacokinetic, and toxicity properties. Hence, they are best fit for development into NSCLC therapeutic agents. In addition, experimental validation of in vivo and in vitro assays for ADME traits is required.

Authors' contribution

Conceptualization: Erazua, E. A.

Data curation: Erazua, E. A.; Oyebamiji, A. K.

Formal Analysis: Oyebamiji, A. K.

Funding acquisition: Not applicable.

Investigation: Erazua, E. A.; Oyebamiji, A. K.

Methodology: Akintelu, S. A.; Adewole, D. P.; Adelakun A. O.

Project administration: Adeleke, B. B.

Resources: Erazua, E. A.; Oyebamiji, A. K.

Software: Oyebamiji, A. K.; Adelakun A. O.

Supervision: Adeleke, B. B.

Validation: Oyebamiji, A. K.; Akintelu, S. A.

Visualization: Erazua, E. A.; Adewole, D. P.

Writing – original draft: Erazua, E. A.

Writing – review & editing: Erazua, E. A.; Oyebamiji, A. K.

Data availability statement

All data sets were generated or analyzed in the current study

Funding

Not applicable

Acknowledgments

We are grateful to Computational Chemistry Research Laboratory, Department of Chemistry, University of Ibadan and Mrs. E. T. Oyebamiji as well as Miss

Priscilla F. Oyebamiji for the assistance in the course of this study.

References

- Adepoju, A. J.; Latona, D. F.; Olafare, O. G.; Oyebamiji, A. K.; Abdul-Hammed, M.; Semire, B. Molecular docking and pharmacokinetics studies of *Curcuma longa* (Curcumin) potency against Ebola virus. *Ovidius University Annals of Chemistry* **2022**, *33* (1), 23–35. <https://doi.org/10.2478/auoc-2022-0004>
- Banerjee, P.; Eckert, A. O.; Schrey, A. K.; Preissner, R. ProTox-II: a webserver for the prediction of toxicity of chemicals. *Nucleic Acids Res.* **2018**, *46* (W1), W257–W263. <https://doi.org/10.1093/nar/gky318>
- Becke, A. D. Density-functional thermochemistry. III. The role of exact exchange. *J. Chem. Phys.* **1993**, *98* (7), 5648. <https://doi.org/10.1063/1.464913>
- Beheshti, J.; Bilal, D.; Mackey, T. P.; Limberg, L.; Bartlett, J. C.; Gwizdka, J.; Jacobson, T.; Ishimura, Y. Information literacy: Bridging the gap between theory and practice. *Proceedings of the Association for Information Science and Technology*, **2016**, *53* (1), 1–6. <https://doi.org/10.1002/pr2.2016.14505301019>
- Capra, J. A.; Laskowski, R. A.; Thornton, J. M.; Singh, M.; Funkhouser, T. A. Predicting protein ligand binding sites by combining evolutionary sequence conservation and 3D structure. *PLoS Comput. Biol.* **2009**, *5* (12), 1000585. <https://doi.org/10.1371/journal.pcbi.1000585>
- Cassidy, A.; Myles, J. P.; van Tongeren, M.; Page, R. D.; Liloglou, T.; Duffy, S. W.; Field, J. K. The LLP risk model: An individual risk prediction model for lung cancer. *Br. J. Cancer* **2008**, *98* (2), 270–276. <https://doi.org/10.1038/sj.bjc.6604158>
- Cheng, A.; Dixon, S. L. In silico models for the prediction of dose-dependent human hepatotoxicity. *J. Comput. Aided Mol. Des.* **2003**, *17* (12), 811–823. <https://doi.org/10.1023/B:JCAM.0000021834.50768.c6>
- Collins, L. G.; Haines, C.; Perkel, R.; Enck, R. E. Lung cancer: Diagnosis and management. *Am. Fam. Physician.* **2007**, *75* (1), 56–63.
- Daina, A.; Michielin, O.; Zoete, V. SwissADME: A free web tool to evaluate pharmacokinetics, drug-likeness and medicinal chemistry friendliness of small molecules. *Sci. Rep.* **2017**, *7*, 42717. <https://doi.org/10.1038/srep42717>
- Darvas, F.; Keseru, G.; Papp, A.; Dorman, G.; Urge, L.; Krajcsi, P. In silico and ex silico ADME approaches for drug discovery. *Curr. Top. Med. Chem.* **2002**, *2* (12), 1287–1304. <https://doi.org/10.2174/1568026023392841>

- Devesa, S. S.; Bray, F.; Vizcaino, A. P.; Parkin, D. M. International lung cancer trends by histologic type: Male:female differences diminishing and adenocarcinoma rates rising. *Int. J. Cancer.* **2005**, *117* (2), 294–299 <https://doi.org/10.1002/ijc.21183>
- Dixon, S. L.; Smondyrev, A. M.; Knoll, E. H.; Rao, S. N.; Shaw, D. E.; Friesner, R. A. PHASE: A new engine for pharmacophore perception, 3D QSAR model development, and 3D database screening: 1. Methodology and preliminary results. *J. Comput. Aided Mol. Des.* **2006**, *20* (10–11), 647–671. <https://doi.org/10.1007/s10822-006-9087-6>
- Faidallah, H. M.; Rostom, S. A. F. Synthesis, *in vitro* antitumor evaluation and DNA binding study of novel tetrahydroquinolines and some derived tricyclic and tetracyclic ring systems. *Eur. J. Med. Chem.* **2013**, *63*, 133–143. <https://doi.org/10.1016/j.ejmech.2013.02.006>
- Fathy, U.; Azzam, M. A.; Mahdy, F.; El-Maghraby, S.; Allam, R. M. Synthesis and *in vitro* anticancer activity of some novel tetrahydroquinoline derivatives bearing pyrazol and hydrazide moiety. *J. Heterocycl. Chem.* **2020**, *57* (5), 2108–2120. <https://doi.org/10.1002/jhet.3930>
- Grisoni, F.; Ballabio, D.; Todeschini, R.; Consonni, V. Molecular descriptors for structure–activity applications: A hands-on approach. In *Computational toxicology*. Nicolotti, O. Ed.; Humana Press, 2018; Vol. 1800, 3–53. https://doi.org/10.1007/978-1-4939-7899-1_1
- Hayat, F.; Salahuddin, A.; Umar, S.; Azam, A. Synthesis, characterization, antiamebic activity and cytotoxicity of novel series of pyrazoline derivatives bearing quinoline tail. *Eur. J. Med. Chem.* **2010**, *45* (10), 4669–4675. <https://doi.org/10.1016/j.ejmech.2010.07.028>
- Hollenberg, P. F. Characteristics and common properties of inhibitors, inducers, and activators of CYP enzymes. *Drug Metab. Rev.* **2002**, *34* (1–2), 17–35. <https://doi.org/10.1081/DMR-120001387>
- Ibrahim, M. T.; Uzairu, A.; Uba, S.; Shallangwa, G. A. Quantitative structure-activity relationship, molecular docking, drug-likeness, and pharmacokinetic studies of some non-small cell lung cancer therapeutic agents. *Beni-Suef Univ. J. Basic Appl. Sci.* **2020**, *9*, 49. <https://doi.org/10.1186/s43088-020-00077-5>
- Johnson, T. O.; Adegboyega, A. E.; Iwaloye, O.; Eseola, O. A.; Plass, W.; Afolabi, B.; Rotimi, D.; Ahmed, E.; Albrakati, A.; Batiha, G. E.; Adeyemi, O. S. Computational study of the therapeutic potentials of a new series of imidazole derivatives against SARS-CoV-2. *J. Pharmacol. Sci.* **2021**, *147* (1), 62–71. <https://doi.org/10.1016/j.jphs.2021.05.004>
- Lapa, G. B.; Bekker, O. B.; Mirchink, E. P.; Danilenko, V. N.; Preobrazhenskaya, M. N. Regioselective acylation of congeners of 3-amino-1H-pyrazolo[3,4-b]quinolines, their activity on bacterial serine/threonine protein kinases and *in vitro* antibacterial (including antimycobacterial) activity. *J. Enzyme Inhib. Med. Chem.* **2013**, *28* (5), 1088–1093. <https://doi.org/10.3109/14756366.2012.716056>
- Lipinski, C. A.; Lombardo, F.; Dominy, B. W.; Feeney, P. J. Experimental and computational approaches to estimate solubility and permeability in drug discovery and development settings. *Adv. Drug Deliv. Rev.* **2001**, *46* (1–3), 3–26. [https://doi.org/10.1016/S0169-409X\(00\)00129-0](https://doi.org/10.1016/S0169-409X(00)00129-0)
- Loving, K.; Salam, N. K.; Sherman, W. Energetic analysis of fragment docking and application to structure-based pharmacophore hypothesis generation. *J. Comput. Aided Mol. Des.* **2009**, *23* (8), 541–554. <https://doi.org/10.1007/s10822-009-9268-1>
- Lynch, T.; Price, A. The effect of cytochrome P450 metabolism on drug response, interactions, and adverse effects. *Am. Fam. Physician.* **2007**, *76* (3), 391–396.
- Mandewale, C. M.; Patil, U. C.; Shedje, S. V.; Dappadwad, U. R.; Yamgar, R. S. A review on quinoline hydrazone derivatives as a new class of potent antitubercular and anticancer agents. *Beni-Suef Univ. J. Basic Appl. Sci.* **2017**, *6* (4), 354–361. <https://doi.org/10.1016/j.bjbas.2017.07.005>
- Mekheimer, R. A.; Al-Sheikh, M. A.; Medrasi, H. Y.; Sadek, K. U. Advancements in the synthesis of fused tetracyclic quinoline derivatives. *RSC Adv.* **2020**, *10* (34), 19867–19935. <https://doi.org/10.1039/D0RA02786C>
- Morgensztern, D.; Ng, S. H.; Gao, F.; Govindan, R. Trends in stage distribution for patients with non-small cell lung cancer: A national cancer database survey. *J. Thorac. Oncol.* **2010**, *5* (1), 29–33. <https://doi.org/10.1097/JTO.0b013e3181c5920c>
- Muegge, I.; Rarey, M. Small molecule docking and scoring. In *Computational chemistry review*. Lipkowitz, K. B., Boyd, D. B., Eds.; Wiley Online Library, 2001; Vol. 17, 1–60. <https://doi.org/10.1002/0471224413.ch1>
- Ntie-Kang, F. An *in silico* evaluation of the ADMET profile of the StreptomeDB database. *SpringerPlus* **2013**, *2*, 353. <https://doi.org/10.1186/2193-1801-2-353>
- Oke, A. M.; Adelakun, A. O.; Akintelu, S. A.; Soetan, E. A.; Oyebamiji, A. K.; Ewemoje, T. A. Inhibition of angiotensin converting enzyme by phytochemicals in *Cucurbita pepo* L.: *In silico* Approach. *Pharmacological Research - Modern Chinese Medicine.* **2022**, *4*, 100142. <https://doi.org/10.1016/j.prmcm.2022.100142>
- Opoku-Temeng, C.; Dayal, N.; Soorshjani, M. A.; Sintim, H. O. 3H-pyrazolo [4, 3-f] quinoline haspin kinase inhibitors and anticancer properties. *Bioorg. Chem.* **2018**, *78*, 418–426. <https://doi.org/10.1016/j.bioorg.2018.03.031>

- Oyebamiji, A.K.; and Semire, B. Theoretical studies of anti-corrosion properties of triphenylimidazole derivatives in corrosion inhibition of carbon steel in acidic media via DFT approach. *Anal. Bioanal. Electrochem.* **2018**, *10* (1), 136–146.
- Oyebamiji, A. K.; Fadare, O. A.; Akintelu, S. A.; Semire, B. Biological studies on anthra[1,9-cd]pyrazol-6(2D)-one analogues as anti-vascular endothelial growth factor via in silico mechanisms. *Chemistry Africa* **2021**, *4* (4), 955–963. <https://doi.org/10.1007/s42250-021-00276-2>
- Oyeneyin, O. E.; Iwegbulam, C. G.; Ipinloju, N.; Olajide, B. F.; Oyebamiji, A. K. Prediction of the antiproliferative effects of some benzimidazolechalcone derivatives against MCF-7 breast cancer cell lines: QSAR and molecular docking studies. *Org. Commun.* **2022**, *15* (3), 273–287. <https://doi.org/10.25135/acg.oc.132.2203>
- Parr, R. G.; Szentpály, L.; Liu, S. Electrophilicity index. *J. Am. Chem. Soc.* **1999**, *121* (9), 1922–1924. <https://doi.org/10.1021/ja983494x>
- Pettersen, E. F.; Goddard, T. D.; Huang, C. C.; Couch, G. S.; Greenblatt, D. M.; Meng, E. C.; Ferrin, T. E. UCSF Chimera—A visualization system for exploratory research and analysis. *J. Comput. Chem.* **2004**, *25* (13), 1605–1612. <https://doi.org/10.1002/jcc.20084>
- Puzyn, T.; Leszczynski, J.; Cronin, M. *Recent Advances in QSAR Studies: Methods and applications*, Vol. 8; Springer Dordrecht, 2010. <https://doi.org/10.1007/978-1-4020-9783-6>
- Sahin, S.; Benet, L. Z. The operational multiple dosing half-life: A key to defining drug accumulation in patients and to designing extended-release dosage forms. *Pharm. Res.* **2008**, *25* (12), 2869–2877. <https://doi.org/10.1007/s11095-008-9787-9>
- Salim, E. I.; Jazieh, A. R.; Moore, M. A. Lung cancer incidence in the Arab League countries: Risk factors and control. *Asian Pacific J. Cancer Prev.* **2011**, *12* (1), 17–34.
- Sato, T.; Watanabe, H.; Tsuganezawa, K.; Yuki, H.; Mikuni, J.; Yoshikawa, S.; Kukimoto-Niino, M.; Fujimoto, T.; Wakiyama, T. Y.; Kojim, H.; Okabe, T.; Nagano, T.; Shirouzu, M.; Yokoyama, S.; Tanaka, A.; Honma, T. Identification of novel drug-resistant EGFR mutant inhibitors by in silico screening using comprehensive assessments of protein structures. *Bioorg. Med. Chem.* **2012**, *20* (12), 3756–3767. <https://doi.org/10.1016/j.bmc.2012.04.042>
- Semire, B.; Mutiu, O. A.; Oyebamiji, A. K. DFT and *AB INITIO* methods on NMR, IR and reactivity indices of indol-3-carboxylate and indazole-3-carboxylate derivatives of cannabinoids: Comparative study. *J. Phys. Theor. Chem.* **2017**, *13* (4), 353–377.
- Siegel, R. L.; Miller, K. D.; Jemal, A. Cancer statistics, 2016. *CA: Cancer. J. Clin.* **2016**, *66* (1), 7–30. <https://doi.org/10.3322/caac.21332>
- Stella, G. M.; Luisetti, M.; Inghilleri, S.; Cemmi, F.; Scabini, R.; Zorzetto, M.; Pozzi, E. Targeting EGFR in non-small-cell lung cancer: Lessons, experiences, strategies. *Respiratory Medicine* **2012**, *106* (2), 173–183. <https://doi.org/10.1016/j.rmed.2011.10.015>
- Swierczewska, M.; Lee, K. C.; Lee, S. What is the future of PEGylated therapies? *Expert Opin. Emerg. Drugs* **2015**, *20* (4), 531–536. <https://doi.org/10.1517/14728214.2015.1113254>
- Testa, B.; Krämer, S. D. The Biochemistry of Drug Metabolism – An Introduction: Part 5. Metabolism and Bioactivity. *Chem. Biodivers.* 2009, *6* (5), 591–684. <https://doi.org/10.1002/cbdv.200900022>
- Trott, O.; Olson, A. J. AutoDock Vina: Improving the speed and accuracy of docking with a new scoring function, efficient optimization, and multithreading. *J. Comput. Chem.* **2010**, *31* (2), 455–461. <https://doi.org/10.1002/jcc.21334>
- Vanommeslaeghe, K.; Guvench, O.; MacKerell Jr, A. D. Molecular mechanics. *Curr. Pharm. Des.* **2014**, *20* (20), 3281–3292. <https://doi.org/10.2174/13816128113199990600>
- Veber, D. F.; Johnson, S. R.; Cheng, H.-Y.; Smith, B. R.; Ward, K. W.; Kopple, K. D. Molecular properties that influence the oral bioavailability of drug candidates. *J. Med. Chem.* **2002**, *45* (12), 2615–2623. <https://doi.org/10.1021/jm020017n>
- Veerasamy, R.; Rajak, H.; Jain, A.; Sivadasan, S.; Varghese, C. P.; Agrawal, R. K. Validation of QSAR models - Strategies and importance. *Int. J. Drug Discov.* **2011**, *2* (3), 511–519.
- Wang, H.; Liu, X.; Rice, S. J.; Belani, C. P. Pulmonary rehabilitation in lung cancer. *PM&R* **2016**, *8* (10), 990–996. <https://doi.org/10.1016/j.pmrj.2016.03.010>
- Waziri, I.; Kelani, M. T.; Oyedeji-Amusa, M. O.; Oyebamiji, A. K.; Coetzee, L.-C. C.; Adeyinka, A. S.; Muller, A. J. Synthesis and computational investigation of *N,N*-dimethyl-4-[(*Z*)-(phenylimino)methyl]aniline derivatives: Biological and quantitative structural activity relationship studies. *J. Mol. Struct.* **2023**, *1276*, 134756. <https://doi.org/10.1016/j.molstruc.2022.134756>
- Yang, L.; Feng, J.-K.; Ren, A.-M. Theoretical studies on the electronic and optical properties of two thiophene–fluorene based π -conjugated copolymers. *Polymer* **2005**, *46* (24), 10970–10981. <https://doi.org/10.1016/j.polymer.2005.09.050>
- Yasuda, H.; Park, E.; Yun, C. H.; Sng, N. J.; Lucena-Araujo, A. R.; Yeo, W. L.; Huberman, M. S.; Cohen, D. W.; Nakayama, S.; Ishioka, K.; Yamaguchi, N.; Hanna, M.;

Oxnard, G. R.; Lathan, C. S.; Moran, T.; Sequist, L. V.; Chaft, J. E.; Riely, G. J.; Arcila, M. E.; Soo, R. A.; Meyerson, M.; Eck, M. J.; Kobayashi, S. S.; Costa, D. B. Structural, biochemical, and clinical characterization of epidermal growth factor receptor (EGFR) exon 20 insertion mutations in lung cancer. *Sci. Transl. Med.* **2013**, *5* (216), 216ra177. <https://doi.org/10.1126/scitranslmed.3007205>

Zhang, Z.; Lee, J. C.; Lin, L.; Olivas, V.; Au, V.; LaFramboise, T.; Abdel-Rahman, M.; Wang, X.; Levine, A. D.; Rho, J. K.; Choi, Y. J.; Choi, C. M.; Kim, S. W.; Jang, S. J.; Park, Y. S.; Kim, W. S.; Lee, D. H.; Lee, J. S.; Miller, V. A.; Arcila, M.; Ladanyi, M.; Moonsamy, P.; Sawyers, C.; Boggon, T. J.; Ma, P. C.; Costa, C.; Taron, M.; Rosell, R.; Halmos, B.; Bivona, T. G. Activation of the AXL kinase causes resistance to EGFR-targeted therapy in lung cancer. *Nat. Genet.* **2012**, *44* (8), 852–860. <https://doi.org/10.1038/ng.2330>

Development and validation of a new spectrophotometric method for simultaneous determination of sitagliptin and metformin hydrochloride in tablet pharmaceutical dosage forms using chemometrics technique in comparison with HPLC

Maher Ali Almaqtari¹⁺, Najat Ahmed Al-Odaini¹, Fares Abdullah Alarbagi¹, Hussein Al-Maydama¹

1. Sana'a University, Faculty of Science, Sana'a, Yemen.

+Corresponding author: Maher Ali Almaqtari, **Phone:** +967 773262252, **Email address:** m.almaqtari@su.edu.ye

ARTICLE INFO

Article history:

Received: August 21, 2022

Accepted: November 16, 2022

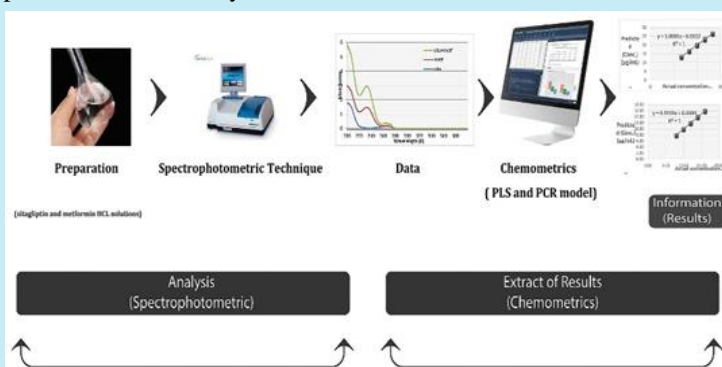
Published: January 11, 2023

Keywords:

1. sitagliptin
2. metformin hydrochloride
3. spectrophotometric method
4. chemometrics technique
5. validation

Section Editors: Assis Vicente Benedetti

ABSTRACT: A new, quick, easy, affordable and eco-friendly simultaneous spectrophotometric method for determining a combined sitagliptin and metformin hydrochloride in pharmaceutical formulations was developed and validated using two chemometrics technique. These two methods are the partial least square (PLS) and principal component regression (PCR). They do not need to do a sample preparation or separation before analysis. Various drug concentrations and instrumental spectra of 25 mixed solutions of a combination of sitagliptin and metformin hydrochloride were used for model construction in the range of 200–270 nm. The R^2 values of 0.9994 and 0.9996 assigned for the PLS of the sitagliptin and metformin hydrochloride and that of 0.9987 and 0.9996 for the PCR of the sitagliptin and metformin hydrochloride, respectively. It is noteworthy that these two models were successfully and effectively used with the commercial pharmaceutical formulations. Finally, the statistical comparison revealed no significant differences with the results of the HPLC reference method. The proposed method is dependable to be adopted as an alternative analytical method in the pharmaceutical industry's quality control.



1. Introduction

Chemically, sitagliptin is (3R)-3-purcino-1-[3-(trifluoromethyl)-5,6-dihydro[1,2,4] triazolo [4,3-a]pyrazin-7 (8H)-yl] -4-(2,4,6-trifluorophenyl) butan-1-one phosphate monohydrate (Fig. 1a). It is used as dipeptidylpeptidase-4 inhibitor; treatment of diabetes mellitus (British Pharmacopoeia Commission, 2020; Swamy *et al.*, 2020).

Metformin HCl is 1,1-dimethylbiguanide hydrochloride and its chemical structure is presented in (Fig. 1b). It is used to treat diabetes mellitus. It is also used to treat polycystic ovarian syndrome. It is taken by mouth and is not linked to weight gain. It is sometimes used as an off-label supplement to help persons who are taking antipsychotics avoid gaining weight (British Pharmacopoeia Commission, 2020).

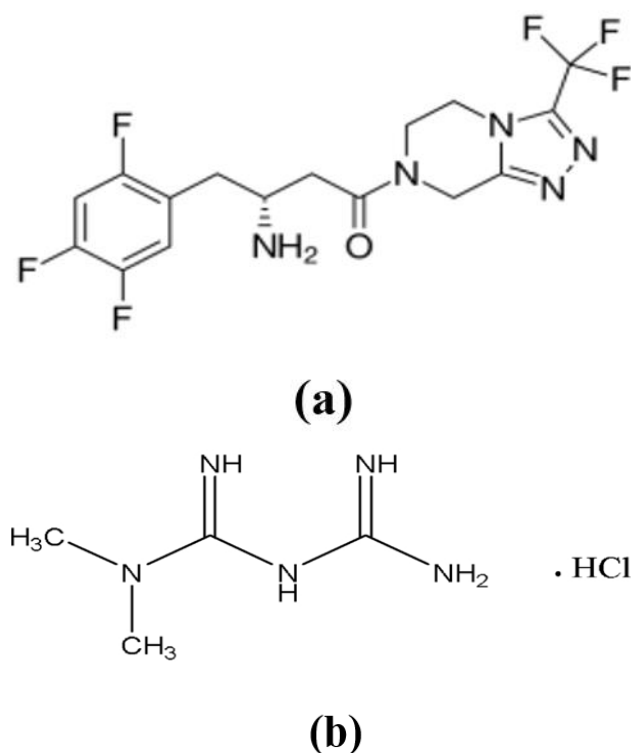


Figure 1. Chemical structure of sitagliptin (a) and metformin hydrochloride (b).

Uddin *et al.* (2019) reported that high-performance liquid chromatography (HPLC) is a technique that collects data from simultaneous separation and determination and is more frequently employed in analytical processes for the analysis of pharmaceutical products. However, it has several disadvantages, including the possibility of being bad for the environment and people's health. The HPLC assay also needed a lot of costly chemicals and supplies.

Furthermore, it takes a lot of time, which delays the marketing and production operations. The expense of HPLC maintenance is likewise substantial. Spectrophotometry, which is simple, dependable, rapid, economical, and most significantly, environmentally benign, may be a useful option for determining a complicated combination in pharmaceutical quality control laboratories. Additionally, the data show that spectrophotometry and chemometrics in conjugation have a promising future and can be used in place of HPLC in both quantitative and qualitative analysis.

The study of chemometrics has significantly influenced analytical chemistry, notably in the field of spectrum analysis, which is crucial for the quality assurance of pharmaceutical formulations including two or more pharmaceuticals with overlapping spectra (K. Patel *et al.*, 2013a; Glavanović *et al.*, 2016).

Chemometrics approaches rely on multivariate analysis, which necessitates that ultraviolet (UV) spectrophotometry methods consider multiple variables at once. The absorbance at each wavelength is taken into account, with many wavelengths being taken into consideration (Gandhi *et al.*, 2017; R. Patel and Mashru, 2019). The principal component regression (PCR) and partial least squares (PLS) are the two most significant chemometrics techniques utilized in multivariate analysis. For the purpose of determining the combination of medications in pharmaceutical formulations, these multivariate calibration methods employ spectrophotometric data coupled with statistical tools, mathematical models, and software (R. Patel and Mashru, 2019). These techniques additionally rely on the mathematical model's calibration using the absorbance data of calibration standards with known concentrations, which is followed by the prediction of the concentration of unknown samples using those samples' absorbance data (Gandhi *et al.*, 2017; R. Patel and Mashru, 2019).

There are many applications for chemometrics in analytical spectroscopy, including UV-visible spectrophotometry (UV-VIS) (Ashour *et al.*, 2015; Attia *et al.*, 2018; Belal *et al.*, 2018; Darbandi *et al.*, 2020; Elfatraty *et al.*, 2016; Gholse *et al.*, 2021; Manouchehri *et al.*, 2016; Moussa *et al.*, 2021; M. Patel *et al.*, 2013b; Phechkrajang *et al.*, 2015; Putri *et al.*, 2021; Sebaiy *et al.*, 2020; 2022; V. D. Singh and V. K. Singh, 2021; Vichare *et al.*, 2010), fluorescence spectroscopy (Manouchehri *et al.*, 2016; Salem *et al.*, 2019; Shinde and Divva, 2015; Walash *et al.*, 2011; Zhu *et al.*, 2016), NIR spectroscopy (Manouchehri *et al.*, 2016; Moroni *et al.*, 2022; Muntean *et al.*, 2017; 2021; Rahman *et al.*, 2020; Sun *et al.*, 2021) and FTIR spectroscopic method (Rahman *et al.*, 2020). Furthermore, chromatography methods like liquid chromatography (Aminu *et al.*, 2019;

Mohammed *et al.*, 2021; Tsvetkova *et al.*, 2012; Vu Dang *et al.*, 2020) along with a number of other analytical chemistry methods, such as flow-injection analysis are used for the pharmaceutical formulations (Ortega-Barrales *et al.*, 2002; Silva *et al.*, 2011).

Uddin *et al.* (2019) reported that the majority of the analytes of interest are accompanied in their dosage forms by other compounds that absorb in the same spectral region, making it impossible to distinguish them using the traditional UV spectral studies. It is challenging to use traditional techniques like extraction because they demand a large amount of solvent, which carries risks of analyte loss or contamination as well as the potential for incomplete separation, which is expensive and time-consuming. However, spectrophotometry, as a quick, accurate, low-cost, and easy technology, may be a wonderful choice when used with chemometric techniques for determining a combined mixture in pharmaceutical quality control. When pharmaceutical product quality monitoring calls for dependable, precise, and quick analytical techniques, they are beneficial. This method, which is quick, accurate, and simple to use, avoids the usage of earlier separation procedures.

Many methods for quantifying sitagliptin and metformin hydrochloride have been published, including chromatographic (Adsul *et al.*, 2018; Krishnan and Mishra, 2020; Kumar *et al.*, 2017) and spectrophotometric approaches (Himabindu *et al.*, 2016; Lotfy *et al.*, 2015). At the time of writing, we had the following information to our knowledge, there is no reference in the analytical literature reviews for the development and validation of simultaneous spectrophotometric method assisted chemometrics methods for the determination of sitagliptin with metformin HCl in pharmaceutical dosage form. This study aims to develop and validate an adequate and reproducible simultaneous spectrophotometric assay method for the determination of sitagliptin and metformin HCl in tablet pharmaceutical dosage forms using chemometrics technique.

2. Materials and methods

2.1 Materials and Reagents

The reference standard of sitagliptin (as phosphate monohydrate) and metformin HCl were obtained from Global Pharma Company, Sana'a, Yemen. All reagents and chemicals used for the spectrophotometric methods were of analytical grade and HPLC grade were used for the HPLC method. Deionized water (with specific

conductance of $0.05 \mu\text{S cm}^{-1}$) was produced in-house and used for the preparation of all samples solutions.

2.2 Instrumentation

Double beam UV-VIS (AnalytiK Jena) model (SPECORD 200) at Sana'a University-Faculty of Science was used for the absorbance measurements. The HPLC system was from JASCO with detector (UV-2070 Plus), pump (PU-2089), an auto sampler (AS-2055 Plus) and a column oven (CO-2067 Plus). Electronic balance (AA-160), Denver Instrument. Electronic balance (GH-252), AND. Electronic balance (GR-120), AND. pH meter (3520), Jenway. Centrifuge (Z326 K), Hermle were also used.

2.3 Development and validations procedures

For the aim of developing an accurate, precise and dependable simultaneous spectrophotometric methods assisted with the chemometrics technique, the analytical methods were established and developed to get the intended results for quantifying the targeted components.

2.3.1 Selection of Solvent

Literature reviews were conducted to identify the proper solvents that aid in dissolving the desired active pharmaceutical ingredients without excipients. Through a series of trial-and-error attempts, a suitable solvent was chosen. Other advantages for selecting the appropriate solvent such as available, easy to use, a cheap, environmentally friendly and for the spectrophotometric method implementation were given a full consideration.

2.3.2 Selection of spectral zones analysis

After the phase of choosing the solvent and before the data is preprocessed, the range of 200–400 nm with a 0.2 nm interval was used to record the individual pure and mixed absorbance spectra of the targeted medicinal components. UV spectra of the mixtures analysis were selected among a suitable wavelength range against a solvent blank providing the greatest amount of information about the two components (Shah and Jasani, 2017).

2.3.3 Construction of the training set

As the training set (calibration set), twenty-five different concentrations of the binary mixture of sitagliptin and metformin HCl were prepared to construct

the model. These mixtures' absorbencies were measured against a blank at intervals of 0.2 nm between 200 and 400 nm.

2.3.4 Construction of chemometric models

The two multivariate calibration models; the PLS and the PCR analysis were established as follows:

- To begin with, binary mixture absorbencies were measured against a blank, and the spectra were saved and extracted into Microsoft Excel in order to develop models;
- Secondly, using absorption data at chosen spectral zones for analysis at intervals of 0.2 nm, the PCR and PLS models were built using the Minitab 17 program;
- Then, the required number of latent variables was obtained using the leave-one-out cross validation method;
- After that, the calibration samples, constants, and coefficients for each wavelength were calculated in order to calculate the predicted concentrations;
- In the end, the predicted concentrations were compared to the actual concentrations in each sample to compute the assay of binary mixture in each sample;
- The root mean square error of cross-validation (RMSECV), which must be as small as possible for a given model, was determined for each method to assess the precision and accuracy of predictions for the models using the following Eq. 1 (Shah and Jasani, 2017):

$$\text{RMSECV} = \sqrt{\frac{\sum(C_{\text{act}} - C_{\text{pre}})^2}{I_c}} \quad (1)$$

where RMSECV = Root mean square error of cross validation; C_{act} = Actual concentration of calibration set; C_{pre} = predicted concentration of calibration set; and I_c = Total number of samples in calibration set.

2.3.5 Validation and construction of the validation set

In order to validate and assess the performance of the suggested and developed spectrophotometric methods assisted chemometric models, these methods were subjected to validation set. Also, the performance criteria of the developed methods including linearity, accuracy, precision (repeatability) and specificity were validated in accordance with the recommendations of International Conference Harmonization and after that determined.

2.4 Developed analytical method procedures for sitagliptin with metformin HCl determination and comparing with reference methods

The performance of the proposed and developed method was determined in accordance with the method validation results. This method was studied and tested for determination of sitagliptin and metformin HCl in marketed pharmaceutical formulations. And they were compared with analysis results of reference method.

2.4.1 Preparation of standard stock solution

Stock solutions of 1670 $\mu\text{g mL}^{-1}$ of sitagliptin and 1000 $\mu\text{g mL}^{-1}$ of metformin hydrochloride were individually prepared in a 100 mL volumetric flask by dissolving 167 mg sitagliptin and 100 mg metformin hydrochloride separately in water.

2.4.2 Preparation of working standard solution

2.4.2.1 Construction of the calibration (training) set

Twenty-five binary mixtures of sitagliptin and metformin hydrochloride were prepared by transferring different aliquots of their standard stock solutions into a series of 50 mL volumetric flasks. The absorbencies of these mixtures were measured between 200 and 400 nm at 0.2 nm intervals against water as a blank.

2.4.2.2 Construction of the validation set

A set of twelve binary mixtures of sitagliptin and metformin hydrochloride was prepared by transferring different volumes into 50 mL volumetric flasks and the procedure under the construction of the training set was repeated.

2.4.2.3 Preparation of spiked samples

Powdered tablets of 25 mg of sitagliptin and 250 mg of metformin hydrochloride were accurately weighed, transferred to a 250 mL volumetric flask and then 200 mL of water was added, the mixture was shaken for 5 min and with frequent shaking the volume completion to 250 mL with the selected solvent was carried out. The solution was then filtered. A 0.5 mL of the filtrate was transferred into 50 mL volumetric flask and calculated amount of sitagliptin and metformin hydrochloride from standard solutions were spiked into sample solution and then diluted with water up to 50 mL. The absorbance was then measured.

2.4.2.4 Analysis of marketed formulations

The developed method was applied to the measurement of a commercially available samples. It was carried out using the marketed formulation with concentration of 50 mg sitagliptin and 500 mg metformin hydrochloride. The tablets solution prepared in the sample preparation section was diluted with water to prepare solutions with concentration of $10.68 \mu\text{g mL}^{-1}$ sitagliptin and of $14 \mu\text{g mL}^{-1}$ metformin hydrochloride. The spectra of the prepared solutions were recorded and then the developed multivariate models PCR and PLS were applied to determine the concentrations of the sitagliptin and metformin HCl.

2.4.2.5 Comparing the suggested method with reference method

Comparison was carried out with the recovery results of the newly developed methods and that of reference method for each of sitagliptin with metformin hydrochloride according to the United States Pharmacopeia (USP, 43). $80 \mu\text{g mL}^{-1}$ sitagliptin was prepared by dissolving 80 mg sitagliptin in acetonitrile: dilute phosphoric acid (5:95) in a 100 mL volumetric flask as standard stock solution; 5 mL of sitagliptin of the standard stock solution was transferred in acetonitrile: dilute phosphoric acid (5:95) in 50 mL volumetric flask. A test sample was prepared by placing 10 tablets containing 500 mg of sitagliptin to 500 mL volumetric flask; 500 mL of acetonitrile: dilute phosphoric acid (5:95) as solvent was added and the solution was shaken for 1 h then a portion of the solution was centrifuged for 10 min; 2 mL of the supernatant solution was transferred into 25 mL volumetric flask and diluted with solvent. The standard and the test sample of sitagliptin were injected through an HPLC system with a mixture of acetonitrile: monobasic potassium phosphate buffer (pH adjusted to 2 with phosphoric acid) (15:85) as the mobile phase at flow rate of 1 mL min^{-1} through a C8 column ($15 \text{ cm} \times 4.6 \text{ mm}$, $5 \mu\text{m}$) and column temperature was 30°C . The UV detection of the sitagliptin was then carried out at 205 nm (United States Pharmacopeia and the National Formulary, 2020).

Metformin hydrochloride was also determined, according to the USP (34), $200 \mu\text{g mL}^{-1}$ metformin hydrochloride was prepared by dissolving 40 mg metformin hydrochloride in acetonitrile: dilute phosphoric acid (5:95) in a 200 mL volumetric flask as

standard stock solution. A test sample was prepared by placing 10 tablets containing 5,000 mg of metformin hydrochloride to 500 mL volumetric flask; 500 mL of acetonitrile: dilute phosphoric acid (5:95) as solvent was added and the solution was shaken for 1 h then a portion of the solution was centrifuged for 10 min; 2 mL of the supernatant solution was transferred into 100 mL volumetric flask and diluted with solvent. The standard and the test sample of metformin hydrochloride were injected through an HPLC system with a mixture of acetonitrile: monobasic potassium phosphate buffer (pH adjusted to 2 with phosphoric acid) (15:85) as the mobile phase at flow rate of 1 mL min^{-1} through a C8 column ($15 \text{ cm} \times 4.6 \text{ mm}$, $5 \mu\text{m}$) and column temperature was 30°C . The UV detection of the sitagliptin was then carried out at 205 nm.

3. Results and discussion

3.1 Method development for sitagliptin and metformin HCl determination

3.1.1 Selection of solvent

In order to choose a suitable solvent, solubility was checked in water, methanol, 0.1 mol L^{-1} NaOH and 0.1 mol L^{-1} HCl. The drug was found to be soluble in methanol, water, 0.1 mol L^{-1} NaOH and 0.1 mol L^{-1} HCl. Therefore, water was selected as diluent that has striking advantages such as easily available, easy to handle, a cheap and environmentally friendly for implementing the spectrophotometric method and Fig. 2 showed the spectra of the sitagliptin and metformin hydrochloride in water.

3.1.2 Selection of spectral zones for analysis

To determine the overlap spectral zones, the absorbance spectra of the pure sitagliptin and metformin hydrochloride samples, and that sample of the mixed sitagliptin with metformin hydrochloride in water were recorded in the range of 200–400 nm with 0.2 nm interval. For the analysis, the UV spectra of the mixtures were selected for a suitable wavelength range (200–270 nm) against water blank. This range provided a great amount of information about the two components as shown in the sitagliptin with metformin hydrochloride spectra (Fig. 2).

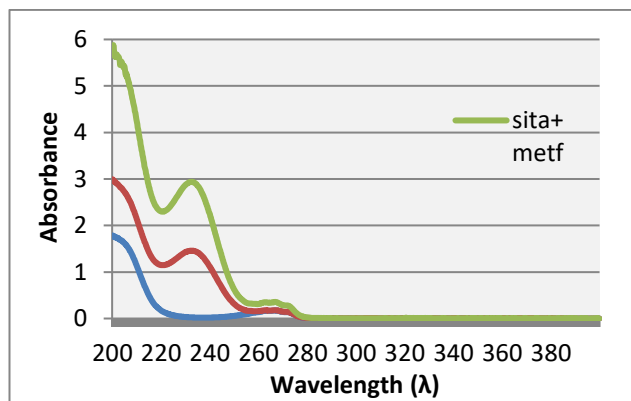


Figure 2. UV absorbance spectra of the pure and mixed samples of sitagliptin and metformin hydrochloride in water solvent.

Table 1. Composition of calibration set.

Mixture No.	Sitagliptin ($\mu\text{g mL}^{-1}$)	Metformin hydrochloride ($\mu\text{g mL}^{-1}$)	Mixture No.	Sitagliptin ($\mu\text{g mL}^{-1}$)	Metformin hydrochloride ($\mu\text{g mL}^{-1}$)
1	13.36	8	14	20.04	14
2	13.36	10	15	20.04	16
3	13.36	12	16	23.38	8
4	13.36	14	17	23.38	10
5	13.36	16	18	23.38	12
6	16.7	8	19	23.38	14
7	16.7	10	20	23.38	16
8	16.7	12	21	26.72	8
9	16.7	14	22	26.72	10
10	16.7	16	23	26.72	12
11	20.04	8	24	26.72	14
12	20.04	10	25	26.72	16
13	20.04	12			

3.1.4 Construction of chemometrics models

The spectra were saved and extracted into Microsoft Excel for model generation. The PCR and PLS models were developed utilizing the absorption data for the selected spectral zones using Minitab 17 software program. After the PCR and PLS models have been constructed, the optimum number of principal components of sitagliptin and metformin hydrochloride were obtained and given in Tables A1–4 of the Appendix.

3.1.5 Determination of the optimum number of the principal components of sitagliptin and metformin hydrochloride for PLS

Selecting the proper number of principal components for the development of model was necessary to obtain good prediction. Leave-one-out cross validation method was used to obtain the necessary optimum number of the principal factors for the PLS model. It was found that the

3.1.3 Construction of the training set

To determine the linear, range from measuring the absorbance at different concentrations for sitagliptin with metformin hydrochloride, the response was found to be linear in the range of 13.36–26.72 $\mu\text{g mL}^{-1}$ for sitagliptin and 8–16 $\mu\text{g mL}^{-1}$ for metformin hydrochloride using 25 different concentrations of sitagliptin and metformin hydrochloride mixtures were prepared to construct the models as shown in Table 1.

optimum number of the principal components were eight for sitagliptin and eight for metformin hydrochloride as mentioned above and as given in Table A1 and A2 of the Appendix.

3.1.6 Determination of the constant and coefficients obtained at each wavelength of sitagliptin and metformin hydrochloride for PLS models

The constant and coefficients at each wavelength were calculated using Minitab 17 program as illustrated in Table A1 of the Appendix.

3.1.7 Determination of the predicted concentrations and the recovery of sitagliptin and metformin hydrochloride for PLS models

The predicted or calculated concentrations in $\mu\text{g mL}^{-1}$ of the sitagliptin and metformin hydrochloride were worked out from the multiple regression Eq. 2:

$$\text{predicted (Calculated)} = \text{Constant} + \sum (\text{Coefficient} \times \text{Absorbance}) \quad (2)$$

The predicted or calculated concentrations of the components were compared with the actual concentrations and the assay of binary mixture were calculated. RMSECV was calculated and found to be low. The low values of RMSECV in Table 2 indicate

both the precision and accuracy of PLS model for sitagliptin and metformin hydrochloride were very high and the R^2 values in Fig. 3 were also of very high linearity.

Table 2. Results of the predicted concentrations with the recovery of sitagliptin and metformin hydrochloride in the binary mixture in each sample for PLS model.

Name	Sitagliptin			Metformin hydrochloride		
Constant	-1.1712			0.4045		
Mixture No.	Actual Conc.	Predicted Conc.	%Recovery	Actual Conc.	Predicted Conc.	%Recovery
1	13.36	13.36	100.00	8.00	7.99	99.88
2	13.36	13.35	99.93	10.00	10.02	100.20
3	13.36	13.36	100.00	12.00	11.98	99.83
4	13.36	13.34	99.85	14.00	14.00	100.00
5	13.36	13.37	100.07	16.00	15.99	99.94
6	16.70	16.73	100.18	8.00	7.99	99.88
7	16.70	16.68	99.88	10.00	10.00	100.00
8	16.70	16.71	100.06	12.00	12.00	100.00
9	16.70	16.67	99.82	14.00	14.01	100.07
10	16.70	16.71	100.06	16.00	16.01	100.06
11	20.04	20.04	100.00	8.00	8.00	100.00
12	20.04	20.04	100.00	10.00	10.02	100.20
13	20.04	20.05	100.05	12.00	12.00	100.00
14	20.04	20.04	100.00	14.00	14.00	100.00
15	20.04	20.08	100.20	16.00	16.00	100.00
16	23.38	23.37	99.96	8.00	8.00	100.00
17	23.38	23.38	100.00	10.00	10.00	100.00
18	23.38	23.37	99.96	12.00	11.99	99.92
19	23.38	23.39	100.04	14.00	14.00	100.00
20	23.38	23.36	99.91	16.00	15.99	99.94
21	26.72	26.71	99.96	8.00	7.99	99.88
22	26.72	26.74	100.07	10.00	10.01	100.10
23	26.72	26.73	100.04	12.00	12.00	100.00
24	26.72	26.71	99.96	14.00	13.99	99.93
25	26.72	26.71	99.96	16.00	16.00	100.00
		Mean%	100		Mean%	99.99
		RSD%	0.09		RSD%	0.089
		RMSECV	0.016		RMSECV	0.01

The linearity of the developed method was tested by constructing a cross-validation of the data in Table 2. The results obtained in Fig. 3 indicated that the developed method possessed high linearity with $R^2 = 1$ within the method linear range (13.36–26.72 $\mu\text{g mL}^{-1}$) for sitagliptin and $R^2 = 1$ within the method linear range (8–16 $\mu\text{g mL}^{-1}$) for metformin hydrochloride. The linearity of the developed method was very high and

most importantly, environmentally friendly with respect to the solvent (water) used. In comparison, Adsul *et al.* (2018) revealed that the linearity of the HPLC methods which carried out in non-eco-friendly solvents and mobile phases was almost similar to our eco-friendly (water) developed method and better than another HPLC method (Kumar *et al.*, 2017).

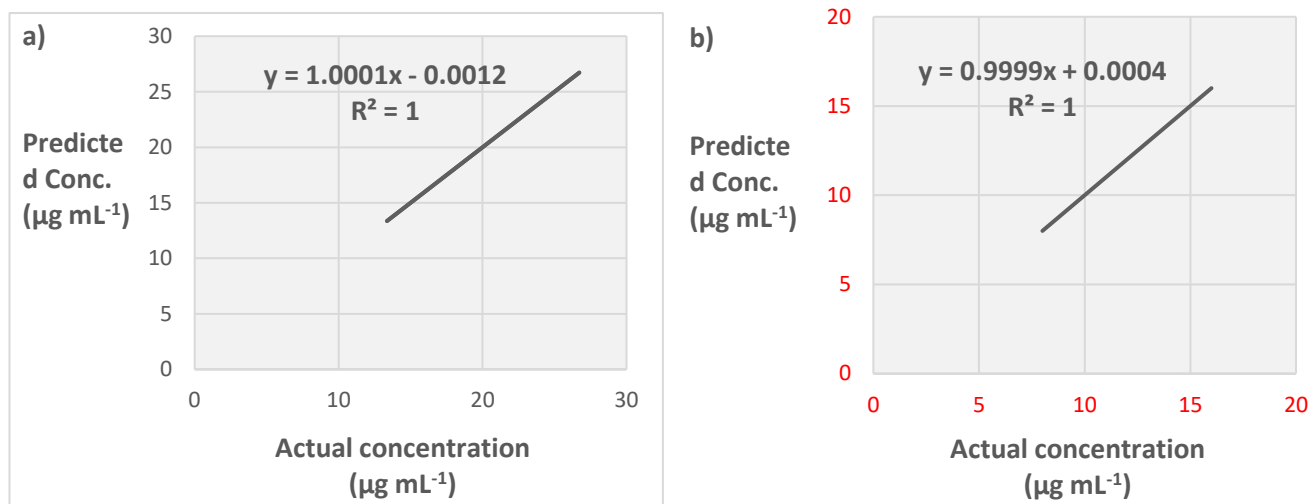


Figure 3. The PLS cross validation for the calibration set of the actual vs. predicted concentration. (a) Sitagliptin; (b) Metformin HCl.

3.1.8 Determination of the optimum number of the principal components and their coefficients of sitagliptin and metformin HCl for PCR

The PCR was computed by using a few principal components and performed regression analysis of these components with concentration in order to determine the principal components coefficients of sitagliptin and

Regression equation of sitagliptin

$$-2.182 + 0.5991 Z_1 + 3.9880 Z_2 + 3.65 Z_3 - 0.92 Z_4 + 1.75 Z_5 - 5.97 Z_6 \quad (3)$$

Regression equation of metformin hydrochloride

$$0.066 + 0.94302 Z_1 - 0.9038 Z_2 - 0.353 Z_3 - 1.524 Z_4 + 1.993 Z_5 + 1.703 Z_6 \quad (4)$$

where Z is the principal components coefficients.

3.1.9 Determination of the predicted concentrations and recovery of sitagliptin and metformin hydrochloride for PCR models

The predicted or calculated concentrations in $\mu\text{g mL}^{-1}$ of the sitagliptin and metformin hydrochloride were calculated from multiple regression Eq. 5:

$$\text{predicted (calculated)} = \text{constant} + \sum (\text{coefficient} \times \text{absorbance}) \quad (5)$$

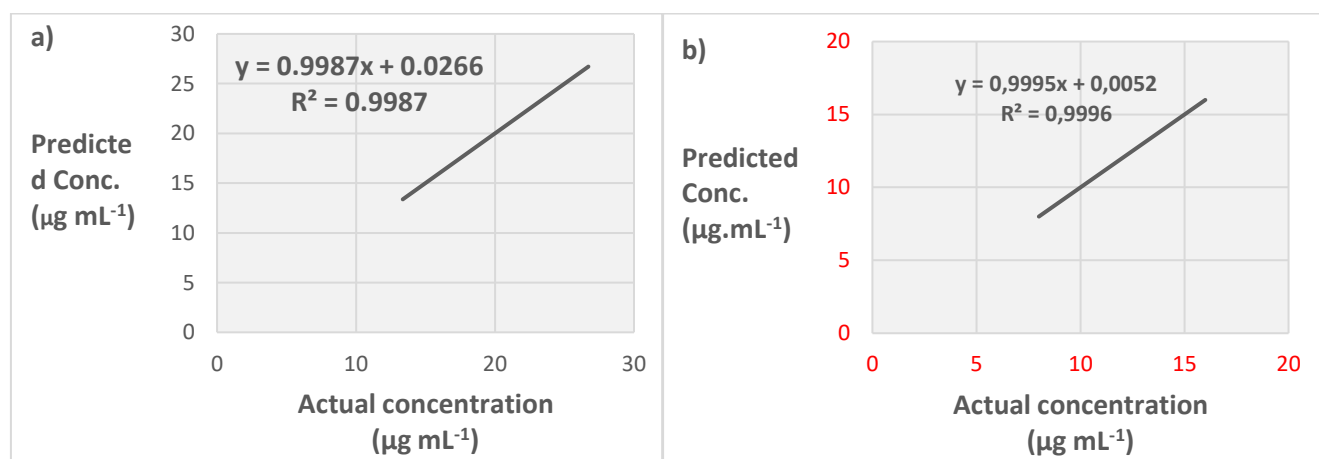
The predicted or calculated concentrations of the sitagliptin and metformin hydrochloride were compared with the actual concentrations and the assay for binary mixture were calculated in each sample. RMSECV was calculated and found to be low. The RMSECV low

metformin hydrochloride for PCR model as illustrated in Table A4 of the Appendix. From the treatment of the principal component's coefficients in (Table A4 of the Appendix) using Minitab 17 program. Regression equations (Eqs. 3 and 4) of sitagliptin and metformin hydrochloride were obtained and used to calculate the predicted concentration as shown below.

values in Table 3 indicate that both the precision and accuracy of PCR model for sitagliptin and metformin hydrochloride were very high, with the R^2 values in Fig. 4 of very high linearity.

Table 3. Results of the predicted concentrations with recovery of sitagliptin and metformin hydrochloride in binary mixture in each sample for PCR models.

Name Constant	Sitagliptin -2.182			Metformin hydrochloride 0.066		
	Mixture NO.	Actual Conc.	Predicted Conc.	%Recovery	Actual Conc.	Predicted Conc.
1	13.36	13.40	100.30	8.00	8.04	100.50
2	13.36	13.15	98.43	10.00	10.07	100.70
3	13.36	13.23	99.03	12.00	11.91	99.25
4	13.36	13.14	98.35	14.00	14.07	100.50
5	13.36	13.39	100.22	16.00	15.98	99.88
6	16.70	16.95	101.50	8.00	7.96	99.50
7	16.70	16.75	100.30	10.00	10.02	100.20
8	16.70	16.61	99.46	12.00	12.02	100.17
9	16.70	16.98	101.68	14.00	13.95	99.64
10	16.70	16.89	101.14	16.00	15.98	99.88
11	20.04	20.05	100.05	8.00	7.96	99.50
12	20.04	20.08	100.20	10.00	9.90	99.00
13	20.04	19.70	98.30	12.00	11.94	99.50
14	20.04	20.01	99.85	14.00	13.96	99.71
15	20.04	20.26	101.10	16.00	16.08	100.50
16	23.38	23.63	101.07	8.00	8.04	100.50
17	23.38	23.45	100.30	10.00	10.10	101.00
18	23.38	23.14	98.97	12.00	12.03	100.25
19	23.38	23.49	100.47	14.00	14.08	100.57
20	23.38	23.50	100.51	16.00	15.96	99.75
21	26.72	26.68	99.85	8.00	8.01	100.13
22	26.72	26.77	100.19	10.00	9.99	99.90
23	26.72	26.55	99.36	12.00	11.95	99.58
24	26.72	26.47	99.06	14.00	13.97	99.79
25	26.72	26.73	100.04	16.00	16.01	100.06
		Mean%	99.99		Mean%	100.00
		RSD%	0.94		RSD %	0.49
		RMSECV	0.169		RMSECV	0.054

**Figure 4.** The PCR cross validation for calibration set of the actual vs. predicted concentration. (a) Sitagliptin; (b) Metformin HCl.

3.2 Validation method for sitagliptin and metformin hydrochloride

3.2.1 Construction of validation set

The results of prediction and the percentage recoveries are represented in Table 4. The predictive

abilities of the models were evaluated by plotting the actual known concentrations against the predicted concentrations that shown in Fig. 5 and 6. A tremendous agreement between the predicted (calculated) and actual concentration of sitagliptin and metformin hydrochloride for PLS and PCR models can be observed in Fig. 5 and 6.

Table 4. Results of validation set of sitagliptin and metformin HCl for PLS and PCR model.

NO.	METHOD		PLS				PCR			
	Sita.	Metf.	Sita.		Metf.		Sita.		Metf.	
	Actual ($\mu\text{g mL}^{-1}$)		Predicted ($\mu\text{g mL}^{-1}$)	%R	Predicted ($\mu\text{g mL}^{-1}$)	%R	Predicted ($\mu\text{g mL}^{-1}$)	%R	Predicted ($\mu\text{g mL}^{-1}$)	%R
1	16.02	8	15.76	98.38	7.71	96.38	16.35	102.06	7.93	99.13
2	16.02	9.6	16.17	100.94	9.36	97.50	16.63	103.81	9.58	99.79
3	13.35	8	13.41	100.45	8.02	100.25	13.55	101.50	8.09	101.13
4	13.35	10	12.96	97.08	9.75	97.50	13.02	97.53	9.85	98.50
5	20.03	10	19.95	99.60	9.80	98.00	20.40	101.85	9.97	99.70
6	20.03	12	20.03	100.00	11.71	97.58	20.56	102.65	11.92	99.33
7	26.7	8	26.66	99.85	7.78	97.25	27.43	102.73	7.98	99.75
8	26.7	10	26.83	100.49	9.58	95.80	27.12	101.57	9.79	97.90
9	16	9.6	16.28	101.75	9.76	101.67	16.33	102.06	9.77	101.77
10	16	12	15.91	99.44	12.03	100.25	15.96	99.75	12.00	100.00
11	24	12	23.91	99.63	11.75	97.92	24.17	100.71	11.92	99.33
12	24	14.4	24.32	101.33	14.09	97.85	24.55	102.29	14.16	98.33
			Mean%	99.91		98.16	Mean%	101.54		99.56
			RSD%	1.22		1.74	RSD%	1.53		1.06

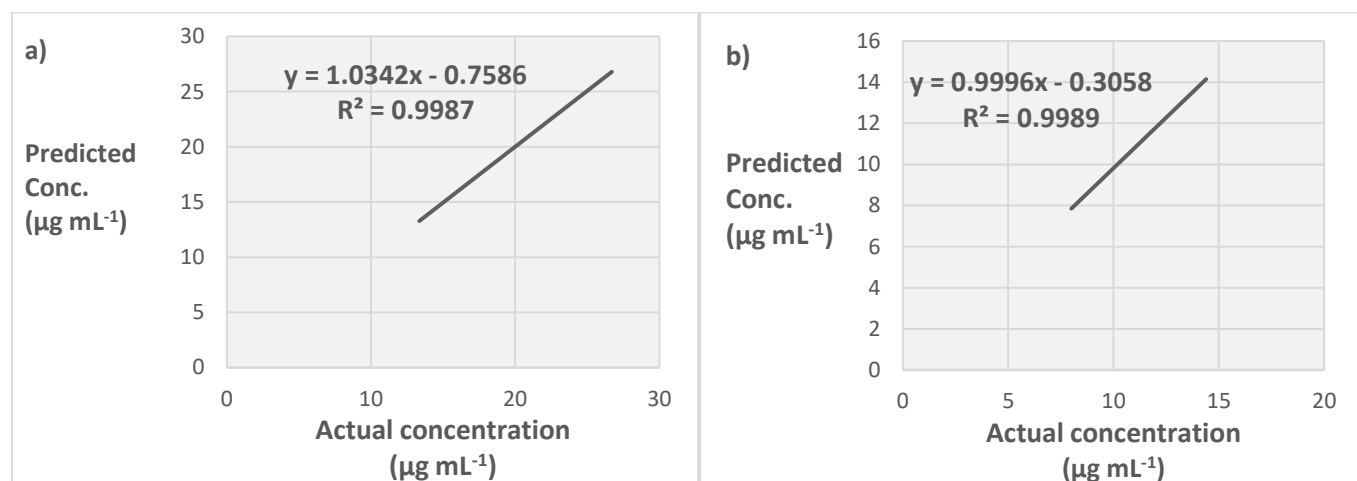


Figure 5. The PLS cross-validation for validation set of the actual vs. predicted concentration. (a) Sitagliptin; (b) Metformin HCl.

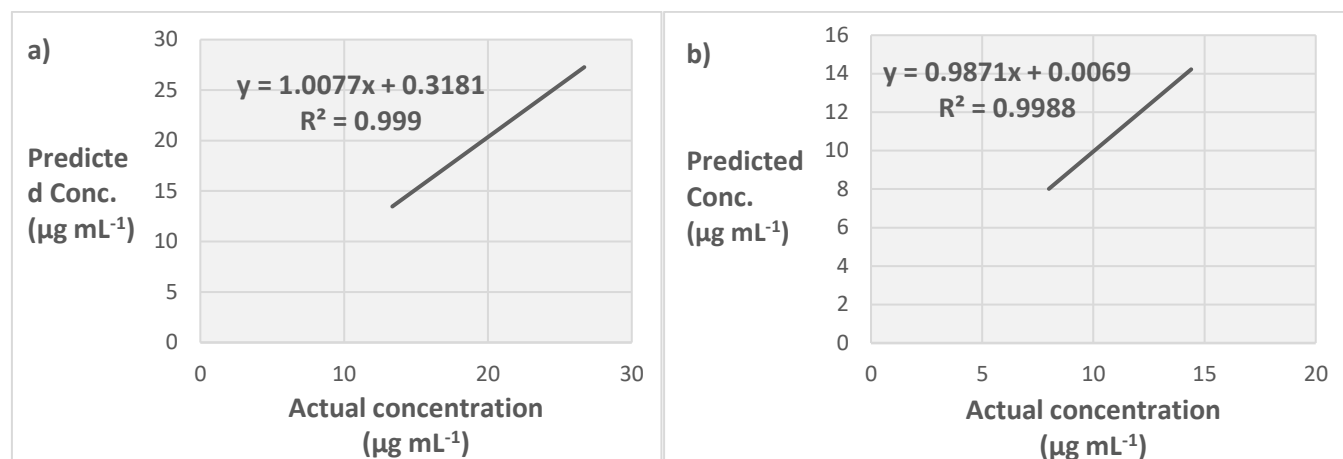


Figure 6. The PCR cross-validation for validation set of the actual vs. predicted concentration. (a) Sitagliptin; (b) Metformin HCl.

3.2.2 Precision (repeatability)

The repeatability (intraday precision) of the developed method was carried out by determining the binary mixture at three different concentrations for sitagliptin and metformin hydrochloride in bulk using three different concentrations (i.e., 13.36/10, 20.04/12 and

26.72/16 $\mu\text{g mL}^{-1}$ of sitagliptin/metformin hydrochloride, respectively) in triplicates sequentially. The results were reported as %RSD. The low values of %RSD were indicative of the high precision of the method. The %RSD values of the developed method were within the acceptable limit as suggested by the USP and the results are presented in Table 5.

Table 5. Results of repeatability and intraday precision using the developed PLS and PCR models.

Amount taken (actual conc.) (mg mL^{-1})		Predicted conc. (mg mL^{-1})				% Recovery				Acceptable % RSD NMT 2%			
Sita.	Metf.	PLS		PCR		PLS		PCR		PLS		PCR	
		Sita.	Metf.	Sita.	Metf.	Sita.	Metf.	Sita.	Metf.	Sita.	Metf.	Sita.	Metf.
13.36	10	13.31	9.56	13.54	9.76	99.63	95.60	101.35	97.60	0.62	0.58	1.17	0.27
13.36	10	13.33	9.60	13.43	9.80	99.78	96.00	100.52	98.00				
13.36	10	13.18	9.67	13.23	9.81	98.65	96.70	99.03	98.10				
20.04	12	19.90	11.55	20.19	11.70	99.30	96.25	100.75	97.50	0.60	0.38	0.33	0.13
20.04	12	20.08	11.62	20.31	11.73	100.20	96.83	101.35	97.75				
20.04	12	20.13	11.63	20.30	11.72	100.45	96.92	101.30	97.67				
26.72	16	26.22	15.51	25.91	15.65	98.13	96.94	96.97	97.81	1.03	0.40	1.15	0.16
26.72	16	26.65	15.63	26.44	15.70	99.74	97.69	98.95	98.13				
26.72	16	26.15	15.54	25.93	15.67	97.87	97.13	97.04	97.94				

% Recovery = (predicted conc. in $\mu\text{g mL}^{-1}$ / Actual conc. in $\mu\text{g mL}^{-1}$) $\times 100$.

3.2.3 Accuracy

Accuracy of the method was investigated using standard addition method for three different percentage levels (i.e., 80, 100, and 120%) by recovery experiments. Known amounts of standard solutions containing sitagliptin and metformin hydrochloride were added to sample solutions under investigation to make up solutions of 80, 100, and 120% levels in triplicates and

scanned at the range 200–400 nm. The amount of the drugs recovered at each percentage level were determined by using the developed PCR and PLS models. The mean percentage recovery for each percentage level was showed low values of %RSD and the percentage recovery was within the acceptable limit (90–110%) as suggested by the USP. This indicates a high accuracy method at all the three levels and the accuracy data are given in Tables 6 and 7.

Table 6. Accuracy data of sitagliptin by PCR and PLS models.

%Level	Sample conc. ($\mu\text{g mL}^{-1}$)	Amount of standard sitagliptin ($\mu\text{g mL}^{-1}$)	Total conc. ($\mu\text{g mL}^{-1}$)	Predicted conc. ($\mu\text{g mL}^{-1}$)		%Recovery		%RSD	
				PLS	PCR	PLS	PCR	PLS	PCR
80%	1	9.68	10.68	11.10	10.97	103.91	102.70	0.86	1.08
				10.91	10.89	102.16	101.94		
				10.98	10.74	102.83	100.54		
100%	1	12.10	13.10	13.37	13.36	102.09	101.99	0.87	0.96
				13.28	13.32	101.37	101.69		
				13.14	13.12	100.34	100.18		
120%	1	14.52	15.52	15.45	15.16	99.55	97.66	0.95	0.20
				15.16	15.10	97.67	97.30		
				15.32	15.15	98.69	97.59		

Table 7. Accuracy data of metformin hydrochloride by PCR and PLS models.

%Level	Sample conc. ($\mu\text{g mL}^{-1}$)	Amount of standard metformin HCl ($\mu\text{g mL}^{-1}$)	Total conc. ($\mu\text{g mL}^{-1}$)	Predicted Conc. ($\mu\text{g mL}^{-1}$)		%Recovery		%RSD	
				PLS	PCR	PLS	PCR	PLS	PCR
80%	10	4	14	13.70	13.87	97.86	99.04	0.54	0.35
				13.79	13.93	98.51	99.50		
				13.85	13.96	98.91	99.73		
100%	10	5	15	15.27	15.17	101.79	101.14	0.49	0.23
				15.37	15.22	102.47	101.48		
				15.42	15.24	102.77	101.59		
120%	10	6	16	16.49	16.14	103.04	100.84	0.09	0.09
				16.50	16.11	103.14	100.69		
				16.52	16.11	103.23	100.68		

3.2.4 Specificity (Spiking Method)

The specificity of the method was checked by adding a certain amount of sitagliptin and metformin

hydrochloride standard into known amount of marketed sample solution as described in the Methodology section. Specificity data are shown in Tables 8 and 9.

Table 8. Results of specificity for sitagliptin using the developed PCR and PLS models.

Name of marketed sample	Sample conc. ($\mu\text{g mL}^{-1}$)	Amount added ($\mu\text{g mL}^{-1}$)	Total conc. ($\mu\text{g mL}^{-1}$)	Predicted conc. ($\mu\text{g mL}^{-1}$)		%Recovery		%RSD	
				PLS	PCR	PLS	PCR	PLS	PCR
Jauntab	1	12.1	13.1	13.37	13.36	102.09	101.99	0.50	0.21
				13.28	13.32	101.37	101.69		
Jaunmet	1	12.1	13.1	13.14	13.12	100.34	100.18	0.20	0.33
				13.18	13.06	100.63	99.71		
Jauncare	1	12.1	13.1	13.13	12.93	100.22	98.69	0.23	0.70
				13.17	13.06	100.54	99.67		

Table 9. Results of specificity for metformin HCl using the developed PCR and PLS models.

Name of marketed sample	Sample conc. ($\mu\text{g mL}^{-1}$)	Amount added ($\mu\text{g mL}^{-1}$)	Total conc. ($\mu\text{g mL}^{-1}$)	Predicted conc. ($\mu\text{g mL}^{-1}$)		%Recovery		%RSD	
				PLS	PCR	PLS	PCR	PLS	PCR
Jauntab	10	5	15	15.27	15.17	101.79	101.14	0.47	0.24
				15.37	15.22	102.47	101.48		
Jaunmet	10	5	15	15.42	15.24	102.77	101.59	0.06	0.00
				15.40	15.24	102.69	101.59		
Jauncare	10	5	15	15.45	15.25	103.03	101.66	0.42	0.22
				15.55	15.30	103.65	101.97		

As it can be appeared from these data, recovery for sitagliptin and metformin hydrochloride using the developed PCR and PLS models are within the acceptable limit (90–110%) This suggests that the methods are free from interference due to the excipients used in the commercial formulation.

The above validation results indicate that method is simple, rapid, economical, precise and accurate beside being eco-friendly. Therefore it can be used for a routine analysis in quality control of mixtures and commercial products containing sitagliptin and metformin hydrochloride.

3.2.5 Analysis of marketed formulations

The applicability of the developed methods for the quantification of sitagliptin and metformin hydrochloride in marketed formulations was carried out using the marketed formulation of 50 mg sitagliptin with 500 mg metformin hydrochloride concentration collected from the local pharmacies in the capital Sana'a. Tables 10 and 11 summarized the data obtained for the sitagliptin and metformin hydrochloride in the analyzed marketed formulations.

Table 10. Assay result for sitagliptin and metformin hydrochloride in tablet (marketed sample) by PLS proposed method.

Name of marketed sample	METHOD		PLS					
	Sita.	Metf.	Sita.			Metf.		
	Measured conc. ($\mu\text{g mL}^{-1}$)		Obtained conc. ($\mu\text{g mL}^{-1}$)	%Recovery	%RSD	Obtained conc. ($\mu\text{g mL}^{-1}$)	%Recovery	%RSD
Jauntab	10.68	14	11.10	103.91	1.20	13.70	97.86	0.47
	10.68	14	10.91	102.16		13.79	98.51	
Jaunmet	10.68	14	10.98	102.83	0.50	13.85	98.91	0.24
	10.68	14	10.91	102.11		13.90	99.25	
Jauncare	10.68	14	11.15	104.40	0.26	13.79	98.52	0.44
	10.68	14	11.19	104.79		13.88	99.14	

Table 11. Assay result for sitagliptin and metformin hydrochloride in tablet (Marketed Sample) by PCR proposed method.

Name of marketed sample	METHOD		PCR					
	Sita.	Metf.	Sita.			Metf.		
	Measured conc. ($\mu\text{g mL}^{-1}$)		Obtained conc. ($\mu\text{g mL}^{-1}$)	%Recovery	%RSD	Obtained conc. ($\mu\text{g mL}^{-1}$)	%Recovery	%RSD
Jauntab	10.68	14	10.97	102.70	0.53	13.87	99.04	0.33
	10.68	14	10.89	101.94		13.93	99.50	
Jaunmet	10.68	14	10.74	100.54	0.64	13.96	99.73	0.06
	10.68	14	10.64	99.63		13.98	99.82	
Jauncare	10.68	14	11.17	104.55	0.43	13.75	98.21	0.27
	10.68	14	11.10	103.91		13.80	98.59	

As it can be seen from these data, the sitagliptin and metformin hydrochloride concentrations were within the acceptable limit (90–110%) according to the USP.

3.2.6 Comparing with reference method

Comparison was carried out, with the aid of SPSS program using F-Test to assure non-significant difference between the recovery results of the newly

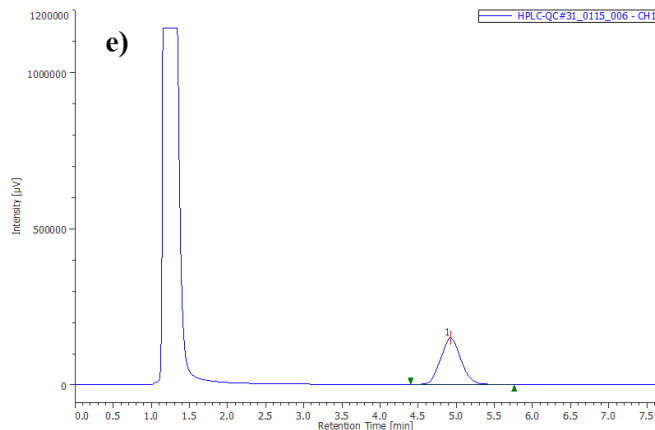
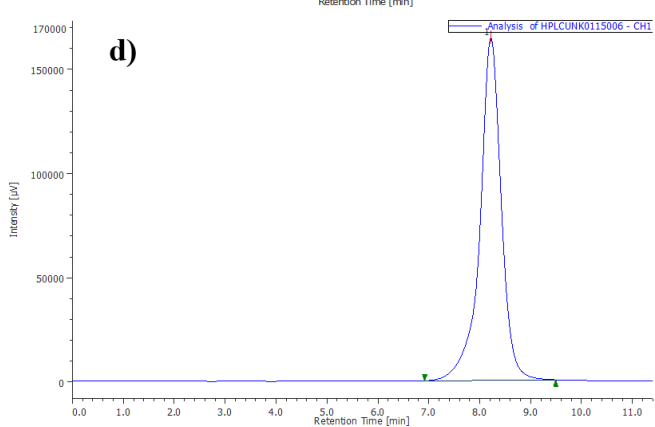
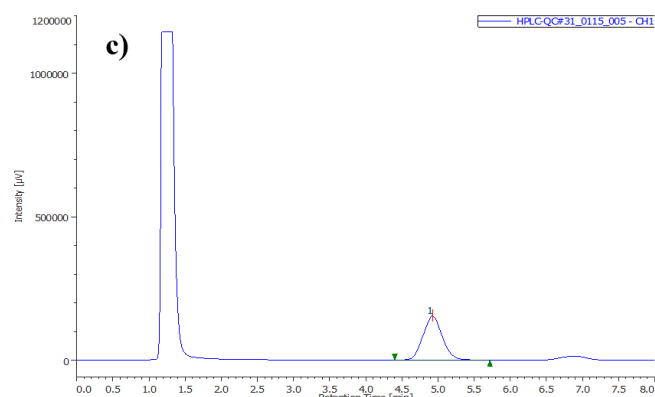
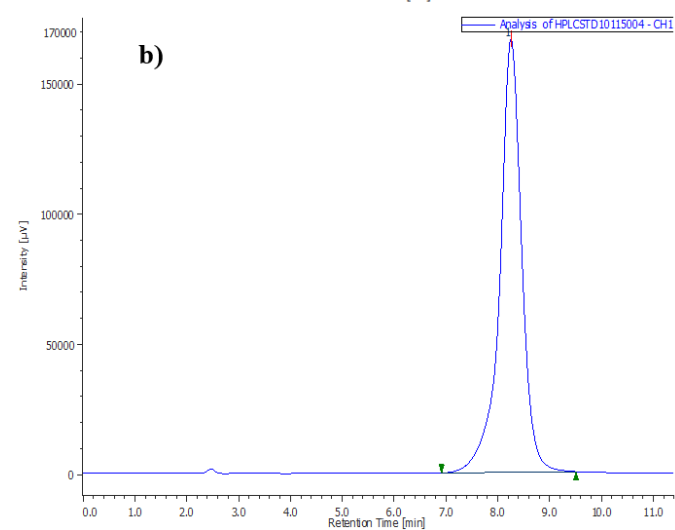
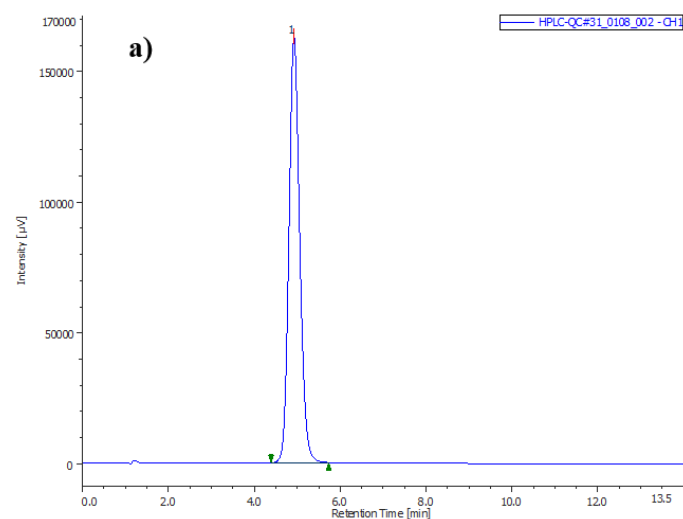
developed methods and that of reference method for both the sitagliptin and metformin hydrochloride. Significance level indicated that null hypothesis was acceptable since the P-value was greater than significance level (Table 12). As for reference methods, sitagliptin and metformin hydrochloride were determined according to the USP as described in the Methodology section.

Table 12. Results of statistical comparison between newly developed method and reference method.

Name of marketed sample	Component	Sitagliptin			Metformin HCl			
		Methods	Reference method (HPLC)	PLS	PCR	Reference method (HPLC)	PLS	PCR
Jauntab			101.62	103.91	102.70	96.87	97.86	99.03
			100.86	102.17	101.94	96.94	98.52	99.50
	Mean%		101.24	103.04	102.32	96.91	96.91	98.19
	RSD%		0.53	1.19	0.53	0.05	0.48	0.33
	F-value			0.20	0.18		0.06	0.01
Jaunmet			98.11	102.82	100.54	97.08	98.91	99.73
			98.32	102.00	99.64	98.60	99.25	99.82
	Mean%		98.22	102.47	100.09	97.84	99.08	99.78
	RSD%		0.15	0.49	0.64	1.10	0.24	0.06
	F-value			0.01	0.06		0.25	0.13

F-value at $p = 0.01$.

Also, the chromatograms in Fig. 7 have showed the results of the analysis for reference method for the determination of sitagliptin and metformin hydrochloride.



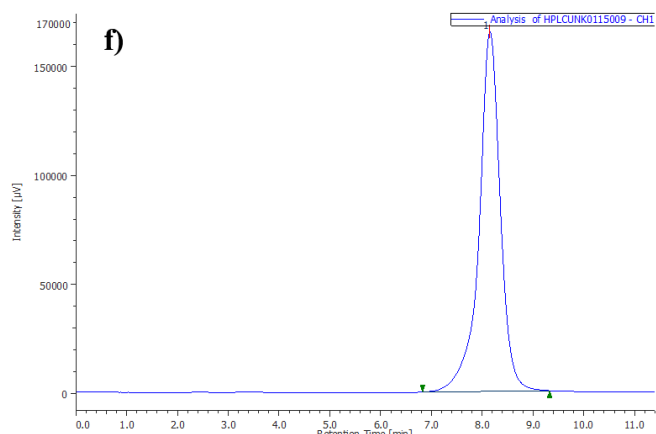


Figure 7. Chromatogram of sitagliptin and metformin HCl standard and commercial samples. (a) Standard sitagliptin; (b) Standard Metformin HCl; (c) Sitagliptin in Jauntab Sample (commercial); (d) Metformin HCl in Jauntab Sample (commercial); (e) Sitagliptin in Jaunmet Sample (commercial); (f) Metformin HCl in Jaunmet Sample (commercial)

4. Conclusions

The proposed chemometrics models (PLS and PCR) has proven to determine simultaneously sitagliptin and metformin HCl in combined mixtures of pharmaceutical dosage forms without excipients interference or each other, and without prior physical separation of the two drugs. Multivariate calibration models were generated using matrices of spectral and concentration data. The validation of the two models and their application to a commercial pharmaceutical dosage form gave excellent results. As a result, the suggested techniques can be applied to regular quality control of the specified medications in their combination dosage form in standard laboratories.

Authors' contribution

Conceptualization: Almaqtari, M. A.
Data curation: Almaqtari, M. A.; Al-Odaini, N. A.
Formal Analysis: Alarbagi, F. A.
Funding acquisition: Not applicable.
Investigation: Alarbagi, F. A.; Al-Maydama, H.
Methodology: Alarbagi, F. A.
Project administration: Almaqtari, M. A.; Al-Odaini, N. A.
Resources: Not applicable.
Software: Alarbagi, F. A.
Supervision: Almaqtari, M. A.; Al-Odaini, N. A.
Validation: Alarbagi, F. A.
Visualization: Al-Odaini, N. A.

Writing – original draft: Alarbagi, F. A.
Writing – review & editing: Al-Maydama, H.

Data availability statement

Data will be available upon request.

Funding

Not applicable

Acknowledgments

The authors would like to thank the Chemistry Department-Faculty of Science, Sana'a University, Global Pharma and Shiba'a pharma Companies, Sana'a, Yemen for providing the laboratory facilities and the reference standards of the samples drugs as a gift.

References

- Adsul, S.; Bidkar, J. S.; Harer, S.; Dama, G. Y. RP-HPLC method development and validation for simultaneous estimation for metformin and sitagliptin in bulk and tablet formulation. *Int. J. Chem. Tech. Res.* **2018**, *11* (11), 428–435. <https://doi.org/10.20902/IJCTR.2018.111149>
- Aminu, N.; Chan, S.-Y.; Khan, N. H.; Farhan, A. B.; Umar, M. N.; Toh, S.-M. A simple stability-indicating HPLC method for simultaneous analysis of paracetamol and caffeine and its application to determinations in fixed-dose combination tablet dosage form. *Acta Chromatogr.* **2019**, *31* (2), 85–91. <https://doi.org/10.1556/1326.2018.00354>
- Ashour, A.; Hegazy, M. A.; Abdel-Kawy, M.; ElZeiny, M. B. Simultaneous spectrophotometric determination of overlapping spectra of paracetamol and caffeine in laboratory prepared mixtures and pharmaceutical preparations using continuous wavelet and derivative transform. *J. Saudi Chem. Soc.* **2015**, *19* (2), 186–192. <https://doi.org/10.1016/j.jscs.2012.02.004>
- Attia, K. A.-S. M.; Abdel-Aziz, O.; Magdy, N.; Mohamed, G. F. Development and validation of different chemometric-assisted spectrophotometric methods for determination of cefoxitin-sodium in presence of its alkali-induced degradation product. *Future J. Pharm. Sci.* **2018**, *4* (2), 241–247. <https://doi.org/10.1016/j.fjps.2018.08.002>

- Belal, F.; Ibrahim, F.; Sheribah, Z.; Alaa, H. New spectrophotometric/chemometric assisted methods for the simultaneous determination of imatinib, gemifloxacin, nalbuphine and naproxen in pharmaceutical formulations and human urine. *Spectrochim. Acta A Mol. Biomol. Spectrosc.* **2018**, *198*, 51–60. <https://doi.org/10.1016/j.saa.2018.02.048>
- British Pharmacopoeia Commission. *Medicines and Healthcare products Regulatory Agency (MHRA). British Pharmacopoeia Commission.* **2020**, *3* (6), 1844.
- Darbandi, A.; Sohrabi, M. R.; Bahmaei, M. Development of a chemometric-assisted spectrophotometric method for quantitative simultaneous determination of Amlodipine and Valsartan in commercial tablet. *Optik.* **2020**, *218*, 165110. <https://doi.org/10.1016/j.ijleo.2020.165110>
- Elfatry, H. M.; Mabrouk, M. M.; Hammad, S. F.; Mansour, F. R.; Kamal, A. H.; Alahmad, S. Development and validation of chemometric-assisted spectrophotometric methods for simultaneous determination of phenylephrine hydrochloride and ketorolac tromethamine in binary combinations. *J. AOAC Inter.* **2016**, *99* (5), 1247–1251. <https://doi.org/10.5740/jaoacint.16-0106>
- Gandhi, S. V.; Waghmare, A. D.; Nandwani, Y. S.; Mutha, A. S. Chemometrics - Assisted UV spectrophotometric method for determination of ciprofloxacin and ornidazole in pharmaceutical formulation. *ARC Journal of Pharmaceutical Sciences.* **2017**, *3* (1), 19–25. <https://doi.org/10.20431/2455-1538.0301005>
- Gholse, Y. N.; Chaple, D. R.; Kasliwal, R. H. Development and validation of novel analytical simultaneous estimation based UV spectrophotometric method for doxycycline and levofloxacin determination. *Biointerface Res. Appl. Chem.* **2021**, *12* (4), 5458–5478. <https://doi.org/10.33263/BRIAC124.54585478>
- Glavanović, S.; Glavanović, M.; Tomišić, V. Simultaneous quantitative determination of paracetamol and tramadol in tablet formulation using UV spectrophotometry and chemometric methods. *Spectrochim. Acta A Mol. Biomol. Spectrosc.* **2016**, *157*, 258–264. <https://doi.org/10.1016/j.saa.2015.12.020>
- Himabindu, T.; Narmadha, S.; Sireesha, D.; Vasudha, B. Development and validation of spectrophotometric method for the simultaneous estimation of metformin hydrochloride and sitagliptinin tablet dosage form. *World J. Pharm. Res.* **2016**, *5* (7), 1011–1018.
- Krishnan, B.; Mishra, K. Quality by design based development and validation of RP-HPLC method for simultaneous estimation of sitagliptin and metformin in bulk and pharmaceutical dosage forms. *Int. J. Pharm. Investig.* **2020**, *10* (4), 512–518. <https://doi.org/10.5530/ijpi.2020.4.89>
- Kumar, V. P.; Kavitha, M.; Patro, S.; Bhavya, C.; Bag, A. K. Development and validation of new analytical method for the simultaneous estimation of metformin and sitagliptin in bulk and dosage form by RP-HPLC. *World J. Pharm. Res.* **2017**, *6* (3), 1691–1700.
- Lotfy, H. M.; Mohamed, D.; Mowaka, S. A comparative study of smart spectrophotometric methods for simultaneous determination of sitagliptinand metformin hydrochloride in their binary mixture. *Spectrochim. Acta A Mol. Biomol. Spectrosc.* **2015**, *149*, 441–451. <https://doi.org/10.1016/j.saa.2015.04.076>
- Manouchehri, F.; Izadmanesh, Y.; Aghaee, E.; Ghasemi, J. B. Experimental, computational and chemometrics studies of BSA-vitamin B6 interaction by UV-Vis, FT-IR, fluorescence spectroscopy, molecular dynamics simulation and hard-soft modeling methods. *Bioorg. Chem.* **2016**, *68*, 124–136. <https://doi.org/10.1016/j.bioorg.2016.07.014>
- Mohammed, O. J.; Hamzah, M. J.; Saeed, A. M. RP-HPLC method validation for simultaneous estimation of paracetamol and caffeine in formulating pharmaceutical form. *Res. J. Pharm. Technol.* **2021**, *14* (9), 4743–4748. <https://doi.org/10.52711/0974-360X.2021.00825>
- Moroni, A. B.; Vega, D. R.; Kaufman, T. S.; Calvo, N. L. Form quantitation in desmotropic mixtures of albendazole bulk drug by chemometrics-assisted analysis of vibrational spectra. *Spectrochim. Acta A Mol. Biomol. Spectrosc.* **2022**, *265*, 120354. <https://doi.org/10.1016/j.saa.2021.120354>
- Moussa, B. A.; Mahrouse, M. A.; Fawzy, M. G. Smart spectrophotometric methods for the simultaneous determination of newly co-formulated hypoglycemic drugs in binary mixtures. *Spectrochim. Acta A Mol. Biomol. Spectrosc.* **2021**, *257*, 119763. <https://doi.org/10.1016/j.saa.2021.119763>
- Muntean, D. M.; Alecu, C.; Tomuta, I. Simultaneous quantification of paracetamol and caffeine in powder blends for tableting by NIR-chemometry. *J. Spectroscopy.* **2017**, *2017*, 7160675. <https://doi.org/10.1155/2017/7160675>
- Muntean, D.; Porfire, A.; Alceu, C.; Iurian, S.; Casian, T.; Gavan, A.; Tomuta, I. A non-destructive NIR

- spectroscopic method combined with chemometry for simultaneous assay of paracetamol and caffeine in tablets. *Ro. J. Pharm. Pract.* **2021**, *14* (2), 68-75. <https://doi.org/10.37897/RJPhP.2021.2.2>
- Ortega-Barrales, P.; Padilla-Weigand, R.; Molina-Díaz, A. Simultaneous determination of paracetamol and caffeine by flow injection–solid phase spectrometry using C18 silica gel as a sensing support. *Anal. Sci.* **2002**, *18* (11), 1241–1246. <https://doi.org/10.2116/analsci.18.1241>
- Patel, K. R.; Prajapati, L. M.; Joshi, A. K.; Kharodiya, M. L.; Patel, J. R. Application of chemometrics in simultaneous spectrophotometric quantification of etophylline and theophylline: The drugs with same chromophore. *Iranian Journal of Pharmaceutical Sciences* **2013a**, *9* (3), 17–28.
- Patel, M. N.; Alvi, S. N.; Savalia, M. D.; Kathiria, P. B.; Patel, B. A.; Parmar, S. J. Development and validation of first order derivative spectrophotometric method for simultaneous estimation of paracetamol and caffeine in tablet dosage form. *Inventi Rapid: Pharm Analysis & Quality Assurance.* **2013b**, *2013* (2), 1–5.
- Patel, R.; Mashru, R. Development and validation of chemometric assisted methods and stability indicating RP-HPLC method for simultaneous estimation of rasagiline mesylate and pramipexole in synthetic mixture. *Acta Scientific Pharmaceutical Sciences.* **2019**, *3* (8), 154–168. <https://doi.org/10.31080/ASPS.2019.03.0359>
- Phechkrajang, C. M.; Siriratawan, W.; Narapanich, K.; Thanomchat, K.; Kantanawat, P.; Srikajhondei, W.; Khajornvanitchot, V.; Sakchaisri, K. Development and validation of chemometrics-assisted spectrophotometric method for determination of clotrimazole in the presence of betamethasone valerate. *Mahidol University J. Pharm. Sci.* **2015**, *42* (2), 1–7.
- Putri, D. C. A.; Gani, M. R.; Octa, F. D. Chemometrics-assisted UV spectrophotometric method for simultaneous determination of paracetamol and tramadol in divided powder dosage form. *Int. J. Pharm. Res.* **2021**, *13* (1), 1901–1907. <https://doi.org/10.31838/ijpr/2021.13.01.075>
- Rahman, A.; Sravani, G. J.; Srividya, K.; Priyadharshni, A. D. R.; Narmada, A.; Sahithi, K.; Sai, T. K.; Padmavathi, Y. Development and validation of chemometric assisted FTIR spectroscopic method for simultaneous estimation of valsartan and hydrochlorothiazide in pure and pharmaceutical dosage forms. *J. Young Pharm.* **2020**, *12* (2s), s51-s55. <https://doi.org/10.5530/jyp.2020.12s.46>
- Salem, Y. A.; Hammouda, M. E. A.; El-Enin, M. A. A.; El-Ashry, S. M. Application of derivative emission fluorescence spectroscopy for determination of ibuprofen and phenylephrine simultaneously in tablets and biological fluids. *Spectrochim. Acta A Mol. Biomol. Spectrosc.* **2019**, *210*, 387–397. <https://doi.org/10.1016/j.saa.2018.11.054>
- Sebaïy, M. M.; El-Adl, S. M.; Mattar, A. A. Different techniques for overlapped UV spectra resolution of some co-administered drugs with paracetamol in their combined pharmaceutical dosage forms. *Spectrochim. Acta A Mol. Biomol. Spectrosc.* **2020**, *224*, 117429. <https://doi.org/10.1016/j.saa.2019.117429>
- Sebaïy, M.; Mattar, A. A.; El-Adl, S. M. UV-chemometric method development for resolving the overlapped spectra of aspirin, caffeine and orphenadrine citrate in their ternary pharmaceutical dosage form. *Research Square.* **Preprint**; 2022. <https://doi.org/10.21203/rs.3.rs-1262160/v1>
- Shah, U. H.; Jasani, A. H. Chemometric assisted spectrophotometric methods for simultaneous determination of paracetamol and tolperisone hydrochloride in pharmaceutical dosage form. *Eurasian J. Anal. Chem.* **2017**, *12* (3), 211–222.
- Shinde, M. A.; Divya, O. Simultaneous quantitative analysis of a three-drug combination using synchronous fluorescence spectroscopy and chemometrics. *Current Science.* **2015**, *108* (7), 1348–1354.
- Silva, W. C.; Pereira, P. F.; Marra, M. C.; Gimenes, D. T.; Cunha, R. R.; Silva, R. A.; Munoz, R. A.; Richter, E. M. A simple strategy for simultaneous determination of paracetamol and caffeine using flow injection analysis with multiple pulse amperometric detection. *Electroanalysis.* **2011**, *23* (12), 2764–2770. <https://doi.org/10.1002/elan.201100512>
- Singh, V. D.; Singh, V. K. Chemo-metric assisted UV-spectrophotometric methods for simultaneous estimation of Darunavir ethanolate and Cobicistat in binary mixture and their tablet formulation. *Spectrochim. Acta A Mol. Biomol. Spectrosc.* **2021**, *250*, 119383. <https://doi.org/10.1016/j.saa.2020.119383>
- Sun, X.; Li, H.; Yi, Y.; Hua, H.; Guan, Y.; Chen, C. Rapid detection and quantification of adulteration in Chinese hawthorn fruits powder by near-infrared spectroscopy combined with chemometrics.

Spectrochim. Acta A Mol. Biomol. Spectrosc. **2021**, *250*, 119346. <https://doi.org/10.1016/j.saa.2020.119346>

Swamy, G. K.; Surekha, M. L.; Krishna, M. M. Development and validation of RP-HPLC method for simultaneous estimation of metformin and sitagliptin in bulk and tablet dosage forms. *Journal of Pharmaceutical and Medicinal Chemistry*. **2020**, *6* (1), 15–20.

Tsvetkova, B.; Kostova, B.; Pencheva, I.; Zlatkov, A.; Rachev, D.; Peikov, P. Validated LC method for simultaneous analysis of paracetamol and caffeine in model tablet formulation. *Int. J. Pharm. Pharm. Sci.* **2012**, *4* (Suppl. 4), 680–684.

Uddin, M.; Mondol, A.; Karim, M.; Jahan, R.; Rana, A. Chemometrics assisted spectrophotometric method for simultaneous determination of paracetamol and caffeine in pharmaceutical formulations. *Bangladesh J. Sci. Ind. Res.* **2019**, *54* (3), 215–222. <https://doi.org/10.3329/bjsir.v54i3.42673>

United States Pharmacopeia and the National Formulary (USP 43 - NF 38). The United States Pharmacopeial Convention; 2020. <https://www.uspnf.com/notices/usp-nf-final-print-edition> (accessed 2022-06-09).

Vichare, V.; Mujgond, P.; Tambe, V.; Dhole, S. N. Simultaneous Spectrophotometric Determination of Paracetamol and Caffeine in Tablet Formulation. *Int. J. PharmTech Res.* **2010**, *2* (4), 2512–2516.

Vu Dang, H.; Thu, H. T. T.; Ha, L. D. T.; Mai, H. N. RP-HPLC and UV Spectrophotometric Analysis of Paracetamol, Ibuprofen, and Caffeine in Solid Pharmaceutical Dosage Forms by Derivative, Fourier, and Wavelet Transforms: A Comparison Study. *J. Anal. Methods Chem.* **2020**, *2020*, 8107571. <https://doi.org/10.1155/2020/8107571>

Walash, M. I.; Belal, F. F.; El-Enany, N. M.; El-Maghrabey, M. H. Synchronous fluorescence spectrofluorimetric method for the simultaneous determination of metoprolol and felodipine in combined pharmaceutical preparation. *Chem. Central J.* **2011**, *5*, 70. <https://doi.org/10.1186/1752-153X-5-70>

Zhu, L.; Wu, H.-L.; Xie, L.-X.; Fang, H.; Xiang, S.-X.; Hu, Y.; Liu, Z.; Wang, T.; Yu, R.-Q. A chemometrics-assisted excitation–emission matrix fluorescence method for simultaneous determination of arbutin and hydroquinone in cosmetic products. *Analytical Methods*. **2016**, *8* (24), 4941–4948. <https://doi.org/10.1039/C6AY00821F>

Appendix

Table A1. Results of optimum number of principal factors of sitagliptin for PLS models.

Method	Components to evaluate	Number of components evaluated	Number of components selected		
Cross-validation (Leave-one-out)	Set	10	8		
Model selection and validation for sitagliptin					
Components (pred.)	X Variance	Error	R-sq	Press	R-sq (Pred)
1	0.577399	139.559	0.74980	188.677	0.661736
2	0.999466	1.892	0.99661	2.565	0.995402
3	0.999858	1.036	0.99814	1.568	0.997189
4	0.999888	0.534	0.99904	1.577	0.997172
5	0.999929	0.370	0.99934	1.304	0.997663
6	0.999937	0.116	0.99979	1.390	0.997508
7	0.999946	0.048	0.99991	1.404	0.997482
8	0.999950	0.006	0.99999	1.291	0.997686
9		0.002	1.00000	1.332	0.997612
10		0.001	1.00000	1.335	0.997607

Table A2. Results of optimum number of principal factors of metformin hydrochloride for PLS models.

Method	Components to evaluate	Number of components evaluated	Number of components selected		
Cross-validation (Leave-one-out)	Set	10	8		
Model selection and validation for metformin hydrochloride					
Components (pred.)	X Variance	Error	R-sq	Press	R-sq (Pred)
1	0.743512	14.9504	0.92525	18.7639	0.906180
2	0.999466	0.1424	0.99929	0.1877	0.999062
3	0.999855	0.1157	0.99942	0.1763	0.999119
4	0.999901	0.0742	0.99963	0.1759	0.999120
5	0.999927	0.0394	0.99980	0.1527	0.999237
6	0.999937	0.0143	0.99993	0.1613	0.999194
7	0.999946	0.0059	0.99997	0.1565	0.999217
8	0.999952	0.0023	0.99999	0.1469	0.999265
9		0.0006	1.00000	0.1502	0.999249
10		0.0002	1.00000	0.1523	0.999239

Table A3. The constant and coefficients at each wavelength of sitagliptin and metformin hydrochloride for PLS models.

Sitagliptin				Metformin hydrochloride			
Constant		-1.1712		Constant		0.4045	
Wavelength (nm)	Coefficients	Wavelength (nm)	Coefficients	Wavelength (nm)	Coefficients	Wavelength (nm)	Coefficients
270	-8.554	234.8	0.6532	270	-5.2653	234.8	0.0527
269.8	36.5022	234.6	0.2441	269.8	-3.4147	234.6	0.0577
269.6	-31.8693	234.4	1.2605	269.6	-10.9734	234.4	0.0604
269.4	-25.5432	234.2	0.49	269.4	10.849	234.2	-0.0832
269.2	-65.3233	234	0.1544	269.2	-1.7155	234	0.1432
269	-23.0727	233.8	-0.2522	269	9.9911	233.8	-0.0113
268.8	-11.3679	233.6	-0.5453	268.8	-13.4665	233.6	0.2214
268.6	-5.5928	233.4	-0.344	268.6	4.7408	233.4	0.2054
268.4	-4.1696	233.2	0.8311	268.4	1.394	233.2	0.1359
268.2	-14.1503	233	0.1554	268.2	-4.088	233	0.0633
268	-19.1888	232.8	-0.059	268	-11.7374	232.8	0.1427
267.8	-40.9486	232.6	-0.7372	267.8	-7.8427	232.6	0.0949
267.6	-22.6885	232.4	-0.6594	267.6	-10.4613	232.4	0.1963

267.4	5.516	232.2	0.6939	267.4	2.0351	232.2	-0.0132
267.2	-50.7754	232	0.6551	267.2	13.406	232	0.0935
267	-9.302	231.8	-0.995	267	1.6967	231.8	0.1395
266.8	-10.1594	231.6	-0.2627	266.8	-2.8888	231.6	0.1843
266.6	18.2208	231.4	-0.5025	266.6	-13.25	231.4	0.1687
266.4	6.7485	231.2	0.0497	266.4	2.8032	231.2	0.1305
266.2	23.5144	231	-0.7094	266.2	0.6477	231	0.1136
266	-9.3416	230.8	0.205	266	-8.4888	230.8	0.0976
265.8	21.6262	230.6	0.152	265.8	2.8843	230.6	-0.2017
265.6	15.7812	230.4	-0.069	265.6	-0.3461	230.4	-0.1925
265.4	36.272	230.2	-0.5146	265.4	4.9661	230.2	0.1252
265.2	23.198	230	-0.9981	265.2	-10.2205	230	0.1216
265	22.0233	229.8	-0.7537	265	-8.7358	229.8	0.0951
264.8	4.3131	229.6	0.0623	264.8	3.7949	229.6	0.4342
264.6	-2.4513	229.4	0.3702	264.6	-1.1286	229.4	-0.077
264.4	16.4876	229.2	-0.4447	264.4	-2.8178	229.2	0.4234
264.2	4.741	229	0.6679	264.2	3.2968	229	0.0984
264	13.294	228.8	0.2232	264	0.8386	228.8	0.3764
263.8	2.2629	228.6	-0.7047	263.8	-1.3713	228.6	0.2014
263.6	-9.7468	228.4	-0.2404	263.6	0.98	228.4	-0.0309
263.4	-13.6458	228.2	-0.671	263.4	8.5777	228.2	0.1123
263.2	13.8386	228	-0.7128	263.2	-4.6343	228	0.1859
263	-1.2977	227.8	-0.4311	263	-4.7391	227.8	0.2667
262.8	-4.2576	227.6	-0.6824	262.8	0.7491	227.6	0.378
262.6	8.4991	227.4	-0.1933	262.6	-6.8955	227.4	0.3419
262.4	10.8477	227.2	-1.2674	262.4	-4.3476	227.2	-0.0296
262.2	4.3527	227	-0.1852	262.2	-7.5522	227	0.1174
262	27.7793	226.8	-0.723	262	2.1918	226.8	0.182
261.8	-16.3076	226.6	-1.5414	261.8	0.0193	226.6	0.2658
261.6	22.6114	226.4	-0.1781	261.6	2.6963	226.4	0.4972
261.4	-4.7696	226.2	-2.6872	261.4	-1.5696	226.2	-0.2154
261.2	-3.511	226	-1.0534	261.2	4.3536	226	0.0702
261	7.9681	225.8	-0.165	261	-3.1001	225.8	0.6035
260.8	41.8407	225.6	-0.2283	260.8	-1.8041	225.6	0.4791
260.6	33.643	225.4	-1.6467	260.6	3.999	225.4	0.5571
260.4	13.2769	225.2	-1.2369	260.4	3.9561	225.2	0.2447
260.2	10.0929	225	-0.5339	260.2	3.1868	225	0.3378
260	9.8518	224.8	-1.3898	260	-2.1213	224.8	0.594
259.8	43.043	224.6	-0.8225	259.8	-1.7967	224.6	0.1454
259.6	5.1607	224.4	-0.6431	259.6	-9.4247	224.4	0.1927
259.4	-34.1511	224.2	-1.1628	259.4	-17.384	224.2	0.3319
259.2	11.5158	224	-1.2444	259.2	-6.5233	224	0.305
259	-14.383	223.8	-0.8308	259	7.4788	223.8	0.4529
258.8	14.5878	223.6	-0.4681	258.8	15.1635	223.6	0.4367
258.6	4.5959	223.4	-0.0295	258.6	3.1614	223.4	0.5613
258.4	-18.8881	223.2	-1.6294	258.4	2.0012	223.2	0.1711
258.2	7.6601	223	-0.7336	258.2	11.4035	223	0.5318
258	4.6961	222.8	-1.8822	258	-5.1932	222.8	0.109
257.8	27.7054	222.6	-1.1367	257.8	10.9597	222.6	0.3162
257.6	0.988	222.4	-1.1225	257.6	10.405	222.4	0.3399
257.4	-12.5001	222.2	-0.8589	257.4	8.7258	222.2	0.3429
257.2	-15.2382	222	-1.6734	257.2	-0.8162	222	0.6074
257	-3.0942	221.8	-0.679	257	1.0974	221.8	0.579
256.8	-4.4602	221.6	0.1903	256.8	-1.5909	221.6	0.1961
256.6	1.7788	221.4	0.089	256.6	-5.2308	221.4	0.23
256.4	27.5921	221.2	-1.1892	256.4	9.6734	221.2	-0.0033
256.2	-18.0223	221	-1.5961	256.2	-2.957	221	0.2731
256	33.2932	220.8	-0.1513	256	8.4664	220.8	0.5852
255.8	-2.1517	220.6	-0.158	255.8	0.3689	220.6	0.3382
255.6	-13.3572	220.4	-0.3497	255.6	7.3895	220.4	0.8263
255.4	-18.1868	220.2	-0.3168	255.4	4.4221	220.2	0.6111

255.2	26.0096	220	-0.8101	255.2	7.9959	220	0.2208
255	9.8431	219.8	0.0445	255	9.3932	219.8	0.2442
254.8	-27.3872	219.6	-0.9638	254.8	-1.395	219.6	0.1875
254.6	20.7778	219.4	-1.6612	254.6	-2.7202	219.4	0.1146
254.4	-1.2528	219.2	-1.7879	254.4	-4.9913	219.2	0.2444
254.2	-13.5772	219	-1.2254	254.2	-1.6811	219	0.1439
254	-23.6382	218.8	0.3546	254	-4.9847	218.8	0.4906
253.8	-13.4889	218.6	-1.0438	253.8	8.1626	218.6	0.1345
253.6	2.8508	218.4	-0.5056	253.6	1.9851	218.4	0.1787
253.4	23.3554	218.2	-0.4821	253.4	0.8798	218.2	0.131
253.2	-11.656	218	0.9343	253.2	-4.1621	218	0.3666
253	-10.1518	217.8	-0.8597	253	4.5813	217.8	0.6368
252.8	-7.8638	217.6	-1.1187	252.8	-5.3028	217.6	-0.0903
252.6	1.4537	217.4	-0.5789	252.6	-0.1427	217.4	0.1755
252.4	-11.0952	217.2	-0.15	252.4	-1.3668	217.2	0.1429
252.2	-8.0002	217	0.7244	252.2	1.6172	217	0.097
252	2.9909	216.8	-1.5768	252	-4.355	216.8	-0.0646
251.8	13.7498	216.6	0.008	251.8	-4.7497	216.6	0.1884
251.6	-2.0345	216.4	-0.4139	251.6	1.0337	216.4	-0.067
251.4	-9.1847	216.2	-0.4189	251.4	-4.5599	216.2	0.0647
251.2	2.0637	216	-1.2419	251.2	-1.7805	216	0.2227
251	-7.3252	215.8	-0.2577	251	-1.8669	215.8	-0.1081
250.8	0.5645	215.6	1.3402	250.8	0.8755	215.6	0.058
250.6	-4.0354	215.4	0.3949	250.6	1.6955	215.4	0.2037
250.4	-1.5513	215.2	0.5238	250.4	-0.6681	215.2	-0.1017
250.2	6.2078	215	0.249	250.2	-2.0834	215	-0.1637
250	-5.6244	214.8	-0.3013	250	0.1999	214.8	-0.1404
249.8	-5.9114	214.6	1.2798	249.8	-1.3228	214.6	-0.1157
249.6	-3.5399	214.4	-1.4815	249.6	-1.4603	214.4	0.1955
249.4	-1.0941	214.2	1.7537	249.4	0.9512	214.2	0.4072
249.2	-3.1039	214	1.6824	249.2	0.4518	214	0.173
249	-3.6641	213.8	2.1526	249	-0.9982	213.8	0.2943
248.8	-0.5871	213.6	1.8704	248.8	0.8471	213.6	0.2654
248.6	-3.7437	213.4	0.581	248.6	-1.7456	213.4	-0.444
248.4	0.8308	213.2	-1.3783	248.4	0.4118	213.2	-0.1354
248.2	-0.8122	213	0.792	248.2	0.5814	213	-0.1364
248	0.7908	212.8	1.164	248	-0.9923	212.8	0.0905
247.8	-1.3825	212.6	2.2452	247.8	-0.057	212.6	0.131
247.6	2.7731	212.4	0.1635	247.6	-1.3365	212.4	0.0719
247.4	0.6642	212.2	0.4482	247.4	-0.5276	212.2	0.2397
247.2	0.4524	212	0.4644	247.2	0.6951	212	-0.7323
247	0.1823	211.8	0.3519	247	-0.8055	211.8	0.0588
246.8	-0.1467	211.6	2.3998	246.8	-0.0386	211.6	-0.4235
246.6	-2.5052	211.4	2.1745	246.6	-1.6217	211.4	0.1408
246.4	-0.5324	211.2	0.0758	246.4	-1.0455	211.2	-0.0643
246.2	0.4933	211	0.4929	246.2	-0.0042	211	0.3936
246	1.6089	210.8	1.2011	246	-0.5154	210.8	0.2329
245.8	3.8558	210.6	2.4589	245.8	0.5417	210.6	0.0627
245.6	0.8283	210.4	1.5865	245.6	-0.2551	210.4	-0.6584
245.4	0.6869	210.2	1.3387	245.4	-0.7264	210.2	-0.2923
245.2	0.8776	210	1.0135	245.2	-0.4832	210	0.284
245	0.1365	209.8	1.659	245	0.2298	209.8	0.068
244.8	2.305	209.6	-1.298	244.8	-0.3353	209.6	-0.0156
244.6	0.2397	209.4	-1.4035	244.6	-0.2579	209.4	-0.2137
244.4	0.652	209.2	1.3169	244.4	0.0854	209.2	-0.0601
244.2	-0.8754	209	3.0337	244.2	-0.3155	209	-0.1924
244	1.0819	208.8	0.6519	244	-0.2405	208.8	-0.1346
243.8	2.4943	208.6	2.6027	243.8	0.1475	208.6	0.4873
243.6	0.4038	208.4	-0.8664	243.6	-0.3628	208.4	0.6161
243.4	1.1649	208.2	-0.5923	243.4	-0.3957	208.2	-0.9718
243.2	0.9246	208	0.57	243.2	-0.3946	208	-0.324

243	0.6146	207.8	2.1778	243	-0.2858	207.8	0.1352
242.8	0.0615	207.6	2.404	242.8	-0.4416	207.6	-0.0218
242.6	1.3358	207.4	0.0886	242.6	-0.1321	207.4	0.2638
242.4	2.3687	207.2	-0.2496	242.4	-0.2817	207.2	-0.4744
242.2	0.2692	207	1.8095	242.2	-0.2462	207	0.4651
242	0.515	206.8	2.6284	242	-0.0534	206.8	0.4709
241.8	1.2582	206.6	1.8385	241.8	-0.1296	206.6	-1.4419
241.6	0.5053	206.4	0.7265	241.6	0.1142	206.4	-0.7179
241.4	1.09	206.2	0.1278	241.4	-0.3483	206.2	1.3186
241.2	0.908	206	-2.309	241.2	-0.237	206	-1.4024
241	0.9199	205.8	1.0478	241	0.0217	205.8	0.7645
240.8	-1.2642	205.6	1.0052	240.8	-0.1368	205.6	-0.1055
240.6	0.7109	205.4	-2.4657	240.6	-0.0489	205.4	0.062
240.4	0.3987	205.2	-0.5511	240.4	0.0043	205.2	-0.0275
240.2	1.0164	205	1.2526	240.2	0.0713	205	-0.7603
240	0.5111	204.8	-0.4337	240	-0.0566	204.8	0.0593
239.8	0.5838	204.6	0.3184	239.8	-0.1276	204.6	1.1632
239.6	0.2768	204.4	-1.8168	239.6	-0.2804	204.4	0.4192
239.4	0.1573	204.2	4.7495	239.4	-0.2246	204.2	0.2375
239.2	0.2461	204	-3.6937	239.2	-0.1877	204	-0.5439
239	0.7206	203.8	-1.3017	239	-0.046	203.8	0.4817
238.8	0.7035	203.6	3.4068	238.8	0.237	203.6	-0.1949
238.6	0.7723	203.4	-1.7004	238.6	-0.1562	203.4	0.1481
238.4	1.1926	203.2	1.0425	238.4	0.1137	203.2	0.4436
238.2	0.4957	203	2.7366	238.2	0.1866	203	0.1096
238	0.1993	202.8	0.2214	238	0.0011	202.8	0.9499
237.8	-0.5919	202.6	-0.9995	237.8	-0.1311	202.6	0.005
237.6	-0.2045	202.4	-0.4386	237.6	-0.2809	202.4	-0.1008
237.4	0.2951	202.2	1.5183	237.4	0.0924	202.2	-1.0241
237.2	0.2763	202	3.9352	237.2	-0.0682	202	0.8222
237	0.3454	201.8	-3.9026	237	0.123	201.8	0.185
236.8	0.1578	201.6	-4.6102	236.8	-0.0583	201.6	0.2563
236.6	-0.8305	201.4	-3.1056	236.6	-0.1394	201.4	0.0675
236.4	0.1178	201.2	0.5686	236.4	0.0475	201.2	-0.9555
236.2	0.3159	201	-2.3895	236.2	0.0784	201	0.0037
236	0.6161	200.8	-0.3335	236	0.0782	200.8	-1.1175
235.8	0.9633	200.6	-1.1089	235.8	0.1337	200.6	-0.4999
235.6	0.2546	200.4	0.8255	235.6	-0.0865	200.4	1.5759
235.4	0.3716	200.2	0.2345	235.4	0.042	200.2	-0.4567
235.2	-0.1638	200	2.0276	235.2	0.173	200	1.3505
235	0.409			235	0.0591		

Table A4. Results of the principal components coefficients of sitagliptin and metformin hydrochloride for PCR model.

Mixture No.	Sitagliptin ($\mu\text{g mL}^{-1}$)	Metformin hydrochloride ($\mu\text{g mL}^{-1}$)	Z1	Z2	Z3	Z4	Z5	Z6
1	13.36	8.00	10.84294	2.185204	-0.0434694	0.0576479	-0.0139843	-0.1021771
2	13.36	10.00	12.69862	1.845221	-0.0622337	0.0725021	-0.0115599	-0.1146071
3	13.36	12.00	14.43255	1.621218	-0.0746509	0.0707957	-0.0140199	-0.1112691
4	13.36	14.00	16.44175	1.265448	-0.0755674	0.0880404	-0.0115464	-0.1338847
5	13.36	16.00	18.27641	1.059148	-0.0853648	0.0881577	-0.0111338	-0.1365247
6	16.70	8.00	11.5361	2.966444	-0.0537313	0.0724661	-0.0113965	-0.1132784
7	16.70	10.00	13.4231	2.646652	-0.0779432	0.077781	-0.0093232	-0.1186342
8	16.70	12.00	15.26954	2.319471	-0.0541354	0.0951629	-0.0129627	-0.1177926
9	16.70	14.00	17.10382	2.172555	-0.0758528	0.0893094	0.0015372	-0.1023928
10	16.70	16.00	18.95773	1.866853	-0.0944023	0.0769914	0.0023791	-0.1136455
11	20.04	8.00	12.17808	3.663929	-0.0583895	0.0667501	-0.0093447	-0.102952
12	20.04	10.00	14.02957	3.384557	-0.0636098	0.0895632	-0.0125965	-0.1159239
13	20.04	12.00	15.83709	3.006622	-0.0476592	0.1091312	-0.000479	-0.1135108
14	20.04	14.00	17.75696	2.836101	-0.1076307	0.0624804	-0.013428	-0.119916
15	20.04	16.00	19.77072	2.589099	-0.0620704	0.0841685	-0.0075716	-0.0988977

16	23.38	8.00	13.05221	4.431188	-0.0777075	0.0878319	-0.009271	-0.118186
17	23.38	10.00	14.89838	4.123749	-0.0764096	0.0853351	-0.0015347	-0.104407
18	23.38	12.00	16.63802	3.798361	-0.0655255	0.1114206	0.0043972	-0.0903928
19	23.38	14.00	18.63537	3.59354	-0.0955316	0.0659751	-0.0306461	-0.106344
20	23.38	16.00	20.41229	3.306786	-0.0370991	0.1190475	-0.0191721	-0.0912103
21	26.72	8.00	13.74611	5.092887	-0.0891428	0.105328	-0.0314232	-0.1326535
22	26.72	10.00	15.43337	4.782102	-0.072408	0.0838503	0.0301399	-0.1550265
23	26.72	12.00	17.35671	4.551464	-0.0895119	0.0670222	-0.0563766	-0.1125212
24	26.72	14.00	18.98121	4.28249	-0.0897928	0.0394045	0.0239509	-0.0873848
25	26.72	16.00	21.00168	3.901466	0.010285	0.0441581	-0.017422	-0.1344944